A Priori Efficiency Calculations For Monte Carlo Applications In Neutron Transport

Andreas J. van Wijk

Supervisor: dr. ir. J. Eduard Hoogenboom

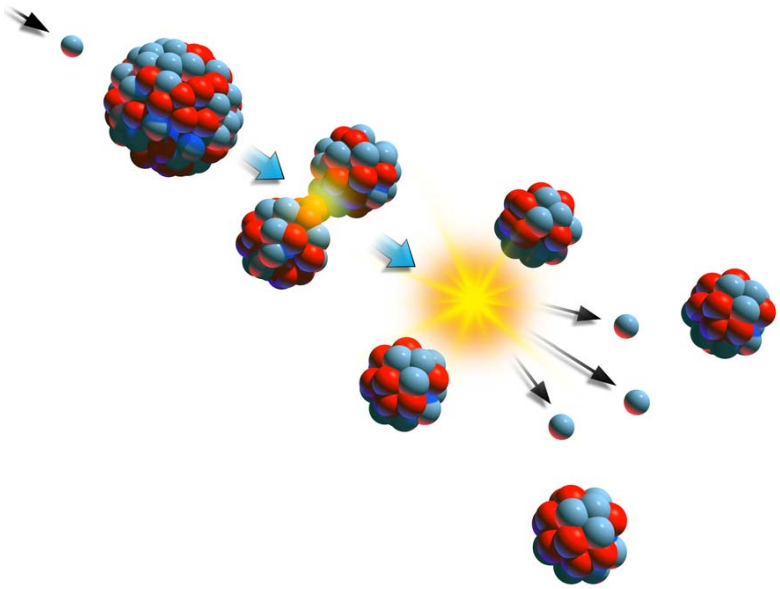

Thesis
Master of science in applied physics
Delft University of Technology
Faculty of Applied Sciences
Department of Radiation Radionuclides and Reactors
Section: Physics of Nuclear Reactors
Delft, January 6, 2010

Abstract

In this research, new theory regarding the a priori calculation of variance and efficiency of a neutron transport Monte Carlo simulation is introduced. Equations describing the expected variance and number of collisions of a neutron history are used to construct a cost function. The cost function can be minimized to obtain an optimal choice of weight window thresholds and/or an optimal choice of a source biasing function in a simulation containing both Russian roulette and splitting, implemented in weight windows.

The theory is verified by applying it to a number of sample cases under the restriction of a two-directional model for the neutron transport, which allows for exact analytical solutions. From a minimum in the cost function it is shown that an optimal choice of weight window thresholds and an optimal source biasing function exists for a specific simulation and can be given a priori.

Attention is also given to the possibility of numerical solutions of the variance and number of collisions equations by means of existing deterministic neutron transport code systems.

To my High school physics teacher Martin Wassink†

Contents

Acknowledgements

I would like to express my gratitude towards my supervisor Eduard Hoogenboom for his unrelenting support and for his enthusiasm throughout the project.
I am also very grateful to my friends and family for providing the necessary relief from the exact sciences.

Chapter 1

Introduction

Although somewhat obscured from everyday life, nuclear technology plays an important role in modern day society. Medical imaging and cancer treatment with radiation both rely on nuclides produced in nuclear facilities and of course, a substantial part of worldwide electricity needs is fulfilled by power generated in nuclear reactors, see Fig. 1.1. Growing concerns about carbon emissions, slow progress in solar and wind technology and diminishing traditional resources have sparked renewed interest in nuclear energy as a viable alternative to traditional power generation methods for the foreseeable future.

Safety issues are always a major concern when it comes to nuclear facilities and having a thorough knowledge of the processes taking place in such facilities is therefore a necessity. Because of the risks and high costs involved in running real life experiments, nuclear scientists investigating these processes resort to computer simulations in most cases. These simulations should of course yield accurate results, preferably within as short a time as possible and with a cost as low as possible.

While there are many research fields within the nuclear sciences it is the transport of neutrons in a nuclear reactor core that is key to the way the reactor will behave, and it is the computer simulation of neutron transport, by means of the Monte Carlo technique, this research focuses on.

Besides Monte Carlo there are a number of *deterministic* methods to simulate neutron transport. These methods usually involve performing some form of numerical analysis to the equation governing neutron transport and describe what the neutrons will do on average. Examples are the 'finite elements' technique [Vermolen, van Kan, and Segal, 2008] or the 'discrete ordinates' method [Dunderstadt and Hamilton, 1976]. One advantage of these treatments is that the solution, if sufficiently accurate, provides full information about the system being studied. One disadvantage is that complicated geometries are usually hard to handle.

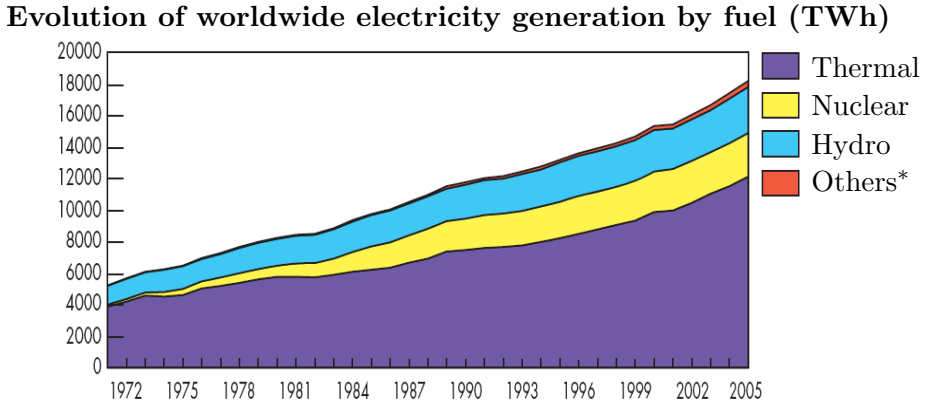

Figure 1.1: Evolution of worldwide electricity generation, International Energy Agency http://www.iea.org/textbase/nppdf/free/2007. In 2005 the total worldwide energy contribution of nuclear was 15.2%.
*Includes geothermal, solar, waste, and renewables.

1.1 The Monte Carlo simulation method

The Monte Carlo method is in essence a stochastic procedure for solving deterministic problems. This statement is as general as the applications of Monte Carlo simulation and it is therefore hard to give a more specific definition. What lies at the heart of Monte Carlo is the notion of random sampling. Samples may be drawn from a parent population, which may describe some physical process, with procedures governed by specific probability laws. By performing statistical analysis[1] on these samples, inferences about the parent population can be made. In case of neutron transport, the average behaviour of the neutrons in the parent population is inferred from the average behaviour of individual, simulated neutrons as we will see later on.

Suppose, as an example, that we want to estimate the value of π. A possible 'real life' Monte Carlo simulation would be to draw a square around a circle on the floor and to *randomly* scatter some rice grains on the floor. By performing the random scattering we've drawn, in a mathematical sense, from a uniform distribution of positions contained by the square and circle. Since we have deterministic expressions for the areas of both the circle and the square we know that the ratio of the number of grains in the circle to the number of grains in the square must, as the number of grains tends to infinity, tend to $\pi r^2/(2r)^2 = \pi/4$. This ratio multiplied by four may therefore be considered a Monte Carlo estimate of π. A more sensible method would be to simply evaluate the expression or to let a computer do the hard work of

[1]Readers who are unfamiliar with statistical concepts like variance and bias are advised to consult appendix A for an introduction to elementary statistical analysis

counting the rice grains. Two such calculations are shown in Fig. 1.2.

Estimating π in this way may seem a lot of work for little gain, and introducing randomness is generally a bad idea when simple problems are concerned. It is only when the processes that have to be simulated become very complex, as is the case in neutron transport, and the number of dimensions increases that Monte Carlo unveils its true potential.

The Monte Carlo method is believed to have been developed at the Los Alamos National Laboratory when computers first made their appearance in the scientific field. The mathematics of Monte Carlo was however developed at a much earlier stage. The name "Monte Carlo" was popularized by physics researchers Stanislaw Ulam, Enrico Fermi, John von Neumann, and Nicholas Metropolis, among others; the name is supposed to be a reference to the Monte Carlo Casino in Monaco where Ulam's uncle would borrow money to gamble [MacKeown, 1997].

Complicated, real-life processes like neutron transport are usually governed by 'known' probability laws. In principle it is possible to incorporate these same laws in the Monte Carlo simulation. If this is the case we will talk of an *analog* simulation; an abstraction of the real life process itself. The conceptual simplicity of analog simulation may be seen as one of Monte Carlo's biggest merits.

On the other hand the probability laws may be wholly artificial; designed for some specific purpose. Usually it is a mix between the two, because analog simulation may be very inefficient in some cases. Suppose for example that one wants to study rare events in some system. These rare events will obviously also be rare in the mathematical analog of the system. Vast stores of data may contain little useful information, leading to a high variance (statistical

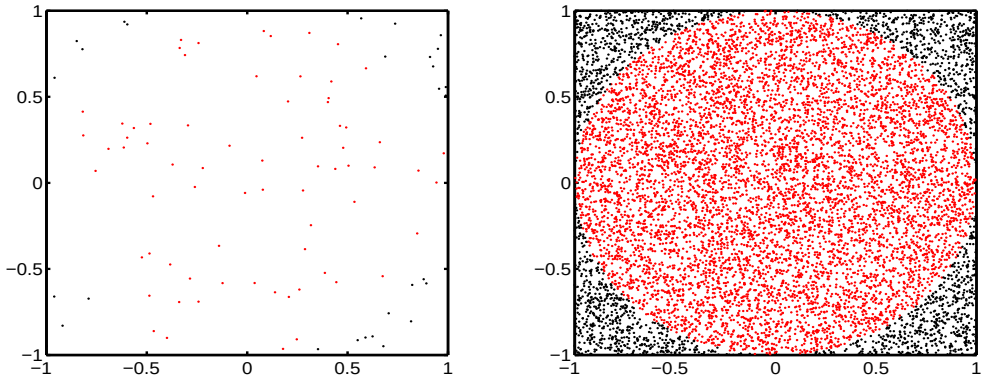

Figure 1.2: Two Monte Carlo simulations for obtaining an estimate of π are shown. The left figure is for 100 'rice grains', leading to an estimate of $\widehat{\pi} = 2.8$, and the right for 10^4 grains, leading to an estimate of $\widehat{\pi} = 3.12$. A simulation with 10^9 grains yields an estimate of $\widehat{\pi} = 3,14159$, which is close to the real value of $\pi = 3,14159265..$

spread) in the estimate following from the simulation. Nothing however prevents one from continuing the abstraction by distorting the probability laws such that the samples collected during simulation will contain more useful information. The only restriction is that the final estimate should be without bias. Simulations containing such modifications will be called *non-analog*.

Over the years there have evolved a multitude of non-analog techniques in the Monte Carlo treatment of neutron transport, all of which aim to reduce the variance and/or to boost the efficiency of a simulation. The researcher is left with the possibility of choosing a strategy for the computation at hand. In practice this usually amounts to making decisions by heuristic arguments and by 'rules of thumb', knowing only after the simulation finishes if the decisions about the strategy were truly the right ones.

It turns out that, as will be shown in later chapters, it is possible to calculate the variance and efficiency of a particular Monte Carlo simulation strategy for neutron transport *a priori*, as opposed to a posteriori (estimated from the samples collected during simulation). This brings forth the possibility of analyzing, comparing and optimizing different strategies before performing the actual simulation and it is exactly that what this research aims to accomplish.

The reason that Monte Carlo simulation has become such a wide spread tool in nuclear reactors analysis is that it has some advantages over deterministic methods. The level of accuracy which can be reached in performing calculations of some aspects of a reactor is unparalleled. This is largely due to the fact that, in principle, even very complicated geometries can be used as an input for the simulation. In deterministic simulations this is simply not possible due to the complex nature of the equations involved. A Monte Carlo simulation furthermore 'focuses on one aspect' of the system. For example, the criticality of the reactor or the flux of neutrons in some part of the reactor may be calculated, whereas deterministic simulations provide the solution to the equations in the entire system and therefore give full information about the problem at hand. Of course, full information may or may not be desirable. Also, Monte Carlo is generally slower than deterministic methods and time-dependent Monte Carlo is still in an infant stage. That's why both practices, Monte Carlo and deterministic simulations, are in use and are undergoing research today.

Details on the mathematical treatment of Monte Carlo for neutron transport will follow in chapter 3. If interested in other Monte Carlo methods like quantum Monte Carlo or Monte Carlo for statistical mechanics, the reader is advised to consult [Thijssen, 2007].

1.2 Scope and goals of this research

This work strives to present and validate both existing and new theory regarding the a priori calculation of variance and efficiency for Monte Carlo

simulations of neutron transport in a way that is complete, readable and has practical significance.

In order to arrive at such theory, chapter 2 provides an introduction to neutron transport in integral form, suitable for Monte Carlo implementation. Also, concepts like adjoint operators and equations are introduced. Chapter 3 deals with the Monte Carlo solution to these transport problems and lays the foundation, in terms of notation and concepts like scoring and sampling, for later chapters.

In chapter 4, equations necessary for the a priori calculation of variance and efficiency are derived. New theory is introduced regarding the calculation of the number of collisions as a measure of computational effort and the variance for a simulation containing both splitting and Russian roulette. From the expressions derived in chapter 4, a cost function is constructed which may be minimized to obtain an optimal choice of weight window thresholds. Although expressions are also derived for the more generally used track-length estimator, the emphasis lies on simulations in which the response is estimated using a collision estimator. This yields more appealing results and allows for analytic solutions more readily.

Chapter 5 provides a number of analytic sample cases to which the theory is applied. A simplified neutron transport model, in which neutrons are only allowed to move in two directions, is introduced. Solutions are provided to the equations necessary for the minimization of cost.

Chapter 6 then provides specific solutions to the sample cases from chapter 5; both a priori, by means of exact analytic solutions, as well as a posteriori, by means of estimates from actual Monte Carlo simulations. From the minimum in the cost function an optimal choice of weight window thresholds is obtained. The possibility of source biasing is also explored and verified.

For the practical implementation of the theory presented in this work, it is necessary to be able to solve the equations describing efficiency by means of existing deterministic neutron transport codes. Existing codes generally solve an integro-differential transport equation. In chapter 7 it is demonstrated how the integral equations derived in this work may be transformed into an integro-differential form that may be suitable.

Since it is the physical nature of the Monte Carlo technique for neutron transport that is most appealing, the author tries to approach the abstract theory from an intuitive, physical point of view rather than providing a formal mathematical derivation of all relevant equations. Hopefully this will lead to a readable and even enjoyable work.

Chapter 2

Integral neutron transport theory

For Monte Carlo purposes, the most common form of the equation describing neutron transport, an integro-differential equation commonly referred to as the Boltzmann equation [Dunderstadt and Hamilton, 1976], is not well suited and it is because of this fact that the transition is made to describing neutron transport in a purely integral form. The following sections provide an introduction to this integral neutron transport theory; emphasizing the physical nature of the processes involved while doing so. This will prove convenient when making the transition to the more abstract theory treated in chapter 4. Also, concepts from adjoint theory will be presented and the necessary notation will be introduced.

2.1 Preliminaries

To fully describe a neutron in a mathematical sense, one would need its position in space $\boldsymbol{r}$, its velocity $\boldsymbol{v}$ and its point in time t. In nuclear reactor physics it has become customary to adopt more convenient variables, although entirely equivalent, for the velocity of the neutron. The velocity vector is essentially decomposed into two components; one characterizing the neutron speed and the second the direction of motion of the neutron.
The speed is characterized by the kinetic energy of the neutron

$$E = \frac{1}{2} m |\boldsymbol{v}|^2 \tag{2.1}$$

The direction is characterized by a unit vector in the direction of motion of the neutron

$$\boldsymbol{\Omega} = \frac{\boldsymbol{v}}{|\boldsymbol{v}|} \tag{2.2}$$

A point in the phase space will from now on be represented as follows

$$P = (\boldsymbol{r}, \boldsymbol{\Omega}, E) \tag{2.3}$$

in which the time variable t is left out here because Monte Carlo calculations are mainly concerned with stationary problems.

The variable that is most commonly used in nuclear reactor physics is the angular neutron flux

$$\phi(P) = \begin{array}{l} \textit{the number of neutrons per unit energy range} \\ \textit{and unit solid angle passing through a surface} \\ \textit{with normal } \boldsymbol{\Omega} \text{ at } P \end{array}$$

In nuclear reactor calculations one is generally interested in some physical property of the system, like the flux of neutrons in some part of the reactor or the dose rate in some volume of material. We shall call this quantity R and refer to it as the detector response. Formally, R is a functional or weighted integral of some response or payoff function $\eta(P)$ and a solution function $\phi(P)$.

$$R = \int \eta(P)\phi(P)dP \tag{2.4}$$

The solution function $\phi(P)$ may be the angular neutron flux. The payoff function $\eta(P)$ then determines what the integral represents.

Cross sections

A concept of importance in nuclear reactor theory is that of cross sections; see [Bell and Glasstone, 1970] or [Dunderstadt and Hamilton, 1976] for a full account. One can define the microscopic cross section σ [cm^2] as

$$\sigma = \frac{\text{Number of reactions/nucleus/sec}}{\text{Number of incident neutrons/cm}^2\text{/sec}} \tag{2.5}$$

The total microscopic cross section σ_t represents the sum over all cross sections of some interaction type, here denoted by the subscript j. j may for example represent elastic scattering, inelastic scattering, fission, or any other distinct interaction.

$$\sigma_t = \sum_j \sigma_j = \sigma_e + \sigma_{in} + \sigma_{n\alpha} + ... \tag{2.6}$$

We define the absorption cross section to characterize any event other than scattering (also including fission)

$$\sigma_a = \sigma_t - \sigma_s \tag{2.7}$$

For the purposes of this thesis it is more convenient to abandon the concept of the microscopic cross section and adopt the macroscopic cross section Σ

[cm^{-1}] as the characterization of interaction types. If the matter consists of components denoted by subscript A, then the total macroscopic cross section is the weighted sum of the microscopic cross sections of interaction type j and component A

$$\Sigma_t(\boldsymbol{r}, E) = \sum_A N_A(\boldsymbol{r}) \sum_j \sigma_{j,A}(E) \tag{2.8}$$

in which $N_A(\boldsymbol{r})$ represents the atomic number density of nuclide A and $\sigma_{j,A}(E)$ denotes the microscopic cross section of interaction type j, provided nuclide A. Note that the macroscopic cross section is written as a function of space and energy and not of direction. For practically all applications in nuclear reactor analysis this simplification holds. For notational convenience however, we might sometimes write $\Sigma_t(P)$. The macroscopic total cross section Σ_t represents the probability of interaction per unit distance traveled. The reciprocal of this quantity is therefore the neutron mean free path. We can ease notation even further by introducing a partial macroscopic cross section

$$\Sigma_{j,A}(\boldsymbol{r}, E) = N_A(\boldsymbol{r})\sigma_{j,A}(E) \tag{2.9}$$

with which Eq. (2.8) reduces to

$$\Sigma_t(\boldsymbol{r}, E) = \sum_A \sum_j \Sigma_{j,A}(\boldsymbol{r}, E) \tag{2.10}$$

In case of an interaction, the particle may undergo a change in direction and energy. For neutrons with direction Ω' and energy E' we define the differential cross section as

$$\Sigma_j(\boldsymbol{r}, \boldsymbol{\Omega}' \to \boldsymbol{\Omega}, E' \to E) = \Sigma_j(\boldsymbol{r}, E') p_j(\boldsymbol{\Omega}' \to \boldsymbol{\Omega}, E' \to E) \tag{2.11}$$

in which $p_j(\boldsymbol{\Omega}' \to \boldsymbol{\Omega}, E' \to E) d\boldsymbol{\Omega} dE$ represents the probability that the neutron coming out of the interaction of type j has a direction $\boldsymbol{\Omega}$ in $d\boldsymbol{\Omega}$ and energy E in dE. For elastic scattering this probability is normalized to unity.

To incorporate fission we introduce $\nu(\boldsymbol{r}, E)$ as the average number of neutrons produced by a fission at $\boldsymbol{r}$ caused by a neutron of energy E. The criticality of a reactor can be conveniently defined as

$$k_{eff} = \frac{\text{Number of neutrons in generation } i+1}{\text{Number of neutrons in generation } i} \tag{2.12}$$

2.2 Integral transport equations

The equation describing neutron transport most common to nuclear physicists is the stationary Boltzmann transport equation

$$\begin{aligned} &\boldsymbol{\Omega} \cdot \nabla \phi(P) + \Sigma_t(\boldsymbol{r}, E)\phi(P) \\ &= \int_{4\pi} \int \Sigma_s(\boldsymbol{r}, E' \to E, \boldsymbol{\Omega}' \to \boldsymbol{\Omega}) \phi(\boldsymbol{r}, E', \boldsymbol{\Omega}') dE' d\boldsymbol{\Omega}' + S(P) \end{aligned} \tag{2.13}$$

It is possible to transform Eq. (2.13) into a purely integral equation which is suitable for Monte Carlo implementation, [Bell and Glasstone, 1970], the derivation of which will be treated in chapter 7 and is of no particular interest at this point. Rather, following an intuitive approach to find the integral equation describing neutron transport will provide the necessary insight into the relevant physical processes. To that end let us first introduce the collision density of neutrons at a point in phase space

$$\psi(P) = \begin{array}{l} \textit{the number of neutrons per unit volume,} \\ \textit{unit energy range and unit solid angle} \\ \textit{entering a collision at } P \end{array}$$

The collision density is related to the angular neutron flux via a simple relation

$$\psi(P) = \Sigma_t(P)\phi(P) \tag{2.14}$$

From Eq. (2.14) it becomes clear that in vacuum there will be no interaction so the collision density is zero, whatever value the neutron flux might be.

Somewhat equivalently it is possible to define an emission density of neutrons

$$\chi(P) = \begin{array}{l} \textit{the number of neutrons per unit volume,} \\ \textit{unit energy range and unit solid angle} \\ \textit{starting a flight path at } P \end{array}$$

Several physical processes may provide the neutrons that constitute the emission and collision densities. There may be a source $S(P)$ of neutrons

$$S(\boldsymbol{r}, \boldsymbol{\Omega}, E) = S(P) \tag{2.15}$$

Neutrons may make a transition to a new collision site, a process which can be described by the transition kernel $T(\boldsymbol{r}' \to \boldsymbol{r}, E, \boldsymbol{\Omega})$, in which

$$T(\boldsymbol{r}' \to \boldsymbol{r}, E, \boldsymbol{\Omega})dV = \begin{array}{l} \textit{the probability for a neutron starting at } \boldsymbol{r}', \\ \textit{with energy } E \textit{ and direction } \boldsymbol{\Omega} \\ \textit{to have its next collision in } dV \textit{ at } r. \end{array}$$

The general form of T in three dimensions, [Lux and Koblinger, 1991], is given by

$$\begin{aligned} &T(\boldsymbol{r}' \to \boldsymbol{r}, E, \boldsymbol{\Omega}) \\ &= \Sigma_t(\boldsymbol{r}, E)\exp\left\{-\int_0^{|\boldsymbol{r}-\boldsymbol{r}'|} \Sigma_t(\boldsymbol{r} - s\boldsymbol{\Omega}, E)ds\right\} \frac{\delta(\boldsymbol{\Omega} - \frac{\boldsymbol{r}-\boldsymbol{r}'}{|\boldsymbol{r}-\boldsymbol{r}'|})}{|\boldsymbol{r} - \boldsymbol{r}'|^2} \end{aligned} \tag{2.16}$$

in which $s = |\boldsymbol{r} - \boldsymbol{r}'|$ represents the path length between two collision points $\boldsymbol{r}$ and $\boldsymbol{r}'$. T is normalized to unity for an infinite system. For a finite system

we can circumvent the normalization 'problem' by imagining the system being surrounded by a purely absorbing medium so that we can take the integral over the entire space volume. Neutrons are simply killed when exiting the system. The transition kernel can thus be understood as a conditional probability density function for a new collision site $\boldsymbol{r}$, given $\boldsymbol{r}', E, \boldsymbol{\Omega}$.

At this point it should be noted that, although time dependence was omitted it can be easily implemented, since if a neutron travels a distance $|\boldsymbol{r} - \boldsymbol{r}'|$ with speed $v = \sqrt{2E/m}$, the time increase will simply be $|\boldsymbol{r} - \boldsymbol{r}'|/v$.

Neutrons in the system may also enter a collision and undergo a change in direction and energy. The collision kernel $C(\boldsymbol{r}, E' \to E, \boldsymbol{\Omega}' \to \boldsymbol{\Omega})$ describes this process;

$$C(\boldsymbol{r}, E' \to E, \boldsymbol{\Omega}' \to \boldsymbol{\Omega}) dE d\boldsymbol{\Omega} = \begin{array}{l} \textit{the probability for a neutron} \\ \textit{entering a collision at } \boldsymbol{r}' \\ \textit{with energy } E' \textit{ and direction } \boldsymbol{\Omega}' \\ \textit{to exit the collision with energy} \\ E \textit{ in } dE \textit{ and direction } \boldsymbol{\Omega} \textit{ in } d\boldsymbol{\Omega} \end{array}$$

In general form, the collision kernel can be written as, [Hoogenboom, 1977]

$$\begin{aligned} &C(\boldsymbol{r}, E' \to E, \boldsymbol{\Omega}' \to \boldsymbol{\Omega}) \\ &= \sum_A \sum_j p_{j,A}(\boldsymbol{r}, E') c_{j,A}(E') p_{j,A}(E' \to E, \boldsymbol{\Omega}' \to \boldsymbol{\Omega}) \end{aligned} \tag{2.17}$$

in which $p_{j,A}(\boldsymbol{r}, E')$ represents the conditional probability of an interaction type j provided a collision with nuclide A

$$p_{j,A}(\boldsymbol{r}, E') = \frac{\Sigma_{j,A}(\boldsymbol{r}, E')}{\Sigma_t(\boldsymbol{r}, E')} \tag{2.18}$$

and $c_{j,A}(E')$ represents the average number of neutrons released in a collision type j with a nuclide A. In case of scattering, $c_{s,A}(E') = 1$; in case of fission the number of neutrons released will be equal to $\nu(E')$.
$p_{j,A}(E' \to E, \boldsymbol{\Omega}' \to \boldsymbol{\Omega})$ represents the joint transfer probability for $(E' \to E)$ and $(\boldsymbol{\Omega}' \to \boldsymbol{\Omega})$ given collision type j with nuclide A. Except for an absorption event this probability is normalized to unity.

The collision density $\psi(P)$ is related to the emission density in the following way

$$\psi(P) = \int T(\boldsymbol{r}' \to \boldsymbol{r}, E, \boldsymbol{\Omega}) \chi(\boldsymbol{r}', E, \boldsymbol{\Omega}) dV' \tag{2.19}$$

as the density of neutrons entering a collision at $\boldsymbol{r}$ with direction $\boldsymbol{\Omega}$ and energy E is formed by the density of neutrons starting a flight at $\boldsymbol{r}'$ with direction $\boldsymbol{\Omega}$ and energy E, traveling to $\boldsymbol{r}$. Alternatively, one can write a relation for the emission density

$$\chi(P) = S(P) + \int_0^\infty \int_{4\pi} C(\boldsymbol{r}, E' \to E, \boldsymbol{\Omega}' \to \boldsymbol{\Omega}) \psi(\boldsymbol{r}, E', \boldsymbol{\Omega}') dE' d\boldsymbol{\Omega}' \tag{2.20}$$

Note that the emission density represents the right hand side of the Boltmann equation, Eq. (2.13).

Using Eq. (2.20) to rewrite Eq. (2.19), one arrives at the transport equation for the collision density $\psi(P)$

$$\psi(P) = S_1(P) + \int K(P' \to P)\psi(P')dP' \tag{2.21}$$

in which $S_1(P)$ represents the source of first collisions

$$S_1(P) = \int_V T(\boldsymbol{r}' \to \boldsymbol{r}, E, \boldsymbol{\Omega})S(\boldsymbol{r}', E, \boldsymbol{\Omega})dV' \tag{2.22}$$

and $K(P' \to P)$ represents the transport kernel for the collision density

$$K(P' \to P) = C(\boldsymbol{r}', E' \to E, \boldsymbol{\Omega}' \to \boldsymbol{\Omega})T(\boldsymbol{r}' \to \boldsymbol{r}, E, \boldsymbol{\Omega}) \tag{2.23}$$

Eq. (2.21) is a so-called Fredholm type integral equation of the second kind [Pipkin, 1991] which will be of particular interest for the Monte Carlo solution procedure discussed in chapter 3. The transport kernel $K(P' \to P)$ represents the probability for a neutron with energy E' and direction $\boldsymbol{\Omega}'$ entering a collision at $\boldsymbol{r}'$, to have a change in energy and direction to E and $\boldsymbol{\Omega}$ and subsequently have a free flight to $\boldsymbol{r}$.

Along the same lines as for the collision density one can derive the transport equation for the emission density $\chi(P)$

$$\chi(P) = S(P) + \int L(P' \to P)\chi(P')dP' \tag{2.24}$$

in which $S(P)$ represents the true source density and $L(P' \to P)$ represents the transport kernel for the emission density

$$L(P' \to P) = T(\boldsymbol{r}' \to \boldsymbol{r}, E', \boldsymbol{\Omega}')C(\boldsymbol{r}, E' \to E, \boldsymbol{\Omega}' \to \boldsymbol{\Omega}) \tag{2.25}$$

It is interesting to note here the difference between the two transport kernels. $L(P' \to P)$ implies first having a flight from $\boldsymbol{r}'$ to $\boldsymbol{r}$ with energy E' and direction $\boldsymbol{\Omega}'$ and subsequently a collision at $\boldsymbol{r}$ to have a change in energy to E and a change in direction to $\boldsymbol{\Omega}$. $K(P' \to P)$ implies first having a collision at $\boldsymbol{r}'$ resulting in a change in energy to E and a change in direction to $\boldsymbol{\Omega}$ and subsequently the flight from $\boldsymbol{r}'$ to $\boldsymbol{r}$ but now, of course, with energy E and direction $\boldsymbol{\Omega}$.

The detector response can now be expressed in terms of any of the three functions encountered in this section

$$R = \int \eta_\phi(P)\phi(P) = \int \eta_\psi(P)\psi(P) = \int \eta_\chi(P)\chi(P) \tag{2.26}$$

The interrelations between the different payoff functions $\eta_\phi(P)$, $\eta_\psi(P)$ and $\eta_\chi(P)$ will be treated shortly.

2.3 Adjoint theory

Adjoint equations and adjoint operators play an important role in the mathematical analysis of complex systems. For the remainder of this work some concepts from adjoint theory will be essential and are therefore briefly discussed below.
Suppose we write Eq. (2.21) in operator form as

$$A\psi(P) = S_1(P) \tag{2.27}$$

We shall call this the *forward* equation. We then proceed to define the equation adjoint to Eq. (2.27) as

$$A^*\psi^*(P) = S_1^*(P) \tag{2.28}$$

in which we recognize three quantities: the adjoint transport operator A^*, an adjoint source term $S_1^*(P)$ and of course the solution to the adjoint equation $\psi^*(P)$.

The definition of the adjoint operator A^* follows from a commutative relation. Suppose $f(P)$ and $g(P)$ are two arbitrary elements in the domain of some operator B, the adjoint operator then obeys

$$\int f(P)Bg(P)dP = \int g(P)B^*f(P)dP \tag{2.29}$$

Finding the adjoint of an operator often involves deriving adjoint boundary conditions (details can be found in [Ronen, 1986]). As a simple example suppose B represents the product operator. In that case obviously $B^* = B$, no adjoint boundary conditions need to be specified and we proceed to call the product operator self-adjoint.
As another example consider the integral operator

$$Kg(P) = \int K(P' \to P)g(P')dP'$$

We see from Eq. (2.29) that

$$\int f(P)Kg(P)dP = \int\int f(P)K(P' \to P)g(P')dP'dP$$
$$= \int g(P') \int K(P' \to P)f(P)dPdP'$$
switch P to P' and vice versa
$$= \int\int g(P)K(P \to P')f(P')dP'dP = \int g(P)K^*f(P)dP$$

and therefore

$$K^*f(P) = \int K(P \to P')f(P')dP' \tag{2.30}$$

Taking the adjoint of an integral operator transposes the kernel.

What remains is finding a suitable adjoint source term $S_1^*(P)$. With suitable in this case we mean that the solution to the adjoint equation should represent something that can aid in solving the forward problem. Now recall that the aim of a calculation was to obtain a detector response, written here as a weighted integral over the collision density

$$R = \int \eta_\psi(P)\psi(P)dP \tag{2.31}$$

in which $\eta_\psi(P)$ is recognized as the payoff function with respect to the collision density $\psi(P)$. Now multiply the forward transport equation, Eq. (2.27), with $\psi^*(P)$ and the adjoint equation, Eq. (2.28), with $\psi(P)$ and integrate over the whole phase space.

$$\begin{aligned} \int \psi^*(P)A\psi(P)dP &= \int \psi^*(P)S_1(P)dP \\ \int \psi(P)A^*\psi^*(P)dP &= \int \psi(P)S_1^*(P)dP \end{aligned} \tag{2.32}$$

Taking the adjoint source $S_1^*(P)$ equal to $\eta_\psi(P)$, the following relation is obtained

$$R = \int \eta_\psi(P)\psi(P)dP = \int S_1(P)\psi^*(P)dP \tag{2.33}$$

which shows that, given this adjoint source definition, $\psi^*(P)$ may be interpreted as the importance or expected contribution to the detector response of a particle entering a collision at P. Integration of this function over the density of first collisions returns the detector response.

Returning to the usual notation we write the transport equation for $\psi^*(P)$ as

$$\psi^*(P) = \eta_\psi(P) + \int K(P \to P')\psi^*(P')dP' \tag{2.34}$$

which again is a Fredholm type integral equation of the second kind, much like the forward equation. In this case, however, the payoff function $\eta_\psi(P)$ acts as a source density and transport is governed by the transposed kernel

$$K(P \to P') = C(\boldsymbol{r}, E \to E', \boldsymbol{\Omega} \to \boldsymbol{\Omega}')T(\boldsymbol{r} \to \boldsymbol{r}', E', \boldsymbol{\Omega}') \tag{2.35}$$

Because the forward and adjoint equations are so closely related the Monte Carlo treatment of forward and adjoint transport is for a great part the same, albeit, in the case of adjoint transport, some extra interpretation of the kernel is necessary. For example, a collision of an adjoint 'pseudo' particle will usually lead to an increase in energy. The Monte Carlo treatment of forward neutron

transport will be treated in chapter 3 and adjoint transport will be covered in appendix B.

The equation adjoint to Eq. (2.24) is written as

$$\chi^*(P) = \eta_\chi(P) + \int L(P \to P')\chi^*(P')dP' \tag{2.36}$$

and the response is expressed as

$$R = \int \eta_\chi(P)\chi(P)dP = \int S(P)\chi^*(P)dP \tag{2.37}$$

$\chi^*(P)$ represents the importance or expected contribution to the detector response of a neutron starting a flight path at P. The transposed kernel $L(P \to P')$ can be written out explicitly

$$L(P \to P') = T(\boldsymbol{r} \to \boldsymbol{r}', E, \boldsymbol{\Omega})C(\boldsymbol{r}', E \to E', \boldsymbol{\Omega} \to \boldsymbol{\Omega}') \tag{2.38}$$

Some other relations between the various relevant functions can be derived. If one substitutes Eq. (2.19) in Eq. (2.31), interchange integration variables and use Eq. (2.37) one finds

$$\begin{aligned} R &= \int_P \eta_\psi(P) \int_V T(\boldsymbol{r}' \to \boldsymbol{r}, E, \boldsymbol{\Omega})\chi(\boldsymbol{r}', E, \boldsymbol{\Omega})dV'dP \\ &\text{switch } \boldsymbol{r} \text{ to } \boldsymbol{r}' \text{ and vice versa} \\ &= \int_P \int_V \eta_\psi(\boldsymbol{r}', E, \boldsymbol{\Omega})T(\boldsymbol{r} \to \boldsymbol{r}', E, \boldsymbol{\Omega})\chi(P)dV'dP \\ &= \int \eta_\chi(P)\chi(P)dP \end{aligned}$$

and, given that this holds for any $\chi(P)$, therefore

$$\eta_\chi(P) = \int T(\boldsymbol{r} \to \boldsymbol{r}', E, \boldsymbol{\Omega})\eta_\psi(\boldsymbol{r}', E, \boldsymbol{\Omega})dV' \tag{2.39}$$

Another useful relation between the payoff functions can be derived from Eq. (2.14). Because

$$R = \int \eta_\phi(P)\phi(P)dP = \int \eta_\phi(P)\frac{\psi(P)}{\Sigma_t(P)}dP = \int \eta_\psi(P)\psi(P)dP$$

we have

$$\eta_\psi(P) = \frac{1}{\Sigma_t(P)}\eta_\phi(P) \tag{2.40}$$

To arrive at a relation between the different adjoint functions, multiply Eq. (2.34), using $\boldsymbol{r}'$ in stead of $\boldsymbol{r}$, with $T(\boldsymbol{r} \to \boldsymbol{r}', E, \boldsymbol{\Omega})$ and integrate over $\boldsymbol{r}'$

to obtain

$$\int T(\boldsymbol{r} \to \boldsymbol{r}', E, \boldsymbol{\Omega})\psi^*(\boldsymbol{r}', E, \boldsymbol{\Omega})dV' = \eta_\chi(P) + \int L(P \to P') \int T(\boldsymbol{r}' \to \boldsymbol{r}'', E', \boldsymbol{\Omega}')\psi^*(\boldsymbol{r}'', E', \boldsymbol{\Omega}')dV''dP'$$

and compare with Eq. (2.36) to see that

$$\chi^*(P) = \int T(\boldsymbol{r} \to \boldsymbol{r}', E, \boldsymbol{\Omega})\psi^*(\boldsymbol{r}', E, \boldsymbol{\Omega})dV' \tag{2.41}$$

using Eq. (2.41) in Eq. (2.34) one finds that

$$\psi^*(P) = \eta_\psi(P) + \int\int C(\boldsymbol{r}, E \to E', \boldsymbol{\Omega} \to \boldsymbol{\Omega}')\chi^*(\boldsymbol{r}, E', \boldsymbol{\Omega}')dE'd\boldsymbol{\Omega}' \tag{2.42}$$

As a final way of expressing the response we write

$$R = \int \phi(P)\eta_\phi(P)dP = \int S(P)\phi^*(P)dP \tag{2.43}$$

and note that the importance functions $\phi^*(P)$ and $\chi^*(P)$ are the same. Both represent the importance or expected contribution to the detector response of a neutron starting a flight at P.

This concludes the derivation of the relevant transport equations and their interrelations. Later on in chapter 4 we will encounter even more, and more complicated, transport equations for processes closely related to the collision and emission densities and the foundations laid in this chapter will be used to manipulate these equations.

Chapter 3

Monte Carlo for neutron transport

In this chapter, a brief description of the process of Monte Carlo simulation with respect to neutron transport will be given. The derivation will again be from an intuitive, physical point of view rather than providing the rigorous mathematical formalism that underlies the Monte Carlo method. For such a rigorous treatment the reader is advised to consult [Spanier and Gelbard, 1969].

Monte Carlo simulation relies heavily on statistical tools. Appendix A therefore deals with a basic introduction to statistics and estimation, introducing some notation on the fly. Readers who have experience in the field may proceed directly to section 3.1 which covers the mathematical formalism of the Monte Carlo procedure along the lines of [Hoogenboom, 1977] and [Lux and Koblinger, 1991]. Appendix B explains how adjoint transport may be accomplished by means of Monte Carlo.

3.1 The theoretical framework of Monte Carlo

Now that the necessary statistical tools, the mathematical description of forward and adjoint transport and the basic ideas behind Monte Carlo simulation have been discussed it is time to cast everything into a formalism which can be employed in computer simulation.

The goal of a simulation is to obtain an estimate of the response R. To illustrate how this can be accomplished by means of Monte Carlo consider the following example. Suppose one is interested in the average of a known function $\varphi(x)$ over some interval $[a, b]$ in a one-dimensional system. The response can in that case be written as

$$R = \frac{1}{b-a} \int_a^b \varphi(x) dx$$

Now we could of course estimate the integral, which represents the area below the graph of $\varphi(x)$, in the same way as we could estimate the value of π; i.e. we could randomly select points in a rectangle containing the function $\varphi(x)$, check the ratio of points below and above the graph, and from this ratio obtain an estimate of the area. There is another method, however, which requires less effort. The integral can also be estimated by

$$\widehat{R} = \frac{1}{N} \sum_{i=1}^{N} \varphi(x_i) \tag{3.1}$$

with the position variable taken randomly from a uniform distribution on the interval $[a, b]$. The random selection of position, which can be achieved by sampling the uniform pdf for positions by generating a random number in a computer, makes it a Monte Carlo simulation. It will be clear that $\widehat{R}$ will provide a reasonable and unbiased estimate, provided that the number of samples N is large enough.

The above methods are of course not very enlightening for neutron transport since they assume the function $\varphi(x)$ to be known. This is for most purposes never the case, since we would then simply evaluate the integral and be done with it. Rather, one has to obtain an estimate of the solution to the transport equation governing neutron transport as well. So generally, in order to obtain an estimate of the response, we will need to estimate the solution function by means of random numbers.

The solution functions encountered in chapter 2 were defined by type two Fredholm integral equations with kernels $K(P' \to P)$, $L(P' \to P)$ and their adjoint counterparts. These equations have a solution in terms of a series development. Consider for example the solution to the emission density, Eq. (2.24), expressed as an infinite Neumann series expansion, [Pipkin, 1991]

$$\begin{aligned} \chi(P) &= \sum_{i=0}^{\infty} \chi_i(P) \qquad (3.2) \\ \chi_0(P) &= S(P) \\ \chi_1(P) &= \int L(P' \to P) S(P') dP' \\ \chi_2(P) &= \int \int L(P' \to P) L(P'' \to P') S(P'') dP'' dP' \end{aligned}$$

This solution converges uniformly, provided that the transport kernel is bounded $\|L\|^2 < 1$ with $\|L\| = \sup \int_a^b \mid L(P' \to P) \mid dP'$ and non-negative. These conditions are satisfied in the case of neutron transport for a non-fissile system. The Monte Carlo solution of Eq. (3.2) then turns out to be remarkably intuitive from a physical point of view (as it should be, since it represents an analog of the physical reality).

From Eq. (3.2) it becomes clear that the emission density at P may be considered as being comprised of neutrons coming from other 'source' points $(P', P'', P''', ...)$, traveling eventually to P and starting a flight there. In this interpretation, each emission (either from a source or after a collision event) of a neutron during its lifetime at a point in phase space constitutes a sample of the emission density at that point in phase space. Since $S(P)$ and the kernel $L(P \to P')$ represent probability densities, the Monte Carlo procedure would involve tracking such a neutron history by randomly sampling the source density $S(P')$ for a birth point P' and randomly sampling the transport kernel $L(P' \to P)$ for new emission points. One is effectively sampling the probability space of neutron 'random walks'; terminology often used in this context.

Following the random walks, or histories, of a large number of neutrons and saving the emission sites results in an estimate of the emission density function in the system.

The series development can also be done for the detector response in terms of the emission density

$$R = \sum_{j=0}^{\infty} R_j = \int \eta_\chi(P) S(P) dP + \int \eta_\chi(P) \int L(P' \to P) S(P') dP' dP + ... \tag{3.3}$$

From Eq. (3.3) it now becomes clear that 'scoring' $\eta_\chi(P_j)$ at every emission site P_j in a neutron history and subsequently summing all these scores leads to a sample or estimate of R.

Scores can also be collected when a particle enters a collision, in which case the scoring function is the payoff function for the collision density: $\eta_\psi(P)$. From Eq. (2.20) and Eq. (2.22) it follows that we actually have a coupled system of equations

$$\begin{aligned}
&\chi_0(P) = S(P) \\
&\psi_0(P) = \int T(\boldsymbol{r}' \to \boldsymbol{r}, E, \boldsymbol{\Omega}) \chi_0(\boldsymbol{r}', E, \boldsymbol{\Omega}) dV' \\
&i + 1 = 1, 2, ..., \infty \\
&\chi_{i+1}(P) = \int C(\boldsymbol{r}, E' \to E, \boldsymbol{\Omega}' \to \boldsymbol{\Omega}) \psi_i(\boldsymbol{r}, E', \boldsymbol{\Omega}') dE' d\boldsymbol{\Omega}' \\
&\psi_{i+1}(P) = \int T(\boldsymbol{r}' \to \boldsymbol{r}, E, \boldsymbol{\Omega}) \chi_{i+1}(\boldsymbol{r}', E, \Omega) dV'
\end{aligned}$$

Source points can be sampled from a pdf which describes the source density $S(P)$. A new position is selected from the transition kernel, which represents a conditional pdf for $\boldsymbol{r}$ given $\boldsymbol{r}'$. This new point represents the first sample of the collision density and a score with respect to the response estimate may be saved here. A new emission point may be randomly selected from the

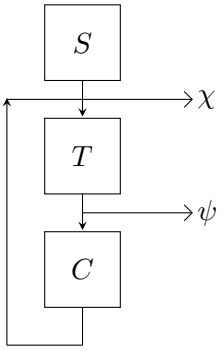

Figure 3.1: A schematic representation of the Monte Carlo treatment of neutron transport showing the positions at which different quantities are obtained and sampled during a neutron history.

collision kernel where a score may also be saved, and so forth. A schematic representation of the formalism is shown in Fig. 3.1 and the appropriate mathematical treatment of analog Monte Carlo is summarized in Table 3.1. The response estimate is then constructed from the scores gathered with the

	Do for N neutrons from $j = 1...N$
	set $i = 0$ and proceed until leakage or absorption
1:	Sample $S(P)$ for initial coordinates $(\boldsymbol{r}_0, E_0, \boldsymbol{\Omega}_0)$
2:	Possibly score $\eta_\chi(P_i)$ at an emission
3:	Sample $T(\boldsymbol{r}_i \rightarrow \boldsymbol{r}_{i+1}, E_i, \boldsymbol{\Omega}_i)$ for next collision site $\boldsymbol{r}_{i+1}$
4:	Possibly score $\eta_\psi(\boldsymbol{r}_{i+1}, E_i, \boldsymbol{\Omega}_i)$ at a collision
5:	Sample $C(\boldsymbol{r}_{i+1}, E_i \rightarrow E_{i+1}, \boldsymbol{\Omega}_i \rightarrow \boldsymbol{\Omega}_{i+1})$ for $(E_{i+1}, \boldsymbol{\Omega}_{i+1})$
	Set $P_i = (\boldsymbol{r}_{i+1}, E_{i+1}, \boldsymbol{\Omega}_{i+1})$ and return to 2:
	Determine $\widehat{R}_j$ from the score collected during history j and proceed with the next neutron history

Table 3.1: Monte Carlo procedure for analog neutron transport

appropriate scoring function during the individual neutron histories: $\widehat{R}_j$, with $j = 1..N$

$$\widehat{R} = \frac{1}{N} \sum_{j=1}^{N} \widehat{R}_j \tag{3.4}$$

and in which N represents the number of neutron histories. The scoring functions η_ψ and η_χ can be as diverse as the physical quantities to be determined. Sometimes there are even multiple possibilities for estimation of a certain quantity. The most common estimators are the *collision estimator* and the

track length estimator. Both will be treated in chapter 4. As an example, suppose one is interested in the average flux in some detector volume V_{det}. The response can in that case be written as

$$R = \frac{1}{V_{det}} \int\int\int_{V_{det}} \phi(P) dV dE d\mathbf{\Omega} = \frac{1}{V_{det}} \int\int\int_{V_{det}} \frac{\psi(P)}{\Sigma_t(P)} dV dE d\mathbf{\Omega}$$

from which the appropriate scoring function is obtained

$$\eta_\psi(P) = \frac{1}{V_{det}\Sigma_t(P)} \qquad \boldsymbol{r} \in V_{det}$$

Every time a neutron enters a collision in the detector volume V_{det}, a score or tally $\eta_\psi(P)$ is recorded and the response is calculated from all scores, call them s_i, gathered during all histories as

$$\widehat{R} = \frac{1}{N} \sum_i s_i \tag{3.5}$$

The statistical tools stated in appendix A apply to a response estimate $\widehat{R}$. Obviously, due to the law of large numbers, increasing the number of neutron histories N will lead to a better estimate with lower variance in the mean. On the other hand this will lead to longer computation times. These criteria can be summarized in the *Figure Of Merit* or FOM, [Lux and Koblinger, 1991]

$$\text{FOM} = \frac{1}{T\text{Var}(\widehat{R})} \tag{3.6}$$

in which T represents the time the calculation took and $\text{Var}(\widehat{R})$ is the relative variance, Eq. (A.7).

Both quantities scale with the number of neutron histories N, which makes the FOM roughly independent of this number. Any non-analog simulation strategy should strive to attain a higher FOM (or to a lower variance depending on ones preference). Since the FOM is calculated from the simulation data, one only knows afterwards if this goal is achieved.

In chapter 4 a cost function is defined as the product of the expected variance and the expected number of collisions resulting from a neutron history. It can be interpreted as the inverse of the figure of merit and as it can be calculated a priori, without performing a simulation, provides one with a tool to compare, analyze and even optimize simulation strategies.

A little extra information on the actual sampling of probability distributions like the transition kernel is required before proceeding with modifications of analog transport.

Sampling probability distributions

Monte Carlo simulation relies on computer generated random[1] numbers, denoted by ρ from this point on, for the sampling of probability distributions. There are numerous ways to perform the actual sampling and as it is not an essential part of this research we will treat two simple examples here and refer the reader to [Lux and Koblinger, 1991] for a full treatment of different possibilities. ρ has a uniform distribution between 0 and 1

$$\text{Prob}(\rho \leq x) = \int_0^x dx' \quad x \in (0,1) \tag{3.7}$$

Suppose a neutron starts a flight and we want to sample the transition kernel, Eq. (2.16), for a new collision site. In a homogeneous system the track length $s = |\boldsymbol{r}' - \boldsymbol{r}|$ has a probability distribution according to $\Sigma_t e^{-\Sigma_t s} \quad s \in [0, \infty)$. We can relate the computer generated random number to the track-length in the following way

$$\rho = P(t) = \int_0^s \Sigma_t e^{-\Sigma_t s'} ds' \quad \rightarrow \quad s = \frac{\ln(1-\rho)}{\Sigma_t} \equiv \frac{-\ln(\rho)}{\Sigma_t}$$

This technique is commonly known as the inverse probability method. Obviously in a non-uniform system the expressions become more complicated.

Another easy example is sampling the collision kernel, Eq. (2.17), in a uniform system where the neutrons are only allowed to move in the positive $\rightarrow$, or negative $\leftarrow$ directions. The collision outcomes are either absorption (leading to termination of the neutron) or scattering, and energy dependence is omitted. The scattering cross section is then formed by the partial cross sections for the positive and negative directions: $\Sigma_s = \Sigma_{\rightarrow} + \Sigma_{\leftarrow}$

The interaction probability under these restrictions is simply $p_j = \Sigma_j / \Sigma_t$ from which it follows that

$$\begin{aligned} j &= a \qquad \text{if } \rho \leq \Sigma_a / \Sigma_t \\ j &= s \qquad \text{otherwise} \end{aligned}$$

and, given a scattering event, the probability to scatter $p_s(\boldsymbol{\Omega}' \rightarrow \boldsymbol{\Omega})$ in either one of the two directions, irrespective of the incoming direction, is given by

$$\begin{aligned} \boldsymbol{\Omega} &= \rightarrow \qquad \text{if } \rho \leq \Sigma_{\rightarrow} / \Sigma_s \\ \boldsymbol{\Omega} &= \leftarrow \qquad \text{otherwise} \end{aligned}$$

For more complex probability distributions, obtaining expressions like the above is usually not that simple.
Now that all the tools are available to perform forward, analog simulations it is time to address possible modifications of the analog game.

[1] Computer generated random numbers are never truly random but with current techniques, for all intents and purposes they are. If true randomness is required, one can for example use random numbers generated from atmospheric noise. It is however very unlikely that the computer generated numbers will not suffice.

3.2 Modifications of the analog game

As mentioned in the introduction, from a mathematical point of view it doesn't matter how one distorts the probability laws governing the analog transport of neutron transport, as long as the resulting Monte Carlo estimate will represent the desired response without bias.

The idea behind modification of the analog game in the context of neutron transport stems from the fact that many particles may never contribute or may carry little significance with respect to the intended response estimate; they may be absorbed or leak long before entering a region of phase space where a score may be recorded. To get an estimate with a reasonable variance in such a situation would involve simulating large amounts of particles, which in turn results in large computing times.

There are a number of ways in which the analog game can be modified, but basically all rely on the possibility to assign a statistical weight W as an extra variable to a particle to account for not sampling the analog probability distribution (pdf) of the respective process. The weight ensures that the final estimate will be unbiased. In analog simulations the particles will always carry a weight equal to one, but this restriction is left out here in light of applications later on. In general, to obtain an unbiased estimate of R, we require

$$\overline{W} \times \overline{\text{pdf}} = W \times \text{pdf} \tag{3.8}$$

in which the overline represents the modified situation.

Three modifications of the analog game most common to neutron transport will be discussed below. Their implications with respect to the variance and efficiency of a simulation will be examined further in chapters 4 and 5.

Implicit Capture

The most intuitive and commonly used form of modification is implicit capture. Whenever a particle collides, the possibility of absorption is accounted for by multiplying the statistical weight W of the particle by the non-absorption probability $\kappa(P) = \Sigma_s(P)/\Sigma_t(P)$. So in stead of possibly terminating a history at collision point P due to absorption, the collision kernel is distorted and the weight is altered according to

$$W' = W\kappa(P) \qquad \kappa(P) \leq 1$$

If a detector is located at P and the particle, born with $W = 1$, has had k collisions at sites $(P_0, P_1 ... P_k)$ before scoring at P, the score will be equal to $\kappa(P_0)\kappa(P_1)...\kappa(P_k)\eta(P)$, whereas the score would have been zero with a greater probability for an analog simulation. Implicit capture therefore reduces variance but increases computational time. Exactly how these effects will manifest themselves mathematically is treated in chapter 4.

Russian roulette and Splitting

Russian roulette is introduced as a means of terminating particles that carry a low statistical weight in order to improve the efficiency of a simulation; increasing variance but decreasing computational effort. If the particle weight W at P is below some threshold $W \leq W_{th}(P)$, the Russian roulette game is played in which case the particle either survives the game with probability $z_1(P)$ and gets assigned a new survival weight $W_s(P)$, or the particle gets killed with probability $z_0(P) = 1 - z_1(P)$. In order to have a statistically fair game it is required that the expected weight after a Russian roulette event is equal to W i.e. $z_1(P)W_s(P) + (1 - z_1(P))0 = W$ or $z_1(P) = W/W_s(P)$

As opposed to terminating particles with low statistical weight by means of Russian roulette, it is common practice to 'split' particles with a weight higher than some user defined threshold weight $W_{split}(P)$ into a number of identical particles in order to increase the probability of scoring. This procedure is called splitting and usually both procedures are implemented in so-called weight windows. The weight window boundaries that define the window may be space and energy dependent and choosing them correctly can significantly improve simulations. The modification of the weight is slightly different in this case

$$N_{split}W' = W \tag{3.9}$$

in which N_{split} represents the number of split particles and W' represents the weigh of the identical particles emerging from the splitting event.

Setting these weight window boundaries in practice usually boils down to performing educated guesses or using iterative methods. A theoretical treatment of how exactly these windows affect the variance and efficiency of a simulation is given in chapter 4 and in chapter 5 some sample cases are studied to examine how this theory can be applied to optimize the choice of weight window thresholds a priori.

Source biasing

The idea behind source biasing stems from the fact that there may very well be source regions in phase space which are of low importance with respect to the response. Suppose for example that detection is done in a small region of a highly absorbing system and that the source is located throughout the system. Particles that have to travel a long distance to reach the detector will have a low probability of scoring a significant amount in any case. In such a situation it will be favorable to bias the spatial distribution of the source such that more particles will be born close to the detector region.

The way in which source biasing is usually implemented in practice, is that the physical source density is biased with the adjoint flux $\phi^*(P)$ in the

following way, [Haghighat and Wagner, 2003]

$$\overline{S}(P) = \frac{\phi^*(P)S(P)}{\int \phi^*(P)S(P)dP} = \frac{\phi^*(P)S(P)}{R}$$

in which the adjoint function and the response may be approximated by an existing, deterministic neutron transport code.

Although $\phi^*(P)$ seems a likely candidate for 'optimal source biasing', as it represents the importance of a particle starting a flight, it remains unclear whether it will give the best result in every situation. There is for example also the adjoint function $\psi^*(P)$ which may yield better results in some cases, or maybe some other function. Let us therefore state a general biasing function $\Gamma(P)$ and implement biasing as

$$\overline{S}(P) = \frac{\Gamma(P)S(P)}{\int \Gamma(P)S(P)dP} \tag{3.10}$$

The modified initial neutron weight will then be equal to

$$\overline{W}(P) = W\frac{\int \Gamma(P)S(P)dP}{\Gamma(P)} \tag{3.11}$$

The tools presented in chapter 4 provide the possibility to investigate an optimal choice for a biasing function.

Another 'rule of thumb' that seems to pay off in practice is to let the biased initial weight of the source particle determine the bounds of the weight window (containing both Russian roulette and splitting). The idea is, according to [Haghighat and Wagner, 2003], that a source particle should neither split nor play Russian roulette immediately, and therefore that the biased initial weight should be located midway between both thresholds in the window.

$$\overline{W}(P) = \frac{W_{split}(P) + W_{th}(P)}{2}$$

and therefore

$$W_{th}(P) \equiv W\frac{\int \Gamma(P)S(P)dP}{\Gamma(P)}\left(\frac{\beta+1}{2}\right)^{-1} \tag{3.12}$$

in which $\beta = W_{split}(P)/W_{th}(P)$ is the ratio of the upper and lower bounds of the weight window. The default value for β in the general purpose Monte Carlo code MCNP is 5, [Laboratories, 2008], and it is observed that the efficiency is fairly insensitive to small deviations from this number.

These rules of thumb all makes sense from an intuitive perspective, but the tools presented in chapter 4 now also provide the possibility to investigate whether or not they provide the best possible result.

To complete the treatment of Monte Carlo for neutron transport, appendix B deals with adjoint Monte Carlo. The equations for variance and efficiency,

derived in the following chapter, are generally adjoint equations which in principle can be solved by means of the Monte Carlo formalism explained there; albeit some extra modifications will be necessary due to modified transport probabilities.

Chapter 4

Theoretical calculation of variance and efficiency

The efficiency of a neutron transport Monte Carlo simulation is measured by the FOM, Eq. (3.6). For the a priori calculation of efficiency it is therefore necessary to arrive at measures for both the variance and computational time of the simulation. As we will see, both can be achieved by exploiting a powerful insight. The score collected during a neutron history is itself probabilistic and therefore has an associated probability score distribution. From this distribution so called moment equations can be constructed, from which the expected variance of a simulation can be obtained.

It turns out to be important where to start the derivation. From Table 3.1 it becomes clear that there are two distinct events during the simulation of a neutron; the start of a neutron flight (following a collision or birth) or a collision event. The notion of a probability score distribution is borrowed from [Lux and Koblinger, 1991], who applied it to a neutron starting a flight and who followed a rigorous and general mathematical approach.

It turns out that looking at a neutron entering a collision yields more appealing results when using a collision estimator. This insight was first put forward by [Hoogenboom, 2004], who derived an equation describing the variance for a simulation with Russian roulette (without using the concept of a probability score distribution). The theory presented in the following may be seen as an extension to the work of both [Lux and Koblinger, 1991] and [Hoogenboom, 2004].

The emphasis lies on simulations using the collisions estimator for obtaining a response estimate because the equations then allow for exact analytic solutions in some cases more readily.

To give a consistent and readable treatment, first an equation for the variance of an analog simulation is derived. Once the concept and necessary notation is sufficiently clear, the transition is made to non-analog games. The

most common of which, using implicit capture to reduce variance in the estimate, is treated in section 4.2. In section 4.3 expressions are derived for the variance of a simulation when both Russian roulette and splitting are applied in a weight window. This requires some new theory to be introduced to account for the splitting procedure.

To estimate the computational time of a simulation, some new theory concerning the estimation of the number of collisions during a particle history is introduced in section 4.4. From the number of collisions and variance, the cost function is constructed which may be minimized to obtain an optimal choice of weight window thresholds and optimal source biasing functions.

In order to give a full treatment, section 4.7 contains the derivation of expressions for track-length estimators, for which it turns out to be favorable to look at neutrons starting a flight.

4.1 The variance equation for analog simulations

When starting a neutron history in an analog simulation, a birth point is sampled from the physical source $S(P)$. A first collision point is then obtained by sampling the transition kernel. A next collision point can be obtained by sampling the transport kernel for the collision density $K(P' \rightarrow P)$. The transport kernel can be normalized to the non-absorption probability $\kappa(P')$ in the following way

$$K_n(P' \rightarrow P) = \frac{K(P' \rightarrow P)}{\kappa(P')} \tag{4.1}$$

in which the subscript n denotes normalization and

$$\begin{aligned} \kappa(P') &= \int C(\boldsymbol{r}', E' \rightarrow E, \boldsymbol{\Omega}' \rightarrow \boldsymbol{\Omega}) T(\boldsymbol{r}' \rightarrow \boldsymbol{r}, E, \boldsymbol{\Omega}) dV dE d\boldsymbol{\Omega} \\ &= \int C(\boldsymbol{r}', E' \rightarrow E, \boldsymbol{\Omega}' \rightarrow \boldsymbol{\Omega}) dE d\boldsymbol{\Omega} = \frac{\Sigma_s(\boldsymbol{r}', E')}{\Sigma_t(\boldsymbol{r}', E')} \end{aligned} \tag{4.2}$$

Along the lines of Coveyou and V. R. Cain [1967] and Lux and Koblinger [1991], we introduce the *Score Probability*

$$\pi[P, s]ds = \begin{array}{l} \textit{the probability for a neutron} \\ \textit{entering a collision at } P \textit{ with unit weight} \\ \textit{to yield, together with its progeny,} \\ \textit{a score } s \textit{ in } ds \end{array} \tag{4.3}$$

In order to obtain an expression for $\pi[P, s]$ it is necessary to consider in detail what might happen to a neutron entering a collision event, and to what score that event will lead. In analog transport there can be two outcomes for a neutron entering a collision. Either the collision event is terminal with

probability $1 - \kappa(P)$, in which case the contribution will simply be the score at that point in phase space: $\eta_\psi(P)$, or the event is not terminal at P and the neutron may experience a next collision event at P', the probability of which is given by the normalized kernel, Eq. (4.1). A schematic of a possible analog neutron history is given in Fig. 4.1. From these events and their respective probabilities, the score probability can now be constructed according to

$$\begin{aligned}\pi[P,s] &= \{1-\kappa(P)\}\,\delta(s-\eta_\psi(P)) + \kappa(P) \\ &\times \int K_n(P \to P')\delta(s-\eta_\psi(P)) * \pi[P',s]dP'\end{aligned} \tag{4.4}$$

in which the $*$ represents convolution with respect to s

$$f(s) * g(s) = \int_{-\infty}^{\infty} f(s-s')g(s')ds'$$

The convolution of two (or more) probability distributions describing independent random variables represents the probability distribution of the sum of the independent random variables. Obviously the score will not be negative but for the evaluation of the integrals this is irrelevant.

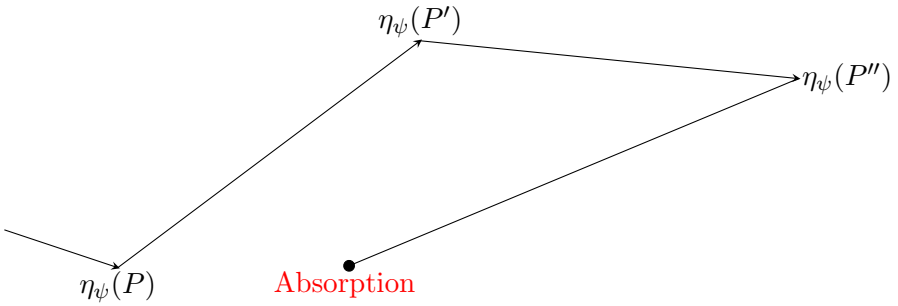

Figure 4.1: A schematic representation of a possible analog neutron history. A score $\eta_\psi(P)$ is recorded at every collision point (P) until termination- in this particular case at the fourth event- or leakage occurs.

The expectation or first moment of the score will be called $M_1(P)$ and the second moment will be called $M_2(P)$.

$$M_1(P) = \int_{-\infty}^{\infty} s\pi[P,s]ds \tag{4.5}$$

$$M_2(P) = \int_{-\infty}^{\infty} s^2\pi[P,s]ds \tag{4.6}$$

To evaluate the first moment consider the substitution $s' = s - \eta_\psi(P)$ and

therefore $ds' = ds$. Computing the integral then results in

$$\begin{aligned} M_1(P) &= \int_{-\infty}^{\infty} s\pi[P,s]ds \\ &= \{1-\kappa(P)\}\int_{-\infty}^{\infty} s\delta(s-\eta_\psi(P))ds \\ &+ \kappa(P)\int K_n(P\to P')\int_{-\infty}^{\infty}\left\{s'+\eta_\psi(P)\right\}\pi[P',s']ds'dP' \\ &= \eta_\psi(P) + \int K(P\to P')M_1(P')dP' \end{aligned} \tag{4.7}$$

in which the fact is used that all probabilities are normalized. Comparing Eq. (4.7) with Eq. (2.34) shows that

$$\psi^*(P) = M_1(P) \tag{4.8}$$

This result should come as no surprise since the expected present and future contribution to the detector response of a particle entering a collision at P is exactly what $\psi^*(P)$ represents. If we then take the average for particles entering their first collisions we see

$$\begin{aligned} E[M_1(P)] &= \int S_1(P)M_1(P)dP \\ &= \int S_1(P)\psi^*(P)dP = R \end{aligned} \tag{4.9}$$

which should obviously be true.

In order to calculate the expected variance of the simulation, the second moment $M_2(P)$ of the score is needed. We can proceed to evaluate the integral by considering the substitution $s^2 = s'^2 + 2\eta_\psi(P)s' + \eta_\psi^2(P)$ from which it follows that

$$\begin{aligned} M_2(P) &= \int_{-\infty}^{\infty} s^2\pi[P,s]ds \\ &= \{1-\kappa(P)\}\int_{-\infty}^{\infty} s^2\delta(s-\eta_\psi(P))ds \\ &+ \kappa(P)\int K_n(P\to P') \\ &\times \int_{-\infty}^{\infty}\left\{s'^2+2\eta_\psi(P)+\eta_\psi^2(P)\right\}\pi[P',s']ds'dP' \\ &= \eta_\psi^2(P) + 2\eta_\psi(P)\kappa(P)\int K_n(P\to P')M_1(P')dP' \\ &+ \kappa(P)\int K_n(P\to P')M_2(P')dP' \\ &= I_0(P) + \int K(P\to P')M_2(P')dP' \end{aligned} \tag{4.10}$$

Because of the transposed kernel, Eq. (4.10) represents an adjoint type equation with a source term that will be of special importance in chapter 5

$$I_0(P) = \eta_\psi(P)\left(2M_1(P) - \eta_\psi(P)\right) \tag{4.11}$$

The variance is obtained by evaluating the moments of particles entering their first collision

$$\text{Var} = \int S_1(P)M_2(P)dP - \left\{\int S_1(P)M_1(P)dP\right\}^2 \tag{4.12}$$

Although solving Eq. (4.12) will generally be quite a daunting undertaking and it may seem as though there is little to be gained from an equation that is more complex than the actual neutron transport equation itself. From a theoretical point of view Eq. (4.12) is very interesting. It serves as a benchmark by which to compare possible variance reduction schemes. In principle Eq. (4.10) (more on that issue in later chapters) can be solved with an existing deterministic neutron transport code or by means of the adjoint Monte Carlo formalism from appendix B.

4.2 The variance equation with implicit capture

Implicit capture is used in practically every general purpose Monte Carlo code, usually in conjunction with Russian roulette and possibly splitting. The variance of the simulation is reduced by ensuring that more neutrons contribute to the detector response estimate, because the particles never get killed in a collision event. Particles therefore have a greater probability of scoring but can also have considerably longer lifetimes, especially in a system with low leakage.

Implicit capture is accomplished by multiplying the weight of a particle at every collision with the non-absorption probability $\kappa(P)$, to account for not terminating the particle due to absorption, and letting the history of the particle run until it exits the system. If the particle enters a collision at P, the score is recorded as $W\eta_\psi(P)$. Later the implication of Russian roulette will be discussed as a means of terminating histories of neutrons which carry a low statistical weight to regain some of the computational time lost by implementing the implicit capture scheme.

Since particles are never killed, the probability score equation contains no terminal contribution. The weight before implicit capture W is reduced to $\kappa(P)W$. The probability score equation will now also be a function of particle weight W and can be written as

$$\pi[P, W, s] = \int K_n(P \to P')\pi[P', \kappa(P)W, s - W\eta_\psi(P)]dP' \tag{4.13}$$

in which the convolution is already written out. The first moment of the score is then calculated as follows

$$\begin{aligned} M_1(P,W) &= \int_{-\infty}^{\infty} s\pi[P,W,s]ds \\ &= W\eta_\psi(P) + \int K_n(P \to P')M_1(P',\kappa(P)W)dP' \end{aligned} \tag{4.14}$$

which is not a very useful result at first glance. It should be noted however that the expected score for a particle with weight W is equal to the weight times the expected score for a particle with weight one.

$$M_1(P,W) = WM_1(P) \tag{4.15}$$

Putting this result to good use on Eq. (4.14) and dividing by W results in the first moment of the score for a simulation with implicit capture

$$M_1(P) = \eta_\psi(P) + \int K(P \to P')M_1(P')dP' \tag{4.16}$$

Eq. (4.16) shows that implicit capture does not introduce bias in the final estimate.

The second moment is evaluated in a similar fashion

$$\begin{aligned} M_2(P,W) &= \int_{-\infty}^{\infty} s^2\pi[P,W,s]ds \\ &= \int K_n(P \to P') \int_{-\infty}^{\infty} \left\{ s'^2 + 2W\eta_\psi(P) + W^2\eta_\psi^2(P) \right\} \\ &\times \pi[P',\kappa(P)W,s']ds'dP' \\ &= W^2 I_0(P) + \int K_n(P \to P')M_2(P',\kappa W)dP' \end{aligned} \tag{4.17}$$

in which $I_0(P)$ is as in Eq. (4.11).
In this particular situation $M_2(P,W) = W^2M_2(P)$, since W does not influence the transport at any point during the neutron history. This is, however, usually not the case and the reader should be mindful of this fact. Applying the result to Eq. (4.18) and dividing by W^2 yields

$$M_2(P) = I_0(P) + \kappa(P) \int K(P \to P')M_2(P')dP' \tag{4.18}$$

The statement that implicit capture reduces variance was already made clear by heuristic arguments. Eq. (4.18) however provides a sound theoretical basis for applying implicit capture as a means of reducing variance. Since $\kappa(P) \leq 1$ the second moment is reduced with respect to the analog situation, and from Eq. (4.12) thereby also the variance.

A means of estimating the increase of 'computational effort' as a result of implementing implicit capture is given in section 4.4. In the next section the application of Russian roulette and splitting is examined.

4.3 The variance equation with Russian roulette and splitting

There are numerous ways in which the Russian roulette and splitting technique can be implemented; the most common of which is treated here and in the remainder of this work. Deriving moment equations for the other versions should pose no real challenge using the formalism presented in this chapter.

A schematic of the situation is presented in Fig. 4.2. Russian roulette will be played after the weight of a particle is altered due to implicit capture; after the particle scores at a collision but before sampling the collision kernel for a new energy and direction. Whether or not the particle plays the game is determined by the Russian roulette threshold weight $W_{th}(P)$. Note that this threshold may be a function of all phase space variables. The particle subsequently either survives the Russian roulette event and emerges with a survival weight $W_s(P)$ or it is terminated. The survival weight is a multiple of the Russian roulette threshold weight.

In case of a splitting event, the particle is split into a number of particles N_{split} when its weight, after implicit capture, equals or exceeds a defined threshold weight $W_{split}(P)$. The threshold weight is again a multiple of the Russian roulette threshold weight.

The particle may experience a total of three, mutually exclusive events with probabilities dependent on the weight with which the particle enters the event and on the position in phase space at which the particle enters the collision. This weight with which the particle enters the event will be called the *pre-event* weight. Obviously, the weight after the event will be called the *post-event* weight. The three event possibilities are depicted in Table 4.1.

1.	Termination by RR; with probability $z_0(P, W)$
2.	Survival of the event; with probability $z_1(P, W)$
3.	Splitting into N_{split} fragments; with probability $z_N(P, W)$

Table 4.1: Weight window event probabilities

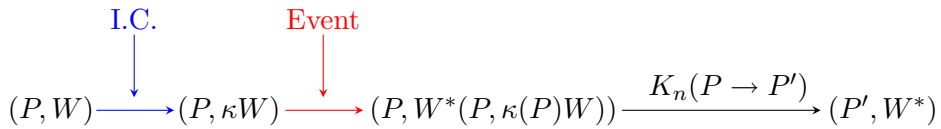

Figure 4.2: A schematic representation of the event. A neutron enters a collision at P with a weight W, experiences a weight reduction due to implicit capture and subsequently plays the event. Depending on the event outcome, the neutron is allowed to experience a new collision with a post-event weight W^* at P', the probability of which is given by the normalized transport kernel K_n.

In order to have statistically fair events, the event probabilities take the following form

$$z_1(P,W) = \begin{cases} W/W_s(P) & W \leq W_{th} \\ 1 & W_{th}(P) < W < W_{split}(P) \\ 0 & W \geq W_{split}(P) \end{cases} \tag{4.19}$$

$$z_0(P,W) = \begin{cases} 1 - W/W_s(P) & W \leq W_{th} \\ 0 & W_{th}(P) < W < W_{split}(P) \\ 0 & W \geq bW_{th}(P) \end{cases} \tag{4.20}$$

$$z_N(P,W) = \begin{cases} 0 & W \leq W_{th} \\ 0 & W_{th}(P) < W < W_{split}(P) \\ 1 & W \geq W_{split}(P) \end{cases} \tag{4.21}$$

Which makes sure that $z_0(P,W) + z_1(P,W) + z_N(P,W) = 1$.
The post-event weight is written as

$$W^*(P,W) = \begin{cases} W_s(P) & W \leq W_{th} \\ W & W_{th}(P) < W < W_{split}(P) \\ W/N_{split} & W \geq W_{split}(P) \end{cases} \tag{4.22}$$

In order to proceed it is also necessary to introduce some further notation concerning multiple convolutions. Let a repeated convolution over distribution functions have the following form.

$$\begin{aligned} &\prod_{j=1}^{N} * f_j(s) = f_1(s) * f_2(s) * ... * f_N(s) \\ &= \int \int ... \int f_N(u_{N-1}) f_{N-1}(u_{N-2}) ... f_2(u_1) \\ &\times f_1(s - u_{N-1} - u_{N-2} - ... - u_1) du_1 du_2 ... du_{N-1} \end{aligned} \tag{4.23}$$

Since we examine a particle entering a collision with weight W, the actual event is played with a pre-event weight $\kappa(P)W$ because of implicit capture. In case of a terminal event the score will be $W\eta_\psi(P)$ as before. In case of a non-terminal event the particle may proceed after the first collision and gather a score $W\eta_\psi(P) \leq s$. For a splitting event N_{split} particles may proceed with a reduced weight to gather a score $W\eta_\psi(P) \leq s$ together. With these definitions it is now possible to construct the score probability equation for a

neutron entering a collision at P with a weight W.

$$\begin{aligned}
&\pi[P,W,s] = z_0(P,\kappa(P)W)\delta(s - W\eta_\psi(P)) \\
&+ z_1(P,\kappa(P)W)\int K_n(P \to P') \\
&\times \delta(s - W\eta_\psi(P)) * \pi[P', W^*(P,\kappa(P)W), s]dP' \\
&+ z_N(P,\kappa W)\int K_n(P \to P') \\
&\times \delta(s - W\eta_\psi(P)) * \prod_{j=1}^{N_{split}} *\pi[P', W^*(P,\kappa(P)W), s]dP'
\end{aligned} \tag{4.24}$$

In order to proceed with the first moment we will need that the expectation of multiple convolutions over probability density functions add, Micoulaut [1976]

$$\begin{aligned}
\langle s\rangle_{f_1 * f_2 * \ldots * f_N} &= \int_{-\infty}^{\infty} s \prod_{j=1}^{N} * f_j(s)ds \\
&= \langle s\rangle_{f_1} + \langle s\rangle_{f_2} + \ldots + \langle s\rangle_{f_N} = \sum_{j=1}^{N} \langle s\rangle_{f_j}
\end{aligned} \tag{4.25}$$

Applying this result to Eq. (4.24) we can evaluate the first moment or expected score for a particle entering a collision at P with weight W

$$\begin{aligned}
&M_1(P,W) = \int_{-\infty}^{\infty} s\pi[P,W,s]ds = z_0(P,\kappa(P)W)W\eta_\psi(P) \\
&+ z_1(P,\kappa(P)W)\int K_n(P \to P')\int_{-\infty}^{\infty} s\delta(s - W\eta_\psi(P)) \\
&* \pi[P', W^*(P,\kappa(P)W), s']ds'dP' \\
&+ z_N(P,\kappa(P)W)\int K_n(P \to P')\int_{-\infty}^{\infty} s\delta(s - W\eta_\psi(P)) \\
&* \prod_{j=1}^{N_{split}} *\pi[P', W^*(P,\kappa(P)W), s]dsdP' \\
&= \eta_\psi(P)W + \{z_1(P,\kappa(P)W) + z_N(P,\kappa(P)W)N_{split}\} \\
&\times \int K_n(P \to P')M_1(P', W^*(P,\kappa(P)W))dP'
\end{aligned} \tag{4.26}$$

This result can be simplified further by applying the event-probability definitions and the fact that $M_1(P,W) = WM_1(P)$. Observe that we can write

$$\{z_1(P,\kappa(P)W) + z_N(P,\kappa(P)W)N_{split}\}\, W^*(P,\kappa(P)W) = \kappa(P)W \tag{4.27}$$

from which it follows, after division by W, that Eq. (4.26) can be written as

$$M_1(P) = \eta_\psi(P) + \int K(P \to P')M_1(P') \tag{4.28}$$

This result was to be expected, since modification of the analog game should not lead to a different expectation value for the score.

The second moment or expected score squared for a neutron entering a collision at P with weight W is written as

$$\begin{aligned}
M_2(P,W) &= \int_{-\infty}^{\infty} s^2 \pi[P,W,s]ds \\
&= z_0(P,\kappa(P)W) \int s^2 \delta(s - W\eta_\psi(P))ds \\
&+ z_1(P,\kappa(P)W) \int K_n(P \to P') \\
&\times \int_{-\infty}^{\infty} s^2 \delta(s - W\eta_\psi(P)) * \pi[P', W^*(P,\kappa(P)W), s]dsdP' \\
&+ z_N(P,\kappa(P)W) \int K_n(P \to P') \\
&\times \int_{-\infty}^{\infty} s^2 \delta(s - W\eta_\psi(P)) * \prod_{j=1}^{N_{split}} *\pi[P', W^*(P,\kappa(P)W), s]dsdP'
\end{aligned} \tag{4.29}$$

In order to proceed, some further investigation of the convolutions in the second and third terms is needed. The second moment of a multiple convolution takes the following form [Micoulaut, 1976]

$$\langle s^2 \rangle_{f_1 * f_2 * \ldots * f_N} = \sum \frac{2!}{j_1! j_2! \ldots j_N!} \langle s^{j_1} \rangle_{f_1} \langle s^{j_2} \rangle_{f_2} \ldots \langle s^{j_N} \rangle_{f_N} \tag{4.30}$$

$$\text{where the summation is such that} \quad \sum_{i=1}^{N} j_i = 2$$

For easy notation call

$$\begin{aligned}
f(s) &\equiv \pi[P', W^*(P,\kappa(P)W), s] \\
g(s) &\equiv \prod_{j=1}^{N_{split}} *\pi[P', W^*(P,\kappa(P)W), s] \\
h(s) &\equiv \delta(s - W\eta_\psi(P))
\end{aligned}$$

and note that the distributions $f(s)$ are the same. With these conventions the result of Eq. (4.30) can be put to work on the second and third terms of Eq. (4.29)

$$\begin{aligned}
\langle s^2 \rangle_g &= \int s^2 g(s)ds = N_{split} \langle s^2 \rangle_f + N_{split}(N_{split} - 1)\langle s \rangle_f^2 \\
\langle s^2 \rangle_{h*g} &= \langle s^2 \rangle_h + \langle s^2 \rangle_g + 2\langle s \rangle_h \langle s \rangle_g
\end{aligned}$$

Further manipulation, returning to the usual notation and using the definitions of the moment equations yields

$$\begin{aligned}\langle s^2\rangle_{h*g} &= W^2\eta_\psi^2(P)\\ &+ N_{split}M_2(P', W^*(P,\kappa(P)W))\\ &+ N_{split}(N_{split}-1)M_1^2(P', W^*(P,\kappa(P)W))\\ &+ 2W\eta_\psi(P)N_{split}M_1(P', W^*(P,\kappa(P)W))\end{aligned} \tag{4.31}$$

and for the second term in Eq. (4.29) we can write

$$\begin{aligned}\langle s^2\rangle_{h*f} &= W^2\eta_\psi^2(P)\\ &+ M_2(P', W^*(P,\kappa(P)W))\\ &+ 2W\eta_\psi(P)M_1(P', W^*(P,\kappa(P)W))\end{aligned} \tag{4.32}$$

Using the results from Eq. (4.31) and Eq. (4.32) in Eq. (4.29) we arrive at

$$\begin{aligned}M_2(P,W) &= W^2\eta_\psi^2(P)\left\{z_0(P,\kappa(P)W) + z_1(P,\kappa(P)W) + z_N(P,\kappa(P)W)\right\}\\ &+ 2W\eta_\psi(P)\left\{z_1(P,\kappa(P)W) + z_N(P,\kappa(P)W)N_{split}\right\}\\ &\times\int K_n(P\to P')M_1(P', W^*(P,\kappa(P)W))dP'\\ &+ \left\{z_1(P,\kappa(P)W) + z_N(P,\kappa(P)W)N_{split}\right\}\\ &\times\int K_n(P\to P')M_2(P', W^*(P,\kappa(P)W))dP'\\ &+ z_N(P,\kappa(P)W)N_{split}(N_{split}-1)\int K_n(P\to P')M_1^2(P', W^*(P,\kappa(P)W))dP'\end{aligned}$$

We can simplify this result further by using the fact that $M_1(P,W) = WM_1(P)$, Eq. (4.27) and the definition of $I_0(P)$ from Eq. (4.11) to arrive at the final expression for the second moment of the score of a neutron entering a collision at P with weight W

$$\begin{aligned}M_2(P,W) &= W^2I_0(P) + \left\{z_1(P,\kappa(P)W) + z_N(P,\kappa(P)W)N_{split}\right\}\\ &\times\int K_n(P\to P')M_2(P', W^*(P,\kappa(P)W))dP'\\ &+ z_N(P,\kappa(P)W)W^2\frac{N_{split}-1}{N_{split}}\kappa(P)\int K(P\to P')M_1^2(P')dP'\end{aligned} \tag{4.33}$$

in which, for the last term, the fact has been used that in case of a splitting event the post-event weight will always be equal to $\kappa(P)W/N_{split}$.

Some remarks can be made with respect to Eq. (4.33). First and foremost it should be noted that the first integral contains the post event weight $W^*(P,\kappa(P)W)$ which will generally not be equal to W. This poses a problem since in this form Eq. (4.33) is not self-consistent and therefore has no direct

solution. In the implicit capture situation this wasn't an issue since we were able to write $W_2(P,W) = W^2 M_2(P)$ (the event outcome was predetermined if you will) but with Russian roulette and splitting the outcome of the event determines the post-event weight and therefore

$$M_2(P,W) \neq W^2 M_2(P) \tag{4.34}$$

If more information about the simulation is available it is however possible to find solutions. Some examples will be given in chapter 5.

It is also possible to obtain the equations for the second moment with only implicit capture, only Russian roulette or analog simulation from Eq. (4.33) by choosing the correct post-event weight and event probabilities. If, for example, we let $W_{split} \to \infty$ the situation for a simulation with only Russian roulette is obtained.

In a 'regular' simulation one would start a particle history with a weight equal to one. The Russian roulette threshold is then some fraction of this starting weight and since the other weight window thresholds are related to the RR threshold it is exactly this and only this ratio that matters. This opens the possibility to maintain W as a variable. Varying W in stead of the threshold W_{th} leads to more appealing results and since it is entirely equivalent it is this strategy that we'll adopt. In order to account for not starting the particle with a weight one, the variance equation, now a function of W, becomes

$$\mathrm{Var}(W) = \int S_1(P) \frac{M_2(P,W)}{W^2} dP - R^2 \tag{4.35}$$

The next section deals with the estimation of computational effort, necessary to arrive at an expression for the efficiency of a simulation.

4.4 The number of collisions equation

One would generally use the computational time taken by the simulation, together with the variance, as a measure for efficiency. From a theoretical point of view there is no way to write an equation for the computational time since it depends on too many factors.

One option is to use the expected number of collisions during a particle history for a particle entering a collision at P. With the framework set up in the previous sections, deriving expressions will prove rather easy. Suppose we define $\pi_c[P,W,m]$ as the probability for a particle entering a collision at P to have, together with its progeny, exactly (since it represents a discrete pdf in

this case) m collisions. The probability collision equations then reads

$$\begin{aligned}\pi_c[P,W,m] &= z_0(P,\kappa(P)W)\delta(m-\varsigma(P)) + z_1(P,\kappa(P)W)\\ &\times \int K_n(P\to P')\delta(m-\varsigma(P)) * \pi[P',W^*(P,\kappa(P)W),m]dP'\\ &+ z_N(P,\kappa W)\int K_n(P\to P')\\ &\times \delta(m-\varsigma(P)) * \prod_{j=1}^{N_{split}} *\pi[P',W^*(P,\kappa(P)W),m]dP' \end{aligned} \tag{4.36}$$

in which the definitions of the different quantities are as in section 4.3. The 'source' $\varsigma(P)$ in this case is not strictly a function of all phase space variables since

$$\varsigma(P) = \begin{cases} 1 & \boldsymbol{r}\in V \\ 0 & \boldsymbol{r}\notin V \end{cases} \tag{4.37}$$

no matter what energy or direction, the particle will collide. We could have written the source as unity, but then the normalization trick, where we imagine the system surrounded by a purely absorbing medium, for the transition kernel no longer holds because the integral should then strictly be taken over the system volume. Writing the source like this retains the generality.

The convolutions are now discrete rather than continuous

$$f(m) * g(m) = \sum_{l=-\infty}^{\infty} f(l)g(m-l) \tag{4.38}$$

Using these conventions and, unfortunately, again a new symbol, the expected number of collision for a particle entering a collision at P with a certain weight W can be written as

$$\begin{aligned} n(P,W) &= \sum_{m=-\infty}^{\infty} m\pi_c[P,W,m] \\ \text{with} \quad & \pi_c[P,W,m] = 0 \quad \text{for} \quad m\le 0 \\ \text{and} \quad & \sum_{m=-\infty}^{\infty}\pi_c[P,W,m] = 1 \end{aligned} \tag{4.39}$$

also note that the event probabilities add up to one and that nothing changes regarding the expectation of multiple convolutions over independent probability mass functions

$$\langle m\rangle_{f_1*f_2*\ldots*f_N} = \sum_{m=-\infty}^{\infty} m\prod_{j=1}^{N} *f_j(m) = \sum_{j=1}^{N}\langle m\rangle_{f_j}$$

Using these results on Eq. (4.36), the expected number of collisions for a particle entering a collision at P with weight W is written as

$$n(P,W) = \varsigma(P) + \{z_1(P,\kappa(P)W) + z_N(P,\kappa(P)W)N_{split}\} \times \int K_n(P \to P')n(P', W^*(P,\kappa(P)W))dP' \tag{4.40}$$

The average value of this quantity for particles entering their first collisions at P with a certain weight W represents the total expected number of collisions for a neutron history

$$N_c(W) = \int S_1(P)n(P,W)dP \tag{4.41}$$

in which $S_1(P)$ accounts for the probability that a source particle may never collide. The issue that a particle starts a history with a weight not equal to one is of no influence on N_c since regardless of the value W, the 'score' for a collision will simply be one. It is again only the ratio between the threshold weight and W that matters.

In the case where W for example doesn't influence the transport, i.e. only implicit capture or analog transport, the weight dependence may de dropped completely. For the implicit capture situation the equation then becomes

$$n(P) = \varsigma(P) + \int K_n(P \to P')n(P')dP' \tag{4.42}$$

and for the analog situation the equation becomes

$$n(P) = \varsigma(P) + \int K(P \to P')n(P')dP' \tag{4.43}$$

Analyzing Eq. (4.42) and Eq. (4.43) shows the exact opposite of what happened for the second moment. For the number of collisions we see that there is now a $\kappa(P)^{-1}$ in front of the integral in Eq. (4.42), stemming from the normalization of the kernel. Since $\kappa(P) \leq 1$ the number of collisions will increase, as was to be expected, with respect to the analog situation.

4.5 Efficiency or cost of a simulation

There a two main concerns when performing a Monte Carlo simulation: the variance should be as low as possible and the computational time should be as short as possible. These criteria were summarized in the 'Figure of merit', which is calculated a posteriori from the simulation data. Since this thesis is concerned with calculating things a priori we define an alternative to the FOM which cancels out the human factor in the equation (bad programming

that leads to long T) and write

$$\begin{aligned} f(W) &= \mathrm{Var}(W) N_c(W) \\ &= \left\{ \int S_1(P) \frac{M_2(P,W)}{W^2} dP - R^2 \right\} \int S_1(P) n(P,W) dP \end{aligned} \tag{4.44}$$

Minimizing this cost function will lead to the best choice of weight window thresholds. This is of course easier said than done since Eq. (4.44) may depend on a variety of parameters, which may in turn be dependent on all phase space variables and of course on W. For very simple situations one may find an analytical expression for the minimum as will be shown in chapter 6.

4.6 Implications of source biasing

In a simulation where the source is biased according to the principles presented in section 3.2, the initial particle weight is altered accordingly. This is irrespective of the moment definitions since they represent expected values for a neutron entering a collision (or starting a flight as we will see in the next section) with a weight W. We only have to account for the fact that the particle enters the $first$ collision with some weight $\overline{W}(P)$. This leads to the following definition for the variance

$$\mathrm{Var}(W) = \int \overline{S_1}(P) \frac{M_2(P, \overline{W}(P))}{W^2} dP - R^2 \tag{4.45}$$

Remember that the division by W^2 came from the fact we allowed to vary the initial weight W in stead of the threshold weight W_{th}, this might lead one to think that we should therefore divide by $\overline{W}^2(P)$. This is not the case since $\overline{W}(P)$ compensates for not sampling the true source distribution $S_1(P)$, which is a different thing.

In practice, the physical source is actually biased, which in turn leads to a biased source of first collisions $\overline{S_1}(P)$. From Eq. (2.22) we find that

$$\overline{S_1}(P) = \int \overline{S}(P) T(\boldsymbol{r}' \rightarrow \boldsymbol{r}, E, \boldsymbol{\Omega}) dV' \tag{4.46}$$

and therefore we have

$$\overline{W}(P) = W \frac{S_1(P)}{\overline{S_1}(P)} \tag{4.47}$$

which can be a challenging expression to evaluate. It is of course also possible to bias the source of first collisions directly, but in practice this will not happen.

For the total expected number of collisions we have

$$N_c(W) = \int \overline{S_1}(P) n(P, \overline{W}(P)) dP \tag{4.48}$$

which shows already that for an analog or implicit capture situation (where N_c is independent of weight), source biasing may have a profound influence on the number of collisions during a particle history.

4.7 Track-length estimators

The track length of a neutron will depend on the coordinate at which the particle starts a flight and the coordinate at which it enters a subsequent collision. Since an expression for the variance should encompass the whole history of the neutron, there is no point in looking at a neutron entering its first collision since there might be a score resulting from the first flight. It is therefore necessary to look at a neutron starting a flight. A schematic of the situation is given in Fig. 4.3. Although usually the track-length estimator will not depend on all phase space variables we will state it as follows to keep matters as general as possible

$$\eta_\psi(\boldsymbol{r}, \boldsymbol{r}', E, \boldsymbol{\Omega}) = \eta_\psi(P, P_e) \tag{4.49}$$

It is important to note that, given a proper choice of scoring function $\eta_\psi(P_e)$, we can obtain an expression for a collision estimator as well, only this time for a neutron starting a flight.

The neutron will start a flight at P with weight W, make a transition to $P_e = (\boldsymbol{r}', E, \boldsymbol{\Omega})$ and score, if $P_e \in V$, an amount $W\eta_\psi(P, P_e)$. At P_e the neutron will first be subjected to implicit capture and subsequently play the event with weight $\kappa(P_e)W$. If the event is non-terminal (either from splitting or survival of the event) the particle(s) may obtain a new energy and direction and experience a new flight from P'. We therefore write the probability score

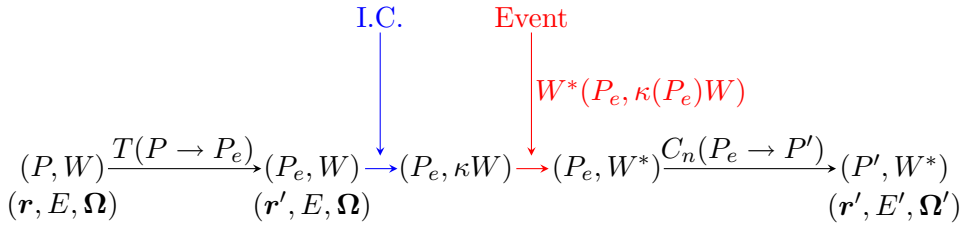

Figure 4.3: A schematic representation of the positions in phase space at which different interactions take place for a neutron starting a flight. The event takes place at P_e.

equation as follows

$$\begin{aligned}\pi_{tl}[P,W,s] &= \int T(P\rightarrow P_e)z_0(P_e,\kappa(P_e)W)\delta(s-W\eta_\psi(P,P_e))dV' \\ &+ \int T(P\rightarrow P_e)z_1(P_e,\kappa(P_e)W)\delta(s-W\eta_\psi(P,P_e)) \\ &* \int\int C_n(P_e\rightarrow P')\pi_{tl}[P',W^*(P_e,\kappa(P_e)W),s]dP' \\ &+ \int T(P\rightarrow P_e)z_N(P_e,\kappa(P_e)W)\delta(s-W\eta_\psi(P,P_e)) \\ &* \int\int C_n(P_e\rightarrow P')\prod_{j=1}^{N_{split}} *\pi_{tl}[P',W^*(P_e,\kappa(P_e)W),s]dP' \end{aligned} \tag{4.50}$$

from which the first moment can be obtained using the convolution expectations of section 4.3

$$\begin{aligned}M_{1tl}(P) &= \int T(P\rightarrow P_e)\eta_\psi(P,P_e)dV' \\ &+ \int L(P\rightarrow P')M_{1tl}(P')dP'\end{aligned} \tag{4.51}$$

and from Eq. (2.39) and Eq. (2.36) we see that we have derived the adjoint emission density or adjoint flux because

$$M_{1tl}(P) = \eta_\chi(P,P_e) + \int L(P\rightarrow P')M_{1tl}(P')dP' = \chi^*(P) \tag{4.52}$$

and that the estimate will therefore be unbiased. The second moment of the score for a particle starting a flight reads

$$\begin{aligned}M_{2tl}(P,W) &= W^2\int T(P\rightarrow P_e)\eta_\psi(P,P_e) \\ &\times\left(\eta_\psi(P,P_e)+2\int\int C(P_e\rightarrow P')M_{1tl}(P')\right)dP' \\ &+ \int T(P\rightarrow P_e)z_N(P_e,\kappa(P_e)W)W^2\frac{N_{split}-1}{N_{split}}\kappa(P_e) \\ &\times\int\int C(P_e\rightarrow P')M_{1tl}^2(P')dP' \\ &+ \int T(P\rightarrow P_e)\left\{z_1(P_e,\kappa(P_e)W)+z_N(P_e,\kappa(P_e)W)N_{split}\right\} \\ &\times\int\int C_n(P_e\rightarrow P')M_{2tl}(P',W^*(P_e,\kappa(P_e)W))dP'\end{aligned} \tag{4.53}$$

The 'immediate payoff' can this time not be simplified further due to the fact that a neutron will first have to make a transition before possibly scoring. Asides from this fact, Eq. (4.33) and Eq. (4.53) bear a striking resemblance.

The second moment term in the variance expression is this time evaluated for particles starting their first flight

$$\mathrm{Var}(W) = \int S(P) \frac{M_{2tl}(P, W)}{W^2} dP - R^2 \tag{4.54}$$

For sake of generality, if the physical source is biased, the variance can be written as

$$\mathrm{Var}(W) = \int \overline{S}(P) \frac{M_{2tl}(P, \overline{W}(P))}{W^2} dP - R^2 \tag{4.55}$$

These expressions are actually more generally applicable than the variance expressions obtained in the previous sections because, given a proper choice of scoring function, Eq. (4.54) and Eq. (4.55) hold for a collision estimator as well. From a practical point of view it is also convenient that the variance expressions now contain the physical source $S(P)$ in stead of the source of first collisions $S_1(P)$. Solving Eq. (4.53) is however going to be more challenging than solving Eq. (4.33).

The expected number of collisions for a neutron starting a flight with a weight W can be written as

$$\begin{aligned} n_{tl}(P, W) = & \int T(P \to P_e) \varsigma_0(P_e) dV' \\ & + \int T(P \to P_e) \left\{ z_1(P_e, \kappa(P_e)W) + z_N(P_e, \kappa(P_e)W) N_{split} \right\} \\ & \times \int C_n(P_e \to P') n_{tl}(P', W^*(P_e, \kappa(P_e)W)) dP' \end{aligned} \tag{4.56}$$

and the total expected number of collision for a particle leaving the biased source with a biased weight $\overline{W}(P) = S(P)/\overline{S}(P)$ is written as

$$N_c(W) = \int \overline{S}(P) n(P, \overline{W}(P)) dP \tag{4.57}$$

Of course, this results should equal the result from Eq. (4.48), provided that both are evaluated with the same physical source distribution.

The necessary tools are now present to compare and optimize a variety of simulation approaches and chapter 5 and 6 will give some examples of how the theory may be used.

Chapter 5

Analytic investigation

This chapter deals with the analytic calculation of efficiency and variance for two simple systems. To allow for analytic solutions, a framework is set up first to deal with the equations derived in previous chapters. A simplified neutron transport model will be introduced, which restricts neutrons to move in only two directions. Under these restrictions it is demonstrated how an integral equation may be transformed into a differential equation which allows to find solutions more readily.

Once the framework has been set up, the moment and number of collisions equations are discussed and solved for the two systems. For non-analog simulation the possibility of optimization is explored by stating the second moment and number of collisions equation in terms of simulation parameters like the Russian roulette threshold weight. From these functions, the cost function can be constructed which may be minimized to obtain an optimal choice for weight window thresholds and/or optimal source biasing functions.

In section 5.3 the introduction is put to good use on a one-group, finite slab system. A full analysis is given of the solution to the transport, moment and number of collisions equations for arbitrary system parameters. From these expressions it is shown how a minimization of the cost function may be accomplished.

In section 5.3 the effects of two groups on the moment and number of collisions equations are explored. In order to not over complicate matters, the system is assumed infinite. The effects of different weight windows in each group are shown and the possibility of source biasing is explored.

The following derivations may be somewhat exhausting. It is the author's belief however that this is necessary in order to fully appreciate the complexity of the equations involved, even for these simple systems.

5.1 The two-directional model for neutron transport

The key feature of the two-directional model as proposed by [Hoogenboom, 2008] is that neutrons are only allowed to move in two directions; either in the positive or the negative direction. This rather extensive simplification of reality brings with it the possibility of analytical solutions to the transport equations, which in turn can be used to validate theory and numerical approximations. Unlike the diffusion approximation, two-directional transport is also suited for Monte Carlo.

In order to gain insight and to have expressions ready for finding solutions later on it will be necessary to cast familiar concepts, like kernels and cross sections, into the two directional approach. It should be noted that at most we are considering a piecewise homogeneous system, so the positional dependence of cross sections can be dropped from now on. Full solutions to the transport equations in such piecewise homogeneous systems can be found by matching coefficients. In section 5.2, the interface conditions necessary to enable matching between different regions will be shown.

We encountered four kernels in the equations governing the transport of the different physical quantities of interest in Monte Carlo simulations. The kernels $L(P' \to P)$, $K(P' \to P)$ and their adjoint counterparts $L(P \to P')$ and $K(P \to P')$. In the two directional approach, a point in phase space P can be represented by the following variables: x represents the position, $\mu = \pm 1$ the cosine of the scattering angle and g a particular energy group.[1]

The procedure is demonstrated for the kernel $K(P' \to P)$ and its transpose. From these expressions it will be clear how to write the other kernel $L(P' \to P)$ and its transpose.

The kernels $K(P' \to P)$ and $K(P \to P')$

Since neutrons are only allowed to move in two directions and the energy is discretized, the kernel $K(P' \to P)$ now represents the possibility for a neutron entering a collision at x' with an energy in group g' and a direction μ', which is either forward or backward, to have a change in energy to group g and a change in direction to μ and afterwards a flight to the next collision site x.

$$K(P' \to P) = C(x', g' \to g, \mu' \to \mu) T(x' \to x, g, \mu) \tag{5.1}$$

in which it should be noted that, due to the piecewise continuity, the spatial dependence of the collision kernel may be dropped. The collision kernel, Eq.

[1] Strictly we could maintain energy as a continuous variable but for practical reasons we will use the group-wise approach most customary to nuclear reactor simulations.

(2.17), can be written out further in the following way

$$C(g' \to g, \mu' \to \mu) = \frac{\Sigma_s^{g'}}{\Sigma_t^{g'}} p(g' \to g, \mu' \to \mu) \tag{5.2}$$

in which, for the systems under consideration, a scattering event is assumed.[2] $p(g' \to g, \mu' \to \mu)$ represents the probability of scattering from $g' \to g$ and from $\mu' \to \mu$, given that there is a scattering event at x'.

The joint probability $p(g' \to g, \mu' \to \mu)$ can be written more conveniently in terms of a conditional probability

$$p(g' \to g, \mu' \to \mu) = p(\mu' \to \mu | g' \to g) p(g' \to g) \tag{5.3}$$

The probability of scattering from group $g' \to g$ can be expressed in terms of scattering cross sections

$$p(g' \to g) = \frac{\Sigma_s^{g'g}}{\sum_{g''} \Sigma_s^{g'g''}} = \frac{\Sigma_s^{g'g}}{\Sigma_s^{g'}} \tag{5.4}$$

What remains is to find an expression for $p(\mu' \to \mu | g' \to g)$.

Given a scattering event from group $g' \to g$ there are two possible outcomes for the direction; $\mu = \pm 1$. So let us define the following differential scattering cross section

$$\Sigma_s^{g'g}(\mu' \to \mu) = \begin{cases} \Sigma_{\rightarrow}^{g'g} & \mu'\mu = +1 \\ \Sigma_{\leftarrow}^{g'g} & \mu'\mu = -1 \end{cases} \tag{5.5}$$

The total scattering cross section, going from group $g' \to g$ is then

$$\Sigma_s^{g'g} = \Sigma_{\rightarrow}^{g'g} + \Sigma_{\leftarrow}^{g'g} \tag{5.6}$$

and the average scattering cosine can be defined as

$$\bar{\mu}_0^{g'g} = \frac{\Sigma_{\rightarrow}^{g'g} - \Sigma_{\leftarrow}^{g'g}}{\Sigma_s^{g'g}} \tag{5.7}$$

After some manipulation, expressing the cross sections $\Sigma_{\rightarrow}^{g'g}$ and $\Sigma_{\leftarrow}^{g'g}$ in terms of the average scattering cosine using Eq. (5.6) and Eq. (5.7), the conditional probability can be expressed as

$$p(\mu' \to \mu | g' \to g) = \frac{1}{2}(1 + \mu'\mu \bar{\mu_0}^{g'g}) \tag{5.8}$$

[2]Interactions like fission may produce neutrons in P but it will be cumbersome to retain these interactions since the system is assumed non-fissile.

Finally the collision kernel can be expressed as

$$C(g' \to g, \mu' \to \mu) = \frac{\Sigma_s^{g'g}}{2\Sigma_t^{g'}}(1 + \mu'\mu\bar{\mu}_0^{g'g}) \tag{5.9}$$

There are some limitations regarding the different cross sections in order to have a physical system. These limitations can be summarized as follows

$$\Sigma_s^{g'} = \sum_g \Sigma_s^{g'g} \tag{5.10}$$

$$\Sigma_t^{g'} = \Sigma_s^{g'} + \Sigma_a^{g'} \tag{5.11}$$

$$|\bar{\mu}_0^{g'g}| \leq 1 \tag{5.12}$$

Also, from now on, if the word isotropic is used it will refer to the average scattering cosine being zero in the two directional approach: $\bar{\mu}_0^{g'g} = 0$. This means that scattering forward or backward is equally likely.

Transitions to other collision sites are governed by the transition kernel $T(x' \to x, g, \mu)$, which can be expressed as

$$T(x' \to x, g, \mu) = \begin{cases} \mu = 1 & \begin{cases} \Sigma_t^g e^{-\Sigma_t^g(x-x')} & x > x' \\ 0 & x < x' \end{cases} \\ \mu = -1 & \begin{cases} \Sigma_t^g e^{-\Sigma_t^g(x'-x)} & x < x' \\ 0 & x > x' \end{cases} \end{cases} \tag{5.13}$$

To complete matters, the transport kernel in the two-directional approach can be written as

$$K(P' \to P) = \begin{cases} \mu = 1 & \begin{cases} \frac{\Sigma_s^{g'g}}{2\Sigma_t^{g'}}(1 + \mu'\bar{\mu}_0^{g'g})\Sigma_t^g e^{-\Sigma_t^g(x-x')} & x > x' \\ 0 & x < x' \end{cases} \\ \mu = -1 & \begin{cases} \frac{\Sigma_s^{g'g}}{2\Sigma_t^{g'}}(1 - \mu'\bar{\mu}_0^{g'g})\Sigma_t^g e^{-\Sigma_t^g(x'-x)} & x < x' \\ 0 & x > x' \end{cases} \end{cases} \tag{5.14}$$

The adjoint kernel is the transpose of the forward kernel; effectively all the primes reverse so we can be brief about the derivation and simply state the full kernel. Be mindful though that when doing adjoint Monte Carlo, one adopts a different approach as can be seen in appendix B.

$$K(P \to P') = \begin{cases} \mu' = 1 & \begin{cases} \frac{\Sigma_s^{gg'}}{2\Sigma_t^g}(1 + \mu\bar{\mu}_0^{gg'})\Sigma_t^{g'} e^{-\Sigma_t^{g'}(x'-x)} & x' > x \\ 0 & x' < x \end{cases} \\ \mu' = -1 & \begin{cases} \frac{\Sigma_s^{gg'}}{2\Sigma_t^g}(1 - \mu\bar{\mu}_0^{gg'})\Sigma_t^{g'} e^{-\Sigma_t^{g'}(x-x')} & x' < x \\ 0 & x' > x \end{cases} \end{cases} \tag{5.15}$$

Sources and other two-directional quantities

Quantities like the collision density or the source of first collisions have two components; one in the positive (+) and one in the negative (−) direction. Generally speaking, the 'total' group-wise quantity in the forward case (meaning total flux in some group, total collision density in some group, total source etc.) is the sum over the two angles of the group-wise angular quantities. More explicitly, for the forward source density S we have

$$S(x,g) = S^g_+(x) + S^g_-(x) \tag{5.16}$$

in which some convenient notation has been introduced.

Adjoint quantities, like the moments, the adjoint emission density and scoring functions have a somewhat different interpretation. The total quantity, irrespective of direction, in some group is the average of the angular quantities rather than the sum. More explicitly, for the second moment $M_2(x,g)$ we have

$$M_2(x,g) = \frac{1}{2}\left(M^g_{2+}(x) + M^g_{2-}(x)\right) \tag{5.17}$$

It is also possible, much like in the case of 'regular' transport theory, to define a net current quantity which we'll state here as J_A, with the subscript A indicating the quantity of interest. The emission current, as an example, is then defined as

$$J_\chi(x,g) = \chi^g_+(x) - \chi^g_-(x) \tag{5.18}$$

In a similar fashion one could proceed to sum or average over the different groups but this is trivial and generally one is more interested in group-wise quantities anyhow.

5.2 Equivalent differential equations

In this section an example is given of how a solution to the integral equations of chapters 2 and 4 can be obtained. Under the restrictions of the two-directional model, the integral kernels are such that a solution can be obtained by transforming into a differential equation that can be solved, provided proper boundary conditions.

As an example of how an equivalent differential equation can be derived, let us look at the importance function $\chi^*(P)$, Eq. (2.36), which can be rewritten in the two-directional approach

$$\chi^{*g}(x,\mu) = \eta^g_\chi(x,\mu) + \sum_{\mu'}\sum_{g'}\int L(P \to P')\chi^{*g'}(x',\mu')dx' \tag{5.19}$$

which leads, using the kernel definition of Eq. (5.15), with some modification, and the definitions of current and total group-wise quantities, to an angular equation pair

$$\chi_+^{*g}(x) = \eta_{\chi+}^g(x) + \sum_{g'} \int_x^b \Sigma_s^{gg'} e^{-\Sigma_t^g(x'-x)} \left\{ \chi^{*g'}(x') + \bar{\mu}_0^{gg'} J_{\chi^*}^{g'}(x') \right\} dx' \tag{5.20}$$

$$\chi_-^{*g}(x) = \eta_{\chi-}^g(x) + \sum_{g'} \int_a^x \Sigma_s^{gg'} e^{-\Sigma_t^g(x-x')} \left\{ \chi^{*g'}(x') - \bar{\mu}_0^{gg'} J_{\chi^*}^{g'}(x') \right\} dx' \tag{5.21}$$

in which a, b are the boundaries of the system. Strictly speaking, the cross sections may still depend on position but this dependence will at most be region-wise so one can first state the differential equation for a region in which the cross sections are constant and later match coefficients.

In order to proceed to a differential equation we have to take the derivative of Eq. (5.20) and Eq. (5.21) with respect to position.

$$\frac{d\chi_+^{*g}(x)}{dx} = \frac{d\eta_{\chi+}^g(x)}{dx} - \sum_{g'} \Sigma_s^{gg'} \left(\chi^{*g'}(x) + \bar{\mu}_0^{gg'} J_{\chi^*}^{g'}(x) \right) + \Sigma_t^g \left(\chi_+^g(x) - \eta_{\chi+}^g(x) \right) \tag{5.22}$$

$$\frac{d\chi_-^{*g}(x)}{dx} = \frac{d\eta_{\chi-}^g(x)}{dx} + \sum_{g'} \Sigma_s^{gg'} \left(\chi^{*g'}(x) - \bar{\mu}_0^{gg'} J_{\chi^*}^{g'}(x) \right) - \Sigma_t^g \left(\chi_-^g(x) - \eta_{\chi-}^g(x) \right) \tag{5.23}$$

in which the Leibniz differentiation rule for integrals has been used, [Christiano, 1959]

$$\frac{d}{dx} \int_{a(x)}^{b(x)} f(x,x')dx' = f(x,b(x))b'(x) - f(x,a(x))a'(x) + \int \frac{\partial}{\partial x} f(x,x')dx' \tag{5.24}$$

From Eq. (5.22) and Eq. (5.23) we can obtain the derivatives of the total

group-wise quantity and the current by summing or subtracting respectively.

$$\frac{d\chi^{*g}(x)}{dx} = \frac{d\eta^g_\chi(x)}{dx} + \Sigma^g_{tr} J^g_{\chi^*}(x) - \Sigma^g_t J^g_{\eta_\chi}(x) - \sum_{g' \neq g} \Sigma^{gg'}_s \bar{\mu}^{gg'}_0 J^{g'}_{\chi^*}(x) \tag{5.25}$$

$$\frac{dJ^g_{\chi^*}(x)}{dx} = \frac{dJ^g_{\eta_\chi}(x)}{dx} + \Sigma^g_r \chi^{*g}(x) - \Sigma^g_t \eta^g_\chi(x) - \sum_{g' \neq g} \Sigma^{gg'}_s \chi^{*g'}(x) \tag{5.26}$$

in which we've defined the transport cross section as

$$\Sigma^g_{tr} = \Sigma^g_t - \bar{\mu}^{gg}_0 \Sigma^{gg}_s \tag{5.27}$$

and the removal cross section as

$$\Sigma^g_r = \Sigma^g_t - \Sigma^{gg}_s \tag{5.28}$$

All that is left now is taking the derivative of Eq. (5.25) and using Eq. (5.26) to arrive at the second order non-homogeneous differential equation, equivalent to Eq. (2.36) in the two directional approach.

$$\frac{d^2\chi^{*g}(x)}{dx^2} - k^2_g \chi^{*g}(x) = \frac{d^2\eta^g_\chi(x)}{dx^2} - \bar{\mu}^{gg}_0 \Sigma^{gg}_s \frac{dJ^g_{\eta_\chi}(x)}{dx} - \Sigma^g_t \Sigma^g_{tr} \eta^g_\chi(x) - \sum_{g' \neq g} \Sigma^{gg'}_s \left\{ \Sigma^g_{tr} \chi^{*g'}(x) + \bar{\mu}^{gg'}_0 \frac{dJ^{g'}_{\chi^*}(x)}{dx} \right\} \tag{5.29}$$

in which

$$k_g = \sqrt{\Sigma^g_{tr} \Sigma^g_r} \tag{5.30}$$

Once solutions have been obtained for the group which receives no inscatter, the lowest energy group for the adjoint quantity, the angular importances can be calculated using Eq. (5.26)

$$\chi^{*g}_\pm(x) = \chi^{*g}(x) \pm J^g_{\chi^*}(x) = \chi^{*g}(x) \pm \frac{1}{\Sigma^g_{tr}} \left\{ \frac{d\chi^{*g}(x)}{dx} - \frac{d\eta^g_\chi(x)}{dx} + \Sigma^g_t J^g_{\eta_\chi}(x) - \sum_{g' \neq g} \Sigma^{gg'}_s \bar{\mu}^{gg'}_0 J^{g'}_{\chi^*}(x) \right\} \tag{5.31}$$

Boundary and interface conditions

For a unique solution to Eq. (5.29), both boundary and interface conditions are needed. The procedure for deriving these conditions is described below.

The vacuum condition at the boundary for the forward flux has an adjoint counterpart which can be deduced from Eq. (5.20) and Eq. (5.21). The integrals extending over the boundary will give no contribution; i.e. the outward angular importance is zero at the boundary except for the source contribution. Using the definition of the current we can relate the density to the current at the boundaries

$$J^g_{\chi^*}|_{x=\pm b} = J^g_{\eta_\chi}|_{\pm b} \mp \chi^{*g}|_{\pm b} \tag{5.32}$$

in which b represents the boundary of the system; taken symmetric in this case for notational convenience. Using Eq. (5.25) the boundary condition can be derived

$$\begin{aligned}\frac{d\chi^{*g}}{dx}|_{\pm b} &= \frac{d\eta^g_\chi}{dx}|_{\pm b} - \bar{\mu}_0^{gg}\Sigma^g_s J^g_{\eta_\chi}|_{\pm b} \\ &\mp \Sigma^g_{tr}\chi^{*g}|_{\pm b} - \sum_{g'\neq g}\Sigma^{gg'}_s\bar{\mu}_0^{gg'}\left(J^{g'}_{\eta_\chi}|_{\pm b} \mp \chi^{*g'}|_{\pm b}\right)\end{aligned} \tag{5.33}$$

At the interface between two different regions, conditions for the discontinuity in the importance and the current, which is related to the derivative of the importance, are needed. If we define $\Delta z|_{x_i}$ as the difference in the limit of the function z taken from the right and from the left to the interface x_i, we can see from the average of Eq. (5.20) and Eq. (5.21) and also from Eq. (2.39) that the discontinuity in the importance function and the current vanishes

$$\Delta\chi^{*g}|_{x_i} = \Delta J^g_{\chi^*}|_{x_i} = 0 \tag{5.34}$$

From Eq. (2.39) and Eq. (5.25), the interface condition for the derivative of the importance can be derived

$$\begin{aligned}\Delta\left(\frac{1}{\Sigma^g_{tr}}\frac{d\chi^{*g}}{dx}\right)_{x_i} &= -\Delta\left(\frac{1}{\Sigma^g_{tr}}J_{\eta_\phi}\right)_{x_i} \\ &- J^g_{\eta_\chi}\Delta\left(\frac{\Sigma^g_t}{\Sigma^g_{tr}}\right)_{x_i} - \sum_{g'}^{g'\neq g} J^{g'}_{\chi^*}\Delta\left(\frac{\Sigma^{gg'}_s\bar{\mu}_0^{gg'}}{\Sigma^g_{tr}}\right)_{x_i}\end{aligned} \tag{5.35}$$

5.3 A one-group, isotropic, homogeneous slab

The title of this section suggests nothing very realistic. This unfortunately is a necessity to have any hope of finding exact solutions to the equations derived in chapters 2 and 4. The simple system consists of a slab with a uniform, normalized, isotropic source. All cross sections are constant and scattering is isotropic. The detector response is some average quantity over the system volume like the average flux or the absorption rate. This means that η_ϕ is a constant and therefore also η_ψ. A schematic of the slab is given in

Fig. 5.1. Under these restrictions the integral transport equations are easily transformed (through the procedure outlined in section 5.2) into differential equations and therefore solutions can be obtained quite readily. Also, the solutions will be symmetric and no interface conditions are needed. Consider for example the differential equation equivalent to Eq. (4.7) for the first moment of the score

$$\frac{d^2M_1(x)}{dx^2} - k^2M_1(x) = -\Sigma_t^2\eta_\psi \tag{5.36}$$

$$\frac{dM_1(x)}{dx}|_{x=\pm b} = \mp\Sigma_t M_1(x)|_{x=\pm b} \tag{5.37}$$

$$k = \sqrt{\Sigma_t\Sigma_a}$$

in which $\eta_\psi = \eta_\phi/\Sigma_t$. The solution may be written as

$$M_1(x) = \psi^*(x) = \frac{\eta_\phi}{\Sigma_a}\left\{1 - \frac{\Sigma_s\cosh(kx)}{k\sinh(kb) + \Sigma_t\cosh(\kappa b)}\right\} \tag{5.38}$$

$$M_{1\pm}(x) = M_1(x)$$

The solutions to Eq. (2.21), Eq. (2.24), Eq. (2.36), Eq. (4.11) and Eq. (2.22) are rather similar and are listed below.

$$\psi(x) = \frac{S\Sigma_t}{\Sigma_a}\left\{1 - \frac{\Sigma_t\cosh(kx)}{k\sinh(kb) + \Sigma_t\cosh(kb)}\right\} \tag{5.39}$$

$$\chi(x) = \frac{S\Sigma_t}{\Sigma_a}\left\{1 - \frac{\Sigma_s\cosh(kx)}{k\sinh(\kappa b) + \Sigma_t\cosh(kb)}\right\} \tag{5.40}$$

$$\chi^*(x) = \frac{\eta_\phi}{\Sigma_a}\left\{1 - \frac{\Sigma_t\cosh(kx)}{k\sinh(kb) + \Sigma_t\cosh(kb)}\right\} \tag{5.41}$$

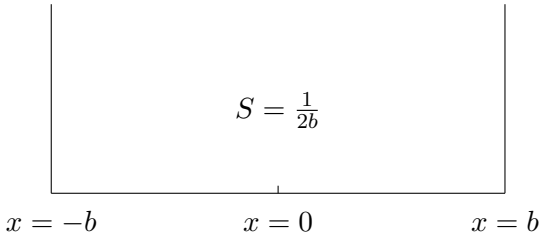

Figure 5.1: A schematic representation of the one-dimensional slab system studied in this section. The system contains a uniform normalized source S and the response represents the average flux in the system.

$$
\begin{aligned}
I_0(x) &= \eta_\psi \left\{ 2M_1(x) - \eta_\psi \right\} \\
&= \eta_\phi^2 \left\{ \frac{2}{k^2} - \frac{1}{\Sigma_t^2} - \frac{2}{k^2} \frac{\Sigma_s \cosh(kx)}{k \sinh(kb) + \Sigma_t \cosh(\kappa b)} \right\}
\end{aligned} \tag{5.42}
$$

$$
S_1(x) = S \left\{ 1 - \exp(-\Sigma_t b) \cosh(\Sigma_t x) \right\} \tag{5.43}
$$

and from Eq. (2.33) the response for this system can be obtained.

$$
\begin{aligned}
R &= \int_V S_1(x) M_1(x) dx \\
&= \frac{2S^2}{k\Sigma_a} \left\{ kb - \frac{\Sigma_t \sinh(kb)}{k \sinh(kb) + \Sigma_t \cosh(kb)} \right\}
\end{aligned} \tag{5.44}
$$

Note that this result could have been obtained from any of the response expressions from sections 2.2 and 2.3.

Since scattering is isotropic, the emission density has no angular dependence and also first moment has no angular dependence. This is because the transposed transport kernel $K(x \to x')$ behaves like the forward kernel $L(x' \to x)$, which can be seen from Eq. (5.15) and Eq. (2.25). This observation is very useful because, given that the source terms are isotropic, all equations governed by this transposed kernel will loose directional dependence; which conveniently holds for all the moment and number of collision equations in the following sections.

Analog simulation and implicit capture

When performing analog simulation or implicit capture, obviously there is no possibility for optimization with respect to weight window thresholds. The variance and cost function expressions in these cases form two ends of a spectrum and may be seen as a reference point by which to compare the Russian roulette and splitting solutions.

Due to the kernel $K(x \to x')$, the second moment equation of the score and the number of collisions equation pose no real challenge. The solutions can be obtained by transforming into a differential equation. Consider the differential equation for the number of collisions in a simulation with only implicit capture (denoted here by a subscript i), obtained from transforming Eq. (4.42)

$$
\begin{aligned}
&\frac{d^2 n_i(x)}{dx^2} = -\Sigma_t^2 \\
&\frac{dn_i(x)}{dx}|_{x=\pm b} = \mp \Sigma_t n_i(x)|_{x=\pm b} \pm \Sigma_t
\end{aligned} \tag{5.45}
$$

in which it is understood that $\varsigma_0 = 1$ for $x \in V$. The solution to Eq. (5.45) can be written as

$$
n_i(x) = 1 + \Sigma_t b + \frac{\Sigma_t^2}{2} \left(b^2 - x^2 \right) \tag{5.46}
$$

and the solution to Eq. (4.43), analog situation, may be obtained in a similar fashion

$$n_a(x) = \frac{\Sigma_t}{\Sigma_a}\left\{1 - \frac{\Sigma_s \cosh(kx)}{k\sinh(kb) + \Sigma_t \cosh(kb)}\right\} \tag{5.47}$$

It becomes clear that the number of collisions increases quite rapidly with increasing b for the implicit capture case. For large systems it may very well be that, from an efficiency perspective, implicit capture is to be avoided. When this turning point occurs depends on how the second moment is influenced by implicit capture.

The second moment equations for this situation are somewhat more complicated due to the source $I_0(x)$. Still, a differential equation is easily obtained and the solutions can be given in terms of the system parameters. The solutions become quite messy and are therefore stated as follows

$$M_{2a}(x) = C_{a0} + C_{a1}\cosh(kx) + C_{a2}x\sinh(kx) \tag{5.48}$$

$$M_{2i}(x) = C_{i0} + C_{i1}\cosh(kx) + C_{i2}\cosh(\sqrt{\Sigma_t^2 - \Sigma_s^2}x) \tag{5.49}$$

in which the coefficients are defined in appendix C.

For a specific choice of system parameters the second moments and number of collisions expressions may be used to calculate the cost of the simulation through Eq. (4.12). These values can be used to compare results from the situation with Russian roulette and splitting, discussed in the next section.

Russian roulette and splitting

In the one-group situation the weight window for Russian roulette and splitting is described by a threshold weight W_{th} beneath which Russian roulette is played. The survival weight W_s and the splitting threshold are multiples of this weight; i.e. $W_s = \alpha W_{th}$ and $W_{split} = \beta W_{th}$, with $\beta > \alpha$ obviously. A schematic of the weight window is given in Fig. 5.3. The number of particles after a splitting event is denoted by N_{split}. Strictly speaking there are four parameters which may be varied to minimize the cost function $f(W, \alpha, \beta, N_{split})$. Recall that W, rather than W_{th} is maintained as a variable and that only the ratio between the two is of importance since it is the ratio between the two that determines what value the parameters would have in a normal simulation, i.e. when starting a history with a weight equal to one. Suppose for example that the threshold is set at $W_{th} = 0.5$ and that the minimum in the cost function is found at $W = 2$ (at some value for $(\alpha, \beta, N_{split})$); the optimal choice for the threshold weight in a regular simulation would then be $W_{th} = 0.25$. In the following, only W is strictly maintained as a variable because (α, β, N) determine the bounds and discontinuities between which $f(W)$ varies. Also, it makes sense to let N_{split} be determined by the size of the window, rather than maintaining it as a 'true' minimization parameter since one can imagine that

there will be no gain in efficiency from letting the particles after a splitting event emerge with either a very high, or a very small weight.

The equations necessary to arrive at a cost equation are Eq. (4.40) and Eq. (4.33) and since all properties are now well defined, finding solutions should not be a problem at this point. There remains however one problem which makes matters a little complicated. The weight after an event $W^*(x', \kappa W)$ is generally not equal to the weight before the event W and therefore the number of collisions and second moment equations have no direct solution. There is a way around this problem fortunately. Since the post event weight is always lower than, or equal to the pre-event weight, the weight will eventually end up at the survival weight $W_s = \alpha W_{th}$. This fact ensures that the second moment and number of collision equations (in one group) may be interpreted as a system of equations, recursively dependent on the solution at survival weight. Once this solution is obtained, the solution at any weight can be constructed from the solution at survival weight, as will be shown below.

The easiest and most intuitive way of demonstrating the point made above is to let the pre-event weight equal the survival weight $W = \alpha W_{th}$ and to let the post event weight also equal the survival weight $W^*(\kappa\alpha W_{th}) = \alpha W_{th}$. This condition requires $\kappa W_s \leq W_{th}$ (or equivalently $\alpha < 1/\kappa$) which is not a very realistic assumption since κ is usually close to one. A more realistic κ, or α, is treated in section 5.3 but for demonstration purposes this needlessly complicates the equations.

Retaining the condition $\kappa W_s \leq W_{th}$ allows for obtaining an explicit ex-

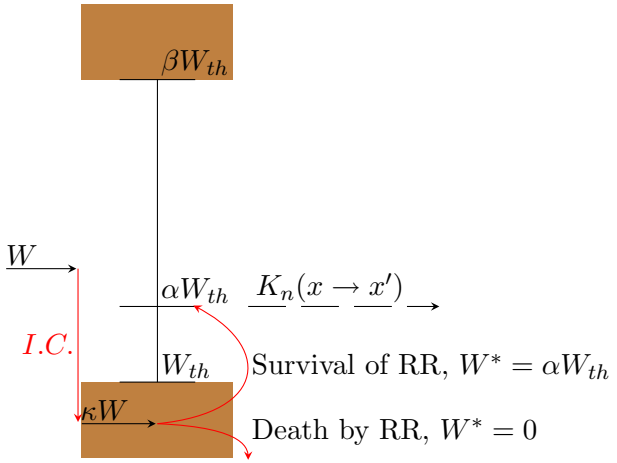

Figure 5.2: A schematic representation of a possible weight window with incoming weight W. The event is played with a pre-event weight κW due to implicit capture, which is below the Russian roulette threshold W_{th}. The particle either gets killed by Russian roulette or survives the event with a post-event weight equal to the survival weight αW_{th}, and the particle is allowed to continue to a new collision point P'; the transport probability of which is given by the normalized kernel K_n.

pression for both second moment and number of collisions directly. From these solutions, recursive expressions for the second moment and number of collisions in different weight ranges can be obtained as will be demonstrated in the following.

Case 1: $W = \alpha W_{th}$ **and** $\kappa W \leq W_{th}$

Or equivalently $\alpha < 1/\kappa$. With these conventions the second moment and number of collisions become simple integral equations

$$M_2(x, \alpha W_{th}) = \alpha^2 W_{th}^2 I_0(x) + \int_{-b}^{b} \frac{\Sigma_s}{2} \exp(-\Sigma_t |x' - x|) M_2(x', \alpha W_{th}) dx' \tag{5.50}$$

$$n(x, \alpha W_{th}) = 1 + \int_{-b}^{b} \frac{\Sigma_s}{2} \exp(-\Sigma_t |x' - x|) n(x', \alpha W_{th}) dx' \tag{5.51}$$

Solutions to Eq. (5.50) can be obtained either directly from the integral equations or from the equivalent differential equations. The solutions read

$$M_2(x, \alpha W_{th}) = C_{M0} + C_{M1} \cosh(kx) + C_{M2} x \sinh(kx) \tag{5.52}$$

$$n(x, \alpha W_{th}) = \frac{\Sigma_t}{\Sigma_a} \left\{ 1 - \frac{\Sigma_s \cosh(kx)}{k \sinh(kb) + \Sigma_t \cosh(kb)} \right\} \tag{5.53}$$

in which the coefficients for the second moment are defined in Appendix C.

From this point on it is only a matter of determining when the weight after an event will be below the threshold, because then $W^* = \alpha W_{th}$ and the equations can be solved. Starting from low weights, in which case Russian roulette will always be played, we will work our way up to high weights, in which case splitting is always done.

Case 2: $W_{th}/\kappa^{N_g} \leq W \leq W_{th}\kappa^{N_g+1}$ **and** $\kappa W < \beta W_{th}$

The index g stands for group and has no meaning is this situation. It is retained to ensure there will be no confusion with N, which represents the number of neutron histories.

Since the weight after a collision will always be less than the splitting threshold we have that $z_N = 0$. Also,

$$\begin{aligned} z_1(\kappa^{N_g+1} W) &= \kappa^{N_g+1} \frac{W}{\alpha W_{th}} \\ W^*(\kappa^{N_g+1} W) &= \alpha W_{th} \\ z_1(\kappa^{N_g} W) &= 1 \\ W^*(\kappa^{N_g} W) &= \kappa^{N_g+1} W \end{aligned}$$

A particle at a higher weight will have to collide a distinct number of times before attaining a pre-event weight which is below the threshold. This observation makes it possible to relate solutions at any weight to the situation at αW_{th}. To that end let us consider the derivation of the number of collisions equation in this weight range, using the following definition for repeated integrations

$$\varsigma_{j+1}(x) = \int K(x \to x')\varsigma_j(x')dx' \tag{5.54}$$

$$\varsigma_0(x) = \begin{cases} 1 & x \in V \\ 0 & x \notin V \end{cases} \tag{5.55}$$

This makes a recursive equation for the number of collisions possible

$$\begin{aligned} n(x, \kappa^{N_g} W) &= \varsigma_0(x) + \kappa^{N_g+1} \frac{W}{\alpha W_{th}} \int K_n(x \to x') n(P', \alpha W_{th}) dP' \\ &= \varsigma_0(x) \left\{ 1 - \kappa^{N_g} \frac{W}{\alpha W_{th}} \right\} + \frac{W}{\alpha W_{th}} n(x, \alpha W_{th}) \\ n(x, \kappa^{N_g-1} W) &= \varsigma(x) + \kappa^{-1} \int K(x \to x') n(x', \kappa^{N_g} W) dx' \\ &= \varsigma_0(x) \left\{ 1 - \kappa^{N_g-1} \frac{W}{\alpha W_{th}} \right\} \\ &\quad + \varsigma_1(x)\kappa^{-1} \left\{ 1 - \kappa^{N_g} \frac{W}{\alpha W_{th}} \right\} + \kappa^{N_g-1} \frac{W}{\alpha W_{th}} n(x, \alpha W_{th}) \\ &\quad \ldots \\ n(x, W) &= \sum_{j=0}^{N_g} \varsigma_j(x) \left(\kappa^{-j} - \frac{W}{\alpha W_{th}} \right) + \frac{W}{\alpha W_{th}} n(x, \alpha W_{th}) \end{aligned} \tag{5.56}$$

equivalently one can define a repeated integration over the source in the second moment equation as

$$I_{j+1}(x) = \int K(x \to x') I_j(x') dx' \tag{5.57}$$

and also a recursive equation is possible

$$M_2(x, W) = W \sum_{j=0}^{N_g} \left(W\kappa^j - \alpha W_{th} I_j(x) \right) + \frac{W}{\alpha W_{th}} M_2(x, \alpha W_{th}) \tag{5.58}$$

We have now expressed the second moment and number of collisions within a certain weight range in terms of the solution at survival weight.

All that is left now is provide solutions to Eq. (5.56) and Eq. (5.58). The repeated integrations can be rewritten as a differential equation from which

the solutions can be obtained. Since both Eq. (5.57) and Eq. (5.54) are defined by the same integral operator, the resulting differential equations will have the same form and the same boundary conditions. As an example we write for I_{n+1}

$$\frac{d^2 I_{n+1}}{dx^2} - \Sigma_t^2 I_{n+1} = -\Sigma_t \Sigma_s I_n \tag{5.59}$$

$$\frac{dI_{n+1}}{dx}|_{x=\pm b} = \mp \Sigma_t I_{n+1}|_{x=\pm b} \tag{5.60}$$

It can be verified by either substitution in the integral or differential equations that the solutions take the following form.

$$I_n(x) = C_n + D_n \cosh(kx) + \sum_{j=0}^{n-1} x^j \left\{ E_{n,j} \cosh(\Sigma_t x) + F_{n,j} \sinh(\Sigma_t x) \right\} \tag{5.61}$$

$$\varsigma_n(x) = A_n + \sum_{j=0}^{n-1} x^j \left\{ B_{n,j} \cosh(\Sigma_t x) + C_{n,j} \sinh(\Sigma_t x) \right\} \tag{5.62}$$

in which the coefficients are defined by filling in the solutions in the equivalent differential equation. Doing so results in

$$C_n = \left(\frac{\Sigma_s}{\Sigma_t} \right)^n C_0 \tag{5.63}$$

$$D_n = D_0 \tag{5.64}$$

$$A_n = \left(\frac{\Sigma_s}{\Sigma_t} \right)^n A_0 \tag{5.65}$$

and for the coefficients in front of a power of x it holds that, under the following restrictions

$$\begin{array}{llll} E_{n,j} = B_{n,j} = 0 & \text{for} & j = odd \\ F_{n,j} = C_{n,j} = 0 & \text{for} & j = even \\ \text{also} \quad j \neq 0 & \text{and} & j \leq n-1 \end{array}$$

the coefficients can be written as

$$E_{n,j} = -\frac{\Sigma_t \Sigma_s F_{n-1,j-1} + j(j-1) F_{n,j+1}}{2j\Sigma_t} \tag{5.66}$$

$$B_{n,j} = -\frac{\Sigma_t \Sigma_s C_{n-1,j-1} + j(j-1) C_{n,j+1}}{2j\Sigma_t} \tag{5.67}$$

$$F_{n,j} = -\frac{\Sigma_t \Sigma_s E_{n-1,j-1} + j(j-1) E_{n,j+1}}{2j\Sigma_t} \tag{5.68}$$

$$C_{n,j} = -\frac{\Sigma_t \Sigma_s C_{n-1,j-1} + j(j-1) C_{n,j+1}}{2j\Sigma_t} \tag{5.69}$$

The last pair of coefficients follows from the boundary condition

$$\begin{aligned} E_{n,0} = &-\frac{1}{\Sigma_t\left(\sinh(\Sigma_t b)+\cosh(\Sigma_t b)\right)} \\ &\times\left(\Sigma_t C_n + D_n\left(\kappa\cosh(\kappa b)+\Sigma_t\sinh(\kappa b)\right)\right. \\ &+\sum_{j=1}^{n-1} E_{n,j}\left\{(jb^{j-1}+\Sigma_t b^j)\cosh(\Sigma_t b)+\Sigma_t b^j\sinh(\Sigma_t b)\right\} \\ &\left.+\sum_{j=1}^{n-1} F_{n,j}\left\{(jb^{j-1}+\Sigma_t b^j)\sinh(\Sigma_t b)+\Sigma_t b^j\cosh(\Sigma_t b)\right\}\right) \end{aligned} \tag{5.70}$$

$$\begin{aligned} B_{n,0} = &-\frac{1}{\Sigma_t\left(\sinh(\Sigma_t b)+\cosh(\Sigma_t b)\right)}\times(\Sigma_t A_n \\ &+\sum_{j=1}^{n-1} B_{n,j}\left\{(jb^{j-1}+\Sigma_t b^j)\cosh(\Sigma_t b)+\Sigma_t b^j\sinh(\Sigma_t b)\right\} \\ &+\sum_{j=1}^{n-1} C_{n,j}\left\{(jb^{j-1}+\Sigma_t b^j)\sinh(\Sigma_t b)+\Sigma_t b^j\cosh(\Sigma_t b)\right\}) \end{aligned} \tag{5.71}$$

The values for all coefficients can de determined by starting with the solution with lowest index $n = 0$. From this known solution, the coefficients with increasing index can be found by filling in the above relations.

The number N_g can be obtained by taking the logarithm of the weight range provided in the title of this section and performing some elementary operations

$$\frac{\ln(W_{th}/W)}{\ln(\kappa)} - 1 \leq N_g \leq \frac{\ln(W_{th}/W)}{\ln(\kappa)}$$

We recognize that the number N_g is a unique integer (as it should be, since a particle makes a unique number of collisions before attaining a weight below the threshold) and therefore we can omit one side of the expression by using a flooring function, written here as: $\lfloor a \rfloor = \mathrm{Max}\{n \in \mathbb{N}_0 | n \leq a\}$. A further constraint stems from the fact that the pre-event weight in this range shouldn't exceed the splitting threshold. All in all this leads to the following

$$\begin{aligned} N_g &= \left\lfloor \frac{\ln(W_{th}/W)}{\ln(\kappa)} \right\rfloor \\ N_g &\in \{0, 1, 2, ...N_{gMax}\} \\ N_{gMax} &= \left\lfloor 1 - \frac{\ln(\beta)}{\ln(\kappa)} \right\rfloor \end{aligned} \tag{5.72}$$

Note at this point that the functions $n(x, W)$ and $M_2(x, W)$ will be discontinuous in weight as the particle, depending on which weight it carries, will need more or less collisions to attain a post-event weight beneath the Russian roulette threshold.

Case 3: $\beta W_{th} \leq \kappa W$ **but** $\kappa^2 W/N_{split} < \beta W_{th}$

In this weight range the particles will definitely split after a collision event but the post-event weight will be below the splitting threshold.

Since $z_1(\kappa W) = 0$, $z_N(\kappa W) = 1$ and $W^*(\kappa W) = \kappa W/N_{split}$ the solution to Eq. (4.33) can be obtained quite readily using the definitions from Case 2 for repeated integrations. For the second moment we have

$$\begin{aligned} M_2(x,W) = I_0(x)\left(W^2 - W\alpha W_{th}\right) + W^2\frac{\kappa}{N}\sum_{j=0}^{N_g}\kappa^j I_{j+1}(x) \\ - W\alpha W_{th}\sum_{j=0}^{N_g} I_{j+1}(x) + \frac{W}{\alpha W_{th}} M_2(x,\alpha W_{th}) \\ + W^2\frac{\kappa}{N_{split}}\left(N_{split}-1\right)\int K(x\rightarrow x')M_1^2(x')dx' \end{aligned} \tag{5.73}$$

and the number of collisions can be obtained in a similar fashion

$$\begin{aligned} n(x,W) = \varsigma_0(x)\left(1 - \frac{W}{\alpha W_{th}}\right) + \frac{N}{\kappa}\sum_{j=0}^{N_g}\left\{\kappa^{-j} - \frac{\kappa W}{N\alpha W_{th}}\right\}\varsigma_{j+1}(x) \\ + \frac{W}{\alpha W_{th}} n(x,\alpha W_{th}) \end{aligned} \tag{5.74}$$

After some manipulation the following result can be obtained for the value N_g

$$\begin{aligned} N_g &= \left\lfloor \frac{\ln(N_{split}W_{th}/W)}{\ln(\kappa)} - 1 \right\rfloor \\ N_g &\in \{N_{gMin}, ..., N_{gMax}\} \\ N_{gMin} &= \left\lfloor \frac{\ln(N_{split}/\beta)}{\ln(\kappa)} \right\rfloor \end{aligned} \tag{5.75}$$

Realistic κ values

For κ close to one (or α larger than $1/\kappa$), the second moment or number of collisions equation at survival weight will not have a direct solution. Rather, the weight needs a number of transitions to come below the threshold weight W_{th}, in which case the post-event weight equals the survival weight again; $W^* = \alpha W_{th}$. As before, the criterion is $W_{th}/\kappa^{N_s} \leq W \leq W_{th}\kappa^{N_s+1}$, with the subscript s denoting the survival weight situation. In terms of the minimization parameters this can be expressed more conveniently as

$$\begin{aligned} N_S &= \left\lfloor -\frac{\ln(\alpha)}{\ln(\kappa)} \right\rfloor \\ N_S &\in \mathbb{N}_0 \end{aligned} \tag{5.76}$$

In order to obtain a solution for $n(P, \alpha W_{th}, N_s)$ it is necessary to evaluate repeated integrations over the source term ς_0 (as was the case in Case 3) and now also over the solution function itself! In general, the equation for the number of collisions at survival weight may be written as

$$f_0(x, N_s) = \sum_{j=0}^{N_s} \kappa^{-j} \varsigma_j(x) + f_{N_s+1}(x, N_s) \tag{5.77}$$

$$\begin{aligned} f_0(x, N_s) &= n(x, \alpha W_{th}, N_s) \\ f_{k+1}(x, N_s) &= \int K(x \to x') f_k(x', N_s) dP' \\ &= \int_{-b}^{b} \frac{\Sigma_s}{2} \exp(-\Sigma_t |x - x'|) f_k(x', N_s) dx' \end{aligned} \tag{5.78}$$

$f_{N_s+1}(x, N_s)$ now represents $N_s + 1$ integrations over the solution itself. The kernel $K(x \to x')$ is fortunately well behaved and the equation basically describes a system of linear integral equations in which the solution function is found in the first and last equation of the set.

Apart from numerical procedures, [Porter and Stirling, 1990], there is unfortunately no general way of solving this type of equation. For very large systems the bounds may be approximated as being infinite and since the kernel essentially only depends on the difference between $|x - x'|$ it may be interpreted as a convolution. When this is the case there are methods involving Fourier transforms, since convolution equals multiplication in the Fourier domain, that offer solutions quite readily, [Pipkin, 1991].

For this particular problem the bounds cannot be simply approximated as infinite. There is hope, however. Because of symmetry one can differentiate the system of integral equations twice with respect to x and obtain a system of differential equation; resulting in an $(N_s+1)^{th}$ order, self consistent differential equation. The procedure is very cumbersome and only the case for $N_s = 1$ is treated here. Let a prime denote differentiation w.r.t. x, discard the N_s dependence for notational convenience and let $S = \varsigma_0(x) + \kappa^{-1}\varsigma_1(x)$. We then have

$$\begin{aligned} f_0'''' &= S'''' + f_2'''' \\ &= S'''' + \Sigma_t^2 f_2 f_2'' - \Sigma_t \Sigma_s f_1'' \\ &= S'''' - \Sigma_t^2 S'' + \Sigma_t^2 f_0'' + \Sigma_t^2 \Sigma_t \Sigma_s \{f_0 - f_1\} \\ &= S'''' - 2\Sigma_t^2 S'' + \Sigma_t^4 S + 2\Sigma_t^2 f_0'' - \Sigma_t^2 k^2 f_0 \end{aligned} \tag{5.79}$$

and also four boundary conditions are needed (actually two will suffice because of symmetry) which can be obtained from the odd derivatives at the boundary.

$$f_0'|_{\pm b} = S'_{\pm b} \mp \Sigma_t (f_0 - S)_{\pm b} \tag{5.80}$$

$$f_0'''|_{\pm b} = S'''_{\pm b} + \Sigma_t^2 \left(f_0' - S'\right)_{\pm b} \mp \Sigma_t \left(f_0'' - S''\right)_{\pm b} \pm \Sigma_t^3 (f_0 - S)_{\pm b} \tag{5.81}$$

Solving Eq. (5.79) analytically is obviously going to be a labour intensive exercise which is best left to a solver like MAPLE[3]. Higher N_s will be even more laborious. Nevertheless, solutions can be obtained for any N_s in principle.

Complete specification of the system

There are several weight window parameters which influence the shape and number of discontinuities of the cost function. First of all, a threshold weight W_{th} has to be chosen. Recall that this is not strictly a minimization parameter since the choice was made to express everything in terms of W rather than W_{th} and it is only the ratio between the two that matters. The number of discontinuities and the shape of $f(W)$ is further determined by the choice of the ratio between survival weight and RR threshold weight $\alpha = W_s/W_{th}$ and the ratio between the splitting threshold and the RR threshold $\beta = W_{split}/W_{th}$. Actually, β only influences the number of discontinuities and their respective positions but it occurs nowhere in the equations describing $f(W)$.

Once the system parameters have been established (i.e. the size, cross sections etc.) it is possible to find a minimum in the cost function for a specific combination of parameters using the functions specified in the three cases. The number of discontinuities for varying parameters α, β, N_{split}, the bounds in the different sums (N_s, N_g) and also the weights, which we shall call W_{disc}, at which they occur are given by

$$
\begin{aligned}
N_S &= \left\lfloor -\frac{\ln(\alpha)}{\ln(\kappa)} \right\rfloor \\
W_{disc} &= \frac{W_{th}}{\kappa^{N_g}} \qquad N_g = 1, 2, ..., N_{gMax} \\
W_{Split} &= \frac{\beta W_{th}}{\kappa} \\
W_{disc} &= \frac{N_{split} W_{th}}{\kappa^{N_g+2}} \qquad N_g = N_{gMin}, ..., N_{gMax} - 1 \\
N_{gMin} &= \left\lfloor \frac{\ln(N_{split}/\beta)}{\ln(\kappa)} \right\rfloor \\
N_{gMax} &= \left\lfloor 1 - \frac{\ln(\beta)}{\ln(\kappa)} \right\rfloor \\
W_{Max} &= \frac{N_{split} \beta W_{th}}{\kappa^2}
\end{aligned}
$$

So, given that no weight boundaries coincide there are in total $2N_{gMax} + 2 - N_{gMin}$ discontinuities in the cost function and therefore also just as many functions to be evaluated.

It is unfortunate that the cost function does not vary smoothly with the minimization parameters and therefore some work is necessary to find the

[3]Maple 13 was used for the calculations in this thesis, http://www.maplesoft.com

global minimum. However, once the solution at survival weight is found, it is simply a matter of working out the bounds and the algebraic equations relating the different weight range solutions to the one at survival weight.

Minimization strategy

The strategy to find the global minimum of the cost would be to first establish the weight discontinuities and the bounds of the different sums from section 5.3, given the system parameters and the minimization parameters. Subsequently the expressions at survival weight $M_2(x, \alpha W_t h)$ and $n(x, \alpha W_t h)$ need to be obtained. The functions at any weight can be expressed in terms of the solutions at survival weight. From these functions $f(W)$ can be constructed by evaluating the integrals Eq. (4.35) and Eq. (4.41) and multiplying the results. This procedure needs to be repeated for a different choice of minimization parameters and so forth. The global minimum of the cost may be located at a discontinuity in W, in which case we cannot simply set the derivative of $f(W)$ to zero and solve for W. Since many expressions need to be evaluated, the calculations performed in this work were done with an automated algorithm written in MAPLE13[4].

Extension to source biased systems

By now the solution to the functions $n(x, W)$ and $M_2(x, W)$ will be fully known. Trying different source biasing strategies is not an operation that will lead to fundamental complications. However, the amount of work that has to be done to find a global minimum in the cost function will most definitely increase.

The way to handle this problem is to first derive the full solutions $M_2(x, W)$ and $n(x, W)$ for the non-biased system and subsequently alter the initial weights according to the procedure of section 3.2, leading to $M_2(x, \overline{W}(x))$ and $n(x, \overline{W}(x))$. The integrals Eq. (4.45) and Eq. (4.48) can in principle be evaluated, but since the non-biased functions contained numerous discontinuities to begin with, the biased versions will contain even more. It is therefore to be preferred to perform discrete spatial biasing; i.e. divide the source region into a number of uniformly biased regions.

5.4 An infinite two-group system

Another interesting system consists of a two-group, infinite system in which up-scattering from group one to two is prohibited. As before, everything is assumed isotropic so directional dependence may be omitted straight away. The most important simplification, however, is that now also spatial depen-

[4] http://www.maplesoft.com

dence can be dropped. This leads to an algebraic system of equations for the moment and number of collisions equations which can be easily solved.

Let M_{1g} denote the first moment in group g, which is either 1 or 2 and follow this notation for other quantities as well. The first moment equation, Eq. (4.7), then takes the following form

$$M_{11} = \eta_{\psi 1} + \frac{\Sigma_s^{11}}{\Sigma_t^1} M_{11} + \frac{\Sigma_s^{12}}{\Sigma_t^1} M_{12}$$
$$M_{12} = \eta_{\psi 2} + \kappa_2 M_{12}$$

which has solutions equal to

$$M_{12} = \frac{\eta_{\psi 2}}{1 - \kappa_2} \tag{5.82}$$

$$M_{11} = \frac{\eta_{\psi 1}\Sigma_t^1(1-\kappa_2) + \eta_{\psi 2}\Sigma_s^{12}}{\Sigma_t^1(1-\kappa_2) + \Sigma_s^{11}(\kappa_2 - 1)} \tag{5.83}$$

The choice for a weight window makes life a bit more complicated, because scattering from group one to group two introduces new weight range possibilities. Furthermore, the weight windows by no means have to be the same in the two groups. To keep matters manageable suppose the weight window boundaries in the first group are a multiple of the window boundaries in the second group; i.e. $W_{th1} = \gamma W_{th2}$. In practice, one would choose a fixed window (α, β) and let the starting weight in the respective group determine the value of γ. A starting weight different from one may for example occur due to source biasing, but more about that later. For the moment suppose $W_{th2} = W_{th}$ and therefore everything is determined in terms of the window parameters of the second group. A schematic of the weight window is given in Fig. 5.4.

The second moment and number of collisions equation can in general be written as

$$\begin{aligned} M_{2g}(W) = {} & W^2 I_{0g} + \left(z_1(\kappa_g W) + N z_N(\kappa_g W)\right)\kappa_g^{-1} \\ & \times \sum_{g'} \frac{\Sigma_s^{gg'}}{\Sigma_t^g} M_{2g'}(W^*(\kappa_g W)) \\ & + z_N(\kappa_g W)\frac{N-1}{N} W^2 \kappa_g \sum_{g'} \frac{\Sigma_s^{gg'}}{\Sigma_t^g} M_{1g}^2 \end{aligned} \tag{5.84}$$

$$\begin{aligned} n_g(W) = {} & 1 + \left(z_1(\kappa_g W) + N z_N(\kappa_g W)\right)\kappa_g^{-1} \\ & \times \sum_{g'} \frac{\Sigma_s^{gg'}}{\Sigma_t^g} n_{g'}(W^*(\kappa_g W)) \end{aligned} \tag{5.85}$$

in which scattering from $2 \rightarrow 1$ is prohibited.

The general idea behind the following derivation again revolves around the fact that, once solutions are found at the survival weight, every solution at a certain weight may be expressed in terms of the solution at survival weight. It should be noted, however, that the survival weights in the two groups may differ; notably by a factor γ. The response, variance and number of collisions may be expressed as

$$R = \sum_g S_{1g} M_{1g} \tag{5.86}$$

$$\mathrm{Var}(W) = \sum_g S_{1g} \frac{M_{2g}(W)}{W^2} - R^2 \tag{5.87}$$

$$N_c(W) = \sum_g S_{1g} n_g(W) \tag{5.88}$$

$$f(W) = \mathrm{Var}(W) N_c(W) \tag{5.89}$$

which, deceivingly, looks a lot simpler than the situation for the space dependent one group system. One has to remember, however, that there are now

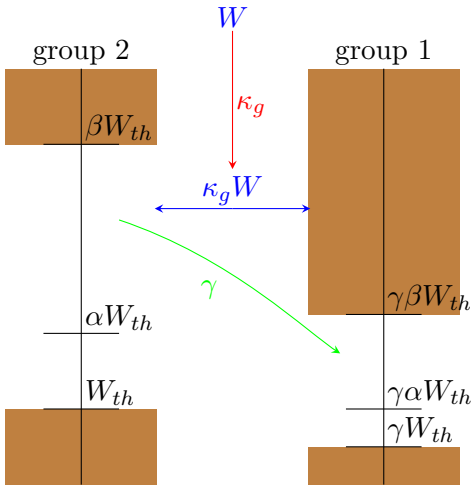

Figure 5.3: A schematic representation of a possible event for a particle colliding with a weight W. Depending on the group g, the pre-event weight will be either $\kappa_1 W$ or $\kappa_2 W$ and the respective group window will be used for the event. For illustration purposes the window scale factor is chosen as $\gamma = 0.5$. This shows that the event may have an entirely different outcome for a particle, depending on the group it is in.

three parameters determining the number of discontinuities and the bounds between which $f(W)$ varies.

For the second group not much changes with respect to the situation for the one-group, finite system and therefore each individual weight range will start with the expressions for this group. The first group also contains contributions from the second group and therefore some more work is needed in order to arrive at solutions; particularly at high weights. Once the full solution for group two, including the possibility of any choice of κ, is obtained the first group is treated.

Solutions for group 2

As in the finite, one-group system the solution at survival weight will be calculated first. From this expression, solutions at any weight will be given. First for the case that splitting does not occur and second, for the case that splitting does occur. Since the procedure of deriving the recursive expressions was treated extensively for the one-group system it will not be necessary to state every derivation explicitly. Also, the solutions are much easier for the infinite system since there is no spatial dependence.

case 1: $W = W_S = \alpha W_{th}$

Let $N_{S2} + 1$ denote the number of collisions, for a particle entering a collision with weight W_s in group 2, necessary to attain a weight beneath the threshold weight W_{th}. Then

$$\begin{aligned} N_{S2} &= \left\lfloor -\frac{\ln(\alpha)}{\ln(\kappa_2)} \right\rfloor \\ N_{S2} &\in \mathbb{N}_0 \end{aligned} \tag{5.90}$$

It can now be easily verified that the solutions for the number of collisions and second moment in the second group, at survival weight (in the second group) are as follows

$$M_{22}(W_S = \alpha W_{th}) = \frac{\alpha^2 W_{th}^2 I_{02} \sum_{j=0}^{N_{S2}} \kappa_2^{2j}}{1 - \kappa_2^{N_{S2}+1}} \tag{5.91}$$

$$n_2(\alpha W_{th}) = \frac{N_{S2} + 1}{1 - \kappa_2^{N_{S2}+1}} \tag{5.92}$$

case 2: $W_{th}/\kappa_2^{N_2} \leq W \leq W_{th}/\kappa_2^{N_2+1}$ **but** $W < \beta W_{th}/\kappa_2$

In this case the particle needs $N_2 + 1$ collisions in the second group to attain a weight below the threshold under the restriction that no splitting is played.

The functions of interest take the following form

$$M_{22}(W) = W^2 I_{02} \sum_{j=0}^{N_2} \kappa_2^{2j} + \kappa_2^{N_2+1} \frac{W}{\alpha W_{th}} M_{22}(\alpha W_{th}) \tag{5.93}$$

$$n_2(W) = N_2 + 1 + \kappa_2^{N_2+1} \frac{W}{\alpha W_{th}} n_2(\alpha W_{th}) \tag{5.94}$$

The number N_2 is determined via

$$\begin{aligned} N_2 &= \left\lfloor \frac{\ln(W_{th}/W)}{\ln(\kappa_2)} \right\rfloor \\ N_2 &\in \{0, 1, 2, ...N_{2Max}\} \\ N_{2Max} &= \left\lfloor 1 - \frac{\ln(\beta)}{\ln(\kappa_2)} \right\rfloor \end{aligned} \tag{5.95}$$

<u>case 3</u>: $\beta W_{th}/\kappa_2 \leq W$ **but** $W < N_{split}\beta W_{th}/\kappa_2^2$

In this case the particle will split after experiencing its first collision. The weight is restricted by the fact that the post-event weight should not be higher than the splitting threshold βW_{th}. The restriction also implies that the post-event contribution in the equations will always be from the weight range of <u>case 2</u> under the same boundary restrictions. Therefore, the second moment and number of collisions can be expressed explicitly in terms of a source contribution and a contribution from the situation at survival weight

$$\begin{aligned} M_{22}(W) = W^2 I_{02} \left\{ 1 + \frac{\kappa_2^2}{N} \sum_{j=0}^{N_2} \kappa_2^{2j} \right\} + \kappa_2^2 W^2 \frac{N_{split} - 1}{N_{split}} M_{12}^2 \\ + \kappa_2^{N_2+2} \frac{W}{\alpha W_{th}} M_{22}(\alpha W_{th}) \end{aligned} \tag{5.96}$$

$$n_2(W) = 1 + N_{split}\,(N_2 + 1) + \kappa_2^{N_2+2} \frac{W}{\alpha W_{th}} n_2(\alpha W_{th}) \tag{5.97}$$

in which the number N_2 is determined via

$$\begin{aligned} N_2 &= \left\lfloor \frac{\ln(NW_{th}/W)}{\ln(\kappa_2)} - 1 \right\rfloor \\ N_2 &\in \{N_{2Min}, ..., N_{2Max}\} \\ N_{2Min} &= \left\lfloor \frac{\ln(N/\beta)}{\ln(\kappa_2)} \right\rfloor \end{aligned}$$

and N_{2Max} is as before

Now that the solutions for the entire weight range of the second group are available for any choice of the parameters $\{\alpha, \beta, \gamma, W, N_{split}\}$, which influence the minimization of the cost function, it is time to consider the first energy group and its solutions for any choice of W.

Solutions for group 1

In order to establish a solution for any choice of W the first priority is to find expressions for the situation at survival weight in the first group $W = \gamma\alpha W_{th}$

case 1: $W = \gamma\alpha W_{th}$

Let the number $N_{S1}+1$ denote the number of collision, for a particle entering its first collision in the first group, necessary to reach a weight below γW_{th}. With this convention it is possible to write down expressions for the number of collisions and the second moment in group one at survival weight.

$$\begin{aligned} M_{21}(\gamma\alpha W_{th}) = {} & Q(\gamma\alpha W_{th})^2 I_{01} \sum_{j=0}^{N_{S1}} \kappa_1^j \left(\frac{\Sigma_s^{11}}{\Sigma_t^1}\right)^j \\ & + Q\left(\frac{\Sigma_s^{11}}{\Sigma_t^1}\right)^{N_{S1}} \left(\frac{\Sigma_s^{12}}{\Sigma_t^1}\right) M_{22}(\gamma\alpha W_{th}) \\ & + Q\left(\frac{\Sigma_s^{12}}{\Sigma_t^1}\right) \sum_{j=1}^{N_{S1}} \kappa_1^{-j} \left(\frac{\Sigma_s^{11}}{\Sigma_t^1}\right)^{j-1} M_{22}(\kappa_1^j \gamma\alpha W_{th}) \end{aligned} \tag{5.98}$$

$$\begin{aligned} n_1(\gamma\alpha W_{th}) = {} & Q \sum_{j=0}^{N_{S1}} \kappa_1^{-j} \left(\frac{\Sigma_s^{11}}{\Sigma_t^1}\right)^j \\ & + Q\left(\frac{\Sigma_s^{11}}{\Sigma_t^1}\right)^{N_{S1}} \left(\frac{\Sigma_s^{12}}{\Sigma_t^1}\right) n_2(\gamma\alpha W_{th}) \\ & + Q\left(\frac{\Sigma_s^{12}}{\Sigma_t^1}\right) \sum_{j=1}^{N_{S1}} \kappa_1^{-j} \left(\frac{\Sigma_s^{11}}{\Sigma_t^1}\right)^{j-1} n_2(\kappa_1^j \gamma\alpha W_{th}) \end{aligned} \tag{5.99}$$

in which it is understood that the sums going from $j = 1$ should be discarded for $N_{S1} = 0$ and

$$\begin{aligned} Q &= \left\{ 1 - \left(\frac{\Sigma_s^{11}}{\Sigma_t^1}\right)^{NS1+1} \right\}^{-1} \\ N_{S1} &= \left\lfloor -\frac{\ln(\alpha)}{\ln(\kappa_1)} \right\rfloor \\ N_{S1} &\in \mathbb{N}_0 \end{aligned} \tag{5.100}$$

Obviously, higher values for N_{S1} mean more work since then more contributions from the second group have to evaluated. However, once a solution is obtained one can proceed to higher weights.

case 2: $\gamma W_{th}/\kappa_1^{N_1} \leq W \leq \gamma W_t h/\kappa_1^{N_1+1}$ **but** $W < \gamma\beta W_{th}/\kappa_1$

In this weight range it is again a matter of relating back to the case at survival weight $W = \gamma\alpha W_{th}$ and of course, evaluating the 'in-scatter' terms from group 2. The complication arising now is that depending on the parameter γ the second group contribution may be from any weight for which a solution is available, which makes it necessary to evaluate every contribution separately. The solutions may be written as

$$\begin{aligned} M_{21}(W) = {} & W^2 I_{01} \sum_{j=0}^{N_1} \kappa_1^j \left(\frac{\Sigma_s^{11}}{\Sigma_t^1}\right)^j \\ & + \frac{W}{\gamma\alpha W_{th}} \left(\frac{\Sigma_s^{11}}{\Sigma_t^1}\right)^{N_1+1} M_{21}(\gamma\alpha W_{th}) \\ & + \frac{W}{\gamma\alpha W_{th}} \left(\frac{\Sigma_s^{11}}{\Sigma_t^1}\right)^{N_1} \left(\frac{\Sigma_s^{12}}{\Sigma_t^1}\right) M_{22}(\gamma\alpha W_{th}) \\ & + \left(\frac{\Sigma_s^{12}}{\Sigma_t^1}\right) \sum_{j=1}^{N_1} \kappa_1^{-j} \left(\frac{\Sigma_s^{11}}{\Sigma_t^1}\right)^{j-1} M_{22}(\kappa_1^j W) \end{aligned} \tag{5.101}$$

$$\begin{aligned} n_1(W) = {} & \frac{W}{\gamma\alpha W_{th}} \left(\frac{\Sigma_s^{11}}{\Sigma_t^1}\right)^{N_1+1} n_1(\gamma\alpha W_{th}) \\ & + \frac{W}{\gamma\alpha W_{th}} \left(\frac{\Sigma_s^{11}}{\Sigma_t^1}\right)^{N_1} \left(\frac{\Sigma_s^{12}}{\Sigma_t^1}\right) n_2(\gamma\alpha W_{th}) \\ & + \left(\frac{\Sigma_s^{12}}{\Sigma_t^1}\right) \sum_{j=1}^{N_1} \kappa_1^{-j} \left(\frac{\Sigma_s^{11}}{\Sigma_t^1}\right)^{j-1} n_2(\kappa_1^j W) \\ & + \sum_{j=1}^{N_1} \kappa_1^{-j} \left(\frac{\Sigma_s^{11}}{\Sigma_t^1}\right)^j \end{aligned} \tag{5.102}$$

in which N_1 is determined via

$$\begin{aligned} N_1 &= \left\lfloor \frac{\ln(W_{th}/W)}{\ln(\kappa_1)} \right\rfloor \\ N_1 &\in \{0, 1, 2, ...N_{1Max}\} \\ N_{1Max} &= \left\lfloor 1 - \frac{\ln(\beta)}{\ln(\kappa_1)} \right\rfloor \end{aligned} \tag{5.103}$$

case 3: $\gamma\alpha W_{th}/\kappa_1 \leq W$ **but** $W < W_{Max}$

In this weight range splitting will occur in the first group. The restriction imposed is, as before, that the post-event weight W^* should not exceed the splitting threshold 'in the same group'. The second group contribution may

very well be in the weight range where splitting occurs. However, solutions are only available up to a certain weight in the second group as well. The maximum allowable weight should be smaller than some value W_{Max}, defined by

$$W < W_{Max} = \text{Min}\left\{\frac{N_{split}^2 \beta W_{th}}{\kappa_1 \kappa_2^2}, \frac{N_{split}\gamma\beta W_{th}}{\kappa_1^2}\right\} \tag{5.104}$$

It should further be noted that the in-group contribution will be from a weight range below the splitting threshold and therefore it is possible to write this term out more explicitly.

$$\begin{aligned} M_{21}(W) &= W^2 I_{01}\left\{1 + \frac{\kappa_1}{N_{split}}\left(\frac{\Sigma_s^{11}}{\Sigma_t^1}\right)\sum_{j=0}^{N_1}\kappa_1^j\left(\frac{\Sigma_s^{11}}{\Sigma_t^1}\right)^j\right\} \\ &+ W^2\kappa_1\frac{N_{split}-1}{N_{split}}\left\{\left(\frac{\Sigma_s^{11}}{\Sigma_t^1}\right)M_{11}^2 + \left(\frac{\Sigma_s^{12}}{\Sigma_t^1}\right)M_{12}^2\right\} + \frac{W}{\gamma\alpha W_{th}}\left(\frac{\Sigma_s^{11}}{\Sigma_t^1}\right)^{N_1+1} \\ &\times\left\{\left(\frac{\Sigma_s^{11}}{\Sigma_t^1}\right)M_{21}(\gamma\alpha W_{th}) + \left(\frac{\Sigma_s^{12}}{\Sigma_t^1}\right)M_{22}(\gamma\alpha W_{th})\right\} \\ &+ N_{split}\left(\frac{\Sigma_s^{12}}{\Sigma_t^1}\right)\sum_{j=0}^{N_1}\kappa_1^{-(j+1)}\left(\frac{\Sigma_s^{11}}{\Sigma_t^1}\right)^j M_{22}(\kappa_1^{j+1}W/N_{split}) \end{aligned} \tag{5.105}$$

$$\begin{aligned} n_1(W) &= 1 + N_{split}\sum_{j=0}^{N_1}\kappa_1^{-(j+1)}\left(\frac{\Sigma_s^{11}}{\Sigma_t^1}\right)^{j+1} + \frac{W}{\gamma\alpha W_{th}}\left(\frac{\Sigma_s^{11}}{\Sigma_t^1}\right)^{N_1+1} \\ &\times\left\{\left(\frac{\Sigma_s^{11}}{\Sigma_t^1}\right)n_1(\gamma\alpha W_{th}) + \left(\frac{\Sigma_s^{12}}{\Sigma_t^1}\right)n_2(\gamma\alpha W_{th})\right\} \\ &+ N_{split}\left(\frac{\Sigma_s^{12}}{\Sigma_t^1}\right)\sum_{j=0}^{N_1}\kappa_1^{-(j+1)}\left(\frac{\Sigma_s^{11}}{\Sigma_t^1}\right)^j n_2(\kappa_1^{j+1}W/N_{split}) \end{aligned} \tag{5.106}$$

in which N_1 is now determined from the post-event weight $\kappa_1 W/N$, from which it follows that

$$\begin{aligned} N_1 &= \left\lfloor \frac{\ln(NW_{th}/W)}{\ln(\kappa_1)} - 1 \right\rfloor \\ N_1 &\in \{N_{1Min}, ..., N_{1Max}\} \\ N_{1Min} &= \left\lfloor \frac{\ln(N/\beta)}{\ln(\kappa_1)} \right\rfloor \end{aligned} \tag{5.107}$$

Full specification

Minimization of any of the functions with regard to the different parameters will be quite a laborious undertaking since the functions are far from smooth

and contain numerous discontinuities whose position, with respect to W, and number may vary with a different choice of parameters. The global minimum may be found at such a discontinuity in which case the standard tool for finding a minimum, i.e. setting the differentiated function equal to zero and solving for the optimal parameter choice, will yield no result. It is therefore necessary to identify all discontinuities and the sum indexes like N_1, N_2 specifying the functions in between in a structured way.

The discontinuities arising from the in-group terms in the second group are defined by

$$\begin{aligned}
W_{disc} &= \frac{W_{th}}{\kappa_2^{N_2}} \qquad N_2 = 1, 2, ..., N_{2max} \\
W_{disc} &= \frac{\beta W_{th}}{\kappa_2} \\
W_{disc} &= \frac{N_{split} W_{th}}{\kappa_2^{N_2+2}} \qquad N_2 = N_{2Min}, ..., N_{2Max} - 1 \\
N_{2Max} &= \left\lfloor 1 - \frac{\ln(\beta)}{\ln(\kappa_2)} \right\rfloor \\
N_{2Min} &= \left\lfloor \frac{\ln(N/\beta)}{\ln(\kappa_2)} \right\rfloor \\
W_{Max} &= \frac{N_{split} \beta W_{th}}{\kappa_2^2}
\end{aligned}$$

which in total make $2N_{2Max} + 2 - N_{2Min}$ discontinuities, just as in the first case.

The discontinuities arising from the in-group terms in the first group are defined by

$$\begin{aligned}
W_{disc} &= \frac{\gamma W_{th}}{\kappa_1^{N_1}} \qquad N_1 = 1, 2, ..., N_{1max} \\
W_{disc} &= \frac{\gamma \beta W_{th}}{\kappa_1} \\
W_{disc} &= \frac{N_{split} \gamma W_{th}}{\kappa_1^{N_1+2}} \qquad N_1 = N_{1Min}, ..., N_{1Max} - 1 \\
N_{1Max} &= \left\lfloor 1 - \frac{\ln(\beta)}{\ln(\kappa_1)} \right\rfloor \\
N_{1Min} &= \left\lfloor \frac{\ln(N/\beta)}{\ln(\kappa_1)} \right\rfloor \\
W_{Max} &= \text{Min} \left\{ \frac{N_{split}^2 \beta W_{th}}{\kappa_1 \kappa_2^2}, \frac{N_{split} \gamma \beta W_{th}}{\kappa_1^2} \right\}
\end{aligned}$$

which totals $2N_{1Max} + 2 - N_{1Min}$ discontinuities.

Since the first group contains in-scatter terms from the second group which carry weights of $\kappa_1^j W$ and $\kappa_1^{j+1} W/N$ it is necessary to evaluate at which weight W these entry-weights will coincide with any of the $2N_{2Max} + 2 - N_{2Min}$ discontinuities in the second group. The larger the values for N_{2Max}, N_{1Max}, the messier it gets obviously. For a good mathematical solver like MAPLE13[5] this will pose no challenge when the in-group solutions are provided.

[5]Maple 13 was used for the calculations in this thesis, http://www.maplesoft.com

Chapter 6

Sample cases

In the following, the equations derived in chapter 5 are applied to specific examples. The cost function is minimized to find an optimal choice of weight window thresholds. Optimal source biasing is also treated in the two-group infinite system. All results are verified by means of Monte Carlo simulations and the results are discussed.

6.1 A one-group, isotropic, homogeneous slab

This particular system is a good starting point for applying the theory of chapters 4 and 5 because, although the equations are more complex than for the case of the two group infinite system, the number of discontinuities as a function of weight is quite limited. The choice of system parameters is specified in table 6.1. For this particular choice of parameters, the absorption is quite high and a neutron born at $x = 0$ will have to traverse $b\Sigma_t = 11$ mean free paths before possibly leaving the system. From this point of view, analog simulation is unattractive. The response is the average flux over the entire system: $\eta_\phi = 1/V$, so increasing the number of collisions, by means of implicit capture, would seem a sensible idea as scoring can occur everywhere in the

$\Sigma_t = 1.1$ cm^{-1}
$\Sigma_s = 0.5$ cm^{-1}
$b = 10$cm
$\kappa \approx 0.4545455$
$k \approx 0.8124$ cm^{-1}
$W_{th} = 0.5$

Table 6.1: A summary of system parameters for the one-group, isotropic, homogeneous slab.

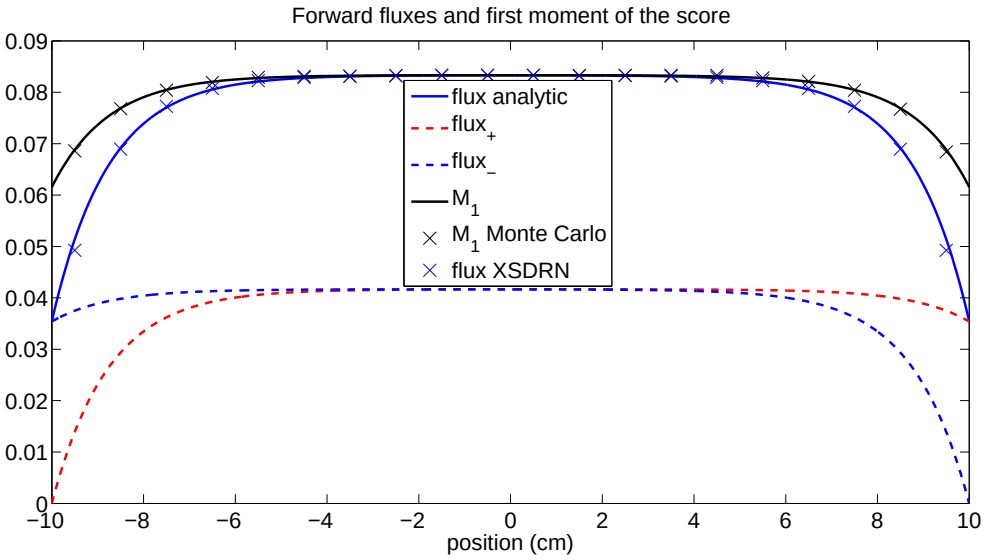

Figure 6.1: The total and directional forward fluxes and the first moment of the score in the system are displayed as a function of position. The first moment obtained with Monte Carlo and the total flux obtained with the discrete ordinates code XSDRN are also displayed. Note that $M_1(x) = M_{1\pm}(x)$.

system. Due to the high absorption, however, the weight of the particle will rapidly fall, leading to a decrease in efficiency. This begs for Russian roulette as a means of terminating particles that carry a low statistical weight. All in all, given this particular choice of system parameters, it is hard to say beforehand which simulation strategy is best and it will be interesting to see to what extent different choices of weight window thresholds will affect the efficiency and variance in the response estimate.

To get a better feeling for the system, the total and directional fluxes and the first moment of the score are displayed in Fig. 6.1. The analytic results from Eq. (2.21) were verified by mean of Monte Carlo and with the discrete ordinates code XSDRN [Green and Petrie, 1998]. Note that the forward flux has directional dependence, but the first moment of the score does not. This makes sense from a physical point of view. Because scattering is isotropic, the importance of a particle entering a collision to the left or right at some position x is, and should, be equal. In a similar fashion, the emission densities (adjoint and forward) and collision densities were calculated. The second moment and number of collisions functions for the analog and implicit capture situations can also be obtained quite readily from the equations derived in section 5.3. Suffice to say that all functions of interest for the calculation of efficiency are symmetric, hyperbolic functions with a similar shape as the first moment of the score in Fig. 6.1.

Method	R	Var
Analog MC	$7.745 \cdot 10^{-2} \pm 2 \cdot 10^{-5}$	$3.0771 \cdot 10^{-3}$
Analog analytically	$7.743322725 \cdot 10^{-2}$	$3.071512766 \cdot 10^{-3}$
IC MC	$7.74345 \cdot 10^{-2} \pm 6 \cdot 10^{-6}$	$3.4063 \cdot 10^{-4}$
IC analytically	$7.743322725 \cdot 10^{-2}$	$3.40052854 \cdot 10^{-4}$

Method	N_c	f
Analog MC	1.7038	$5.243 \cdot 10^{-3}$
Analog analytically	1.703530999	$5.232417211 \cdot 10^{-3}$
IC MC	51.315	$1.748 \cdot 10^{-2}$
IC analytically	51.33333335	$1.745604651 \cdot 10^{-2}$

Table 6.2: Summary of the results obtained for analog simulation and a simulation containing only implicit capture. Results are shown obtained by analytical means and by Monte Carlo simulation. 10^7 particles were used for the MC results. The variance denotes the variance in a response estimate from a single neutron history obviously. The variances in the Monte Carlo estimates of Var and Nc were not calculated.

The results for the analog and implicit capture situations are summarized in table Table 6.2. The Monte Carlo results were obtained by simulating 10^7 particle histories in a simple Monte Carlo neutron transport program, written specifically for this work. Var denotes the variance from a single particle history. The standard deviation in the response estimate is then obtained by calculating $\sigma = \sqrt{\text{Var}/N}$, in which $N = 10^7$.

From Table 6.2 it becomes clear that only implicit capture, without Russian roulette as a means of terminating particles with low weight, seriously deteriorates the efficiency of the simulation because, although a reduction in variance of about one order of magnitude is accomplished, the number of collisions is increased by roughly three times that amount. This is due to the fact that a neutron history will only end if the neutron leaks out of the system.

Russian roulette and splitting

For this particular situation there are four weight window parameters of interest. Obviously there is W, which eventually determines an optimal choice of the weight window lower bound or Russian roulette threshold W_{th}. α represents the ratio of the Russian roulette threshold and the survival weight $\alpha = W_s/W_{th}$. β represents the ratio between the splitting threshold and the Russian roulette threshold $\beta = W_{split}/W_{th}$. β only has influence on the number of discontinuities and their locations in the range of $f(W)$ but not on the overall hight of the function. N_{split} determines the number of fragments after a splitting event

To study the effects of different choices for the weight window param-

eters $(W, \alpha, \beta, N_{split})$, numerous computations were performed with varying thresholds and of course, varying initial weight W. It turns out that, for this particular system, the parameters $(\alpha, \beta, N_{split})$ are of marginal influence in the overall cost and/or variance reduction, albeit that a sensible choice must be made and extreme values should be avoided. The best results were obtained for $(W_{min} = 5.324, \alpha = 2, \beta > 4.84, N_{split} = 2)$. The parameters $(\alpha = 2, \beta > 4.84, N_{split} = 2)$ should not be interpreted as the result of 'true' minimization because, for example, a value of $\beta = 100$ will result in exactly the same minimum of $f(W)$. Despite the fact that the discontinuities will shift, the location at which the minimum occurs and the hight of the minimum remains unchanged for $\beta > 4.84$. This is due to the fact that for this system it is not favorable to implement splitting. Notice that $\beta > W_{min}\kappa/W_{th} = 4.84$. Shifting a little too much can obviously result in a different location and hight of the minimum. $\beta \leq 4.84$ for example may lead to a considerable loss in efficiency. Since the above choice of weight window thresholds does lead to the lowest possible value of f, we will simply call it the global minimum.

In the following, the result of a minimization with $(\alpha = 2, \beta = 9, N_{split} = 2)$ will be shown. From section 5.3 we can see discontinuities in the cost function located at weights

$$W_{disc} = \{1.1; 2.42; 5.324; 9.9; 10.648; 23.4256; < 43.56\}$$

which means that the functions $n(x, W), M_2(x, W)$ are to be evaluated for a total of seven different regions. Splitting occurs from weights higher than $W_{split} = \beta W_{th}/\kappa = 9.9$. The weight is bounded by the fact that a fragment emerging from a splitting event should not split again at its next collision.

The functions $n(x, W), M_2(x, W)$ can be obtained by filling in the numbers in the equations from section 5.3. The variance $\mathrm{Var}(W)$ and number of collisions $N_c(W)$ can be calculated from Eq. (4.35) and Eq. (4.41), the results of which are depicted in Fig. 6.2.

It is clear that the theory presented in previous chapters correctly represents the Monte Carlo results. The seven discontinuities are also distinctly present. The variance reduction flattens out quite quickly whilst the number of collisions keeps increasing with growing W, leading to a decrease in efficiency. We can also clearly see a jump in the number of collision at $W = 9.9$, above which splitting occurs.

From the number of collisions and variance, the cost function can be constructed through Eq. (4.44). This function, along with a detailed view around the minimum and also results from Monte Carlo simulations, is depicted in Fig. 6.3. The global minimum is found right at a weight discontinuity between the $N_g = 2$ and $N_g = 3$ regions, $N_g + 1$ representing the number of collisions necessary to attain a weight beneath the Russian roulette threshold W_{th}.

We can also see that apparently it is favorable from an efficiency perspective to let a particle collide three times (and no more) on average before playing Russian roulette. Splitting is not favorable as the variance barely decreases

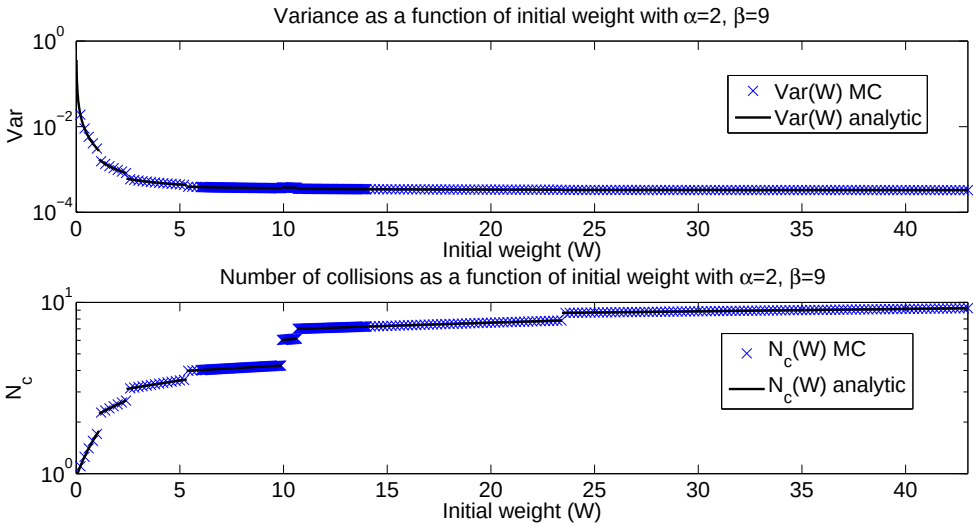

Figure 6.2: The variance and number of collisions are displayed as a function of initial weight W for the entire weight range. The Monte Carlo results were obtained by computing 400 simulations at different starting weights with 10^7 particle histories for each run.

	Minimum w.r.t $f(W)$	Implicit Capture	Analog
W	5.324	n.a	n.a.
Var	$4.360670595 \cdot 10^{-4}$	$3.40052854 \cdot 10^{-4}$	$3.071512766 \cdot 10^{-3}$
N_c	3.545894494	51.33333335	1.703530999
f	$1.546247785 \cdot 10^{-3}$	$1.745604651 \cdot 10^{-2}$	$5.232417211 \cdot 10^{-3}$

Table 6.3: Summary of the analytical solution to the global minimization problem. For comparison also the results for the analog and only implicit capture are depicted.

and the number of collisions increases quite substantially with W. For this particular system we therefore might as well dispose of splitting altogether. The results of the computations for this specific system are summarized in Table 6.3. We can see from these results that for this particular system the cost decrease with an optimal choice of weight window thresholds is roughly a factor of 3.5 with respect to analog simulation. We can also see that implicit capture (without Russian roulette as a means of low particle weight cutoff) increases cost.

In an actual Monte Carlo simulation, where a particle would start a simulation with a weight equal to one, the best choice of weight window thresholds would be as in Table 6.4. Because splitting will never occur we could have omitted both W_{split} and N_{split} in Table 6.4 but for sake of consistency they

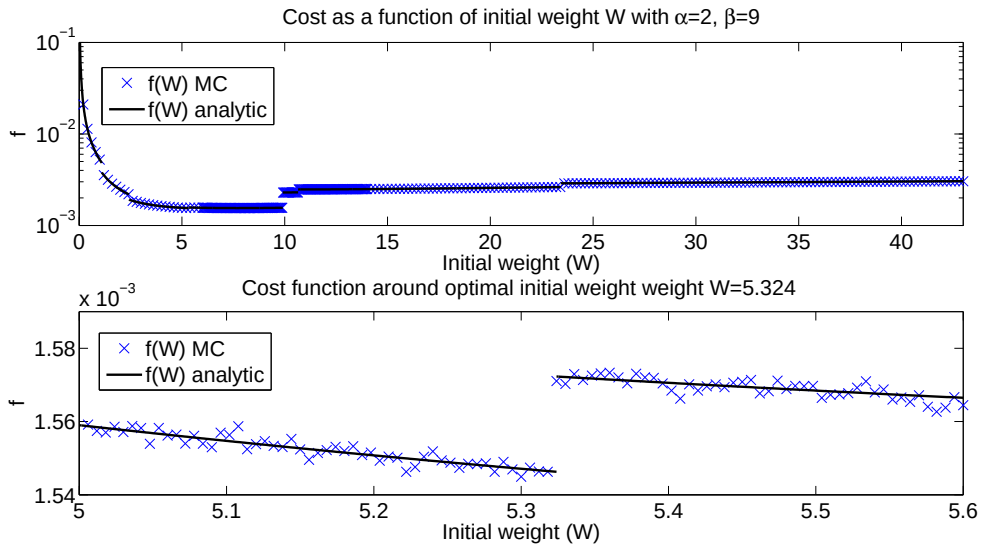

Figure 6.3: The cost function is displayed as a function of initial weight W for the entire weight range and for the range around which the minimum in the cost function can be found: $W_{min} = 5.324$. The minimum occurs at the transition between the $N_g = 2$ and $N_g = 3$ regions. The Monte Carlo results were obtained by computing 400 simulations at different starting weights with 10^7 particle histories for each run.

$W_{th} = 0.0939$
$W_s = 0.1878$
$W_{split} > 0.4545$
$N_{split} = 2$

Table 6.4: Weight window bounds in an actual Monte Carlo simulation, resulting from the minimization of $f(W)$ for the finite, slab system.

are retained.

Further investigation would require spatial variations in weight windows, combined with source biasing. These complications would render exact analytical solutions obsolete and would require numerical solutions to the moment and number of collisions equations. Chapter 7 therefore deals with the derivation of equations which may be suitable for implementation in existing, deterministic neutron transport codes.

6.2 An infinite two-group system

For the infinite two-group system there are numerous variations on the system parameters possible, but for brevity we will restrict ourselves to an interesting

$\Sigma_{t1} = 1$ cm^{-1}	$\Sigma_{t2} = 1$ cm^{-1}
$\Sigma_s^{11} = 0.2$ cm^{-1}	$\Sigma_s^{22} = 0.4$ cm^{-1}
$\Sigma_s^{12} = 0.25$ cm^{-1}	$\Sigma_s^{21} = 0$ cm^{-1}
$S_1 = 0.7$	$S_2 = 0.3$
$M_{11} = 0.5208333$	$M_{12} = 1.6666667$
$\kappa_1 = 0.45$	$\kappa_2 = 0.4$
$R = \psi_2/\Sigma_{t2} = 0.864583$	$W_{th} = 0.5$

Table 6.5: Summary of the system parameters used for cost minimization in the two-group, infinite system. The first moments and the response are also displayed.

case. The choice of system parameters is specified in Table 6.5. The absorption is again quite high and 70% of the source neutrons are born in the first group. The response represents the average flux in the second, thermal group. In this way, the first moment M_{1g} has a substantially different value for each group. Because most particles are born in the first group but the adjoint is higher in the second group, it is reasonable to expect that source biasing with a proper function will be beneficial for the overall efficiency. First we will look at a situation without source biasing.

The equations derived in section 5.4 may be applied to analyze the system and to find a global minimum in the cost function. Several computations were performed to explore the different choices of weight window thresholds. The best result was found at $W = 4.997925$ with $\alpha = 2, \beta \geq 4.5, \gamma = 1$. γ represents the ratio between the first and second group windows $\gamma = W_{th1}/W_{th2}$, which allowed us to express everything in terms of the second group window. The minimization for $\alpha = 2, \beta = 9, \gamma = 1$, along with Monte Carlo results, is shown in Fig. 6.4. Splitting occurs in the second group above weights higher than $W_{split2} = \beta W_{th}/\kappa_2 = 11.25$ and in the first group for weights higher than $W_{split1} = \gamma\beta W_{th}/\kappa_1 = 10$. $\gamma = 1$ makes sense in this situation as there is no biasing and therefore, regardless of the group, the particle is born with a weight equal to the initial weight W. Deviations from $\alpha = 2$ again result in a small change of the total minimal cost but $\alpha = 2$ yields the best result. As was the case in the finite system, splitting is to be avoided for both groups and therefore $\beta > W_{min}\kappa/W_{th} = 4.498$. The efficiency gains from varying these parameters are marginal for this particular situation (as was the case for the finite one-group system) and the real gain comes from finding an optimal initial weight W or equivalently, an optimal choice of Russian roulette threshold.

Source biasing with anything near the importance function M_g yields a lower cost over basically the whole weight range. The best result is found for

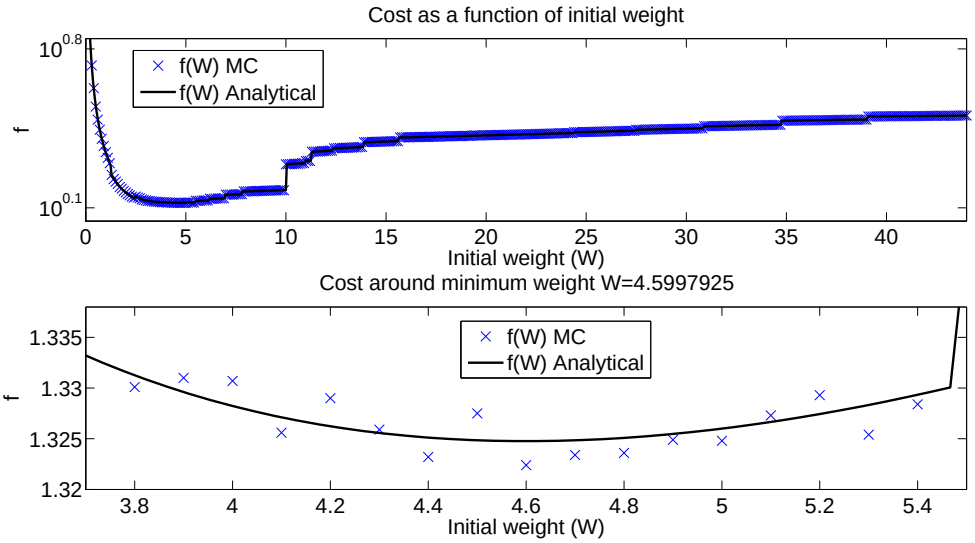

Figure 6.4: Results of a computation of the cost function with $\alpha = 2, \beta = 9, \gamma = 1$ and no source biasing. The Monte Carlo results were obtained by performing 200 simulations at different weights, each with 10^7 particle histories.

a biasing function

$$\Gamma_1 = 0.26$$
$$\Gamma_2 = 0.74$$

which leads, using Eq. (3.10), to a biased source distribution of

$$S_1 = 0.4504$$
$$S_2 = 0.5495$$

This is quite close to the source distribution obtained when biasing with the importance function, but definitely not exactly equal. For comparison, the normalized adjoint in the second group equals $M_{12}/(M_{12} + M_{11}) = 0.7619$, leading to $S_1 = 0.4216, S_2 = 0.5783$. Also note that for the infinite system there is no distinction between the different importance functions, $\chi_g^* = M_{1g}$.

Since, due to biasing, the initial neutron weight is modified, it is to be expected that for optimal results $\gamma \neq 1$, because particles may be born outside the window in that case. From manipulation of Eq. (3.12) it follows that an optimal value for γ should in theory, with this particular choice of biasing function, be $\gamma = \overline{W}_1/\overline{W}_2 = 2.846$ and indeed, this follows from the calculation as well. It has to be said though that, as is the case for other weight window parameters, small deviations from this number usually do not lead to cost increases because γ determines where the discontinuities in the weight range

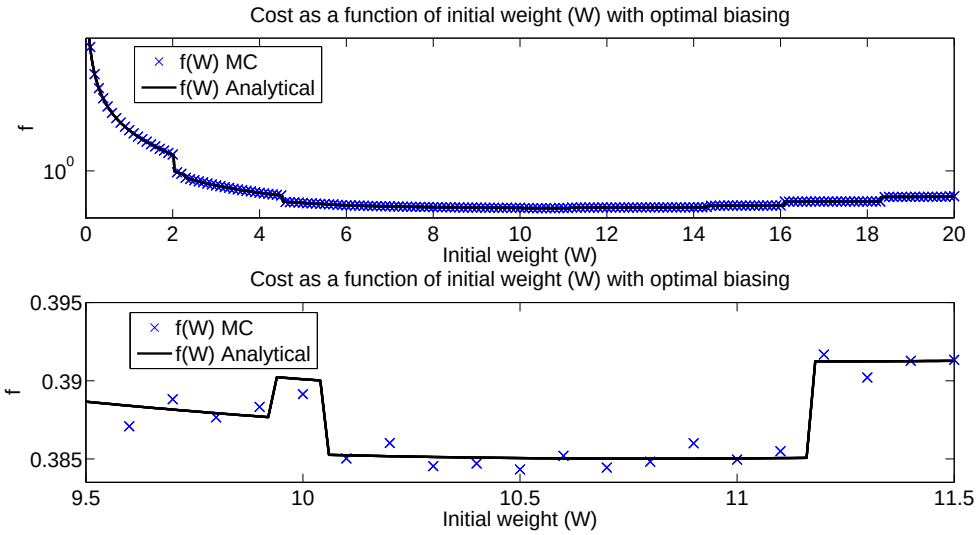

Figure 6.5: Minimization of the cost with $\alpha = 2, \beta = 9, \gamma = 2.8461538$, using the best biasing function. The Monte Carlo results were obtained by performing 200 simulations at different weights, each with 10^7 particle histories.

Minimum w.r.t $f(W)$	Analog	Non-biased	Biased
W	n.a.	4.5997925	10.8003422
Var	2.017361	0.3712423	0.09075254
N_c	1.739583	3.5684577	4.24249895
f	3.509368	1.3247624	0.38501757

Table 6.6: Summary of the analytical solution to the global minimization problem for the infinite two-group system. The results of analog, best non-biased and optimal biased simulations are shown.

of $f(W)$ occur. The minimization with optimal source biasing is depicted in Fig. 6.5.

Implicit capture only, without Russian roulette, obviously has no meaning in the infinite system as the variance would tend to zero and the number of collisions would tend to infinity. The results for the minimizations with and without bias, as well as analog results are shown in Table 6.6. As was the case in the one-group system, the cost decrease with respect to analog simulation in a non-biased simulation with weight windows isn't dramatic. The cost decrease with optimal biasing this time is roughly a factor 10, which shows that group-wise source biasing can be an effective tool for efficiency boosting.

In an actual Monte Carlo simulation with optimal biasing, the weight windows is as in Table 6.7.

$\overline{W}_2 = 0.545946$	$\overline{W}_1 = 1.553846$
$W_{th2} = 0.046295$	$W_{th1} = 0.13176$
$W_{s2} = 0.092589$	$W_{s1} = 0.263523$
$W_{split2} = 0.416653$	$W_{split1} = 1.18586$

Table 6.7: Weight window bounds in an actual Monte Carlo simulation, resulting from the minimization of $f(W)$ for the infinite, two-group system. The biased, initial weights are also depicted.

Further investigation would require extending the theory to include more energy groups. Another possibility is to examine more complicated systems by means of modified deterministic transport codes. Chapter 7 therefore deals with the derivation of equations which may be suitable for implementation in such deterministic codes.

Chapter 7

Integro-differential forms

It has been demonstrated that the theory regarding a priori calculation of variance and efficiency is correct and can be used to obtain an optimal choice of weight window thresholds and biasing functions. In any realistic system there is no hope of finding exact solutions to the variance and efficiency equations and it is therefore necessary to be able to solve them numerically. Numerical approximations may be attempted with Monte Carlo, employing the adjoint Monte Carlo formalism of appendix B with additional modifications arising due to the weight dependence. This may be possible in some cases, but will likely lead to unacceptable computing times when treating realistic systems, because the integrals that need to be solved are more complex than the actual neutron transport problem to begin with.

Another option is to try to use existing deterministic neutron transport codes. These codes solve an integro-differential form of the neutron transport equation, Eq. (2.13). Usually they can also handle the equation adjoint to Eq. (2.13). The equations that need to be solved to find an expression for the efficiency of a Monte Carlo simulation, derived in chapter 4, are not in a form that is suitable for direct implementation in such codes and therefore some interpretation will be necessary. To better see what the differences and similarities are between the equation that is solved with the existing deterministic neutron transport codes and the relevant equations from chapter 4, it is first necessary to transform the purely integral form to an integro-differential form.

As stated in the beginning of chapter 2, the purely integral form of neutron transport, expressed in terms of the collision and emission density, can be obtained from the integro-differential form by applying analytic techniques [Bell and Glasstone, 1970]. The idea of the following derivations is that we will first derive an integral equation from the integro-differential form. Once the solution is obtained we will follow this route backward to arrive at a result which allows an integral equation of a particular form to be written as an integro-differential equation. Applying this result to the equations from chapter 4 allows us to further investigate how to manipulate the existing

deterministic neutron transport codes to cope with the integro-differential form of, for example, the second moment equation or the number of collisions equation.

The equations derived in chapter 4 contained operators with an adjoint kernel $K(P \to P')$. As a consequence it is to be expected that the equivalent integro-differential equation will also be of an adjoint form.

7.1 From integro-differential to integral form

Let us first state the adjoint Boltzmann equation

$$\begin{aligned} &-\boldsymbol{\Omega}\cdot\nabla\chi^*(P)+\Sigma_t(\boldsymbol{r},E)\chi^*(P)\\ &=\int_{4\pi}\int\Sigma_t(\boldsymbol{r},E)C(\boldsymbol{r},E\to E',\boldsymbol{\Omega}\to\boldsymbol{\Omega}')\chi^*(\boldsymbol{r},E',\boldsymbol{\Omega}')dE'd\boldsymbol{\Omega}'+\eta_\phi(P) \end{aligned} \tag{7.1}$$

From Eq. (2.42) it becomes clear that the right hand side of Eq. (7.1) can be rewritten to obtain

$$-\boldsymbol{\Omega}\cdot\nabla\chi^*(P)+\Sigma_t(\boldsymbol{r},E)\chi^*(P)=\Sigma_t(\boldsymbol{r},E)\psi^*(P) \tag{7.2}$$

For sake of simplicity we will assume that the total cross section is a constant. The following derivation can also be done without this simplification but the notation will become needlessly complicated and the final result remains unchanged, [Bell and Glasstone, 1970].

Let us write $\boldsymbol{r}=\boldsymbol{r}_0+s\boldsymbol{\Omega}$, in which $s=|\boldsymbol{r}-\boldsymbol{r}_0|$ represents the path length between the two positions $\boldsymbol{r}$ and $\boldsymbol{r}_0$. Taking the derivative of χ^* with respect to s we see that

$$\frac{d\chi^*(\boldsymbol{r}_0+s\boldsymbol{\Omega})}{ds}=\frac{\partial\chi^*}{\partial x}\frac{dx}{ds}+\frac{\partial\chi^*}{\partial y}\frac{dy}{ds}+\frac{\partial\chi^*}{\partial z}\frac{dz}{ds}=\boldsymbol{\Omega}\cdot\nabla\chi^*(\boldsymbol{r}) \tag{7.3}$$

We may now rewrite Eq. (7.2) as

$$\begin{aligned} &-\frac{d}{ds}\chi^*(\boldsymbol{r}_0+s\boldsymbol{\Omega},E,\boldsymbol{\Omega})+\Sigma_t\chi^*(\boldsymbol{r}_0+s\boldsymbol{\Omega},E,\boldsymbol{\Omega})\\ &=\Sigma_t\psi^*(\boldsymbol{r}_0+s\boldsymbol{\Omega},E,\boldsymbol{\Omega}) \end{aligned} \tag{7.4}$$

Multiplying Eq. (7.4) by an integrating factor $\exp(-\Sigma_t s)$, we get

$$-\frac{d}{ds}\left(\chi^*(\boldsymbol{r}_0+s\boldsymbol{\Omega},E,\boldsymbol{\Omega})e^{-\Sigma_t s}\right)=\Sigma_t e^{-\Sigma_t s}\psi^*(\boldsymbol{r}_0+s\boldsymbol{\Omega},E,\boldsymbol{\Omega}) \tag{7.5}$$

Now integrate Eq. (7.5) from $0\to\infty$

$$\begin{aligned} &-\int_0^\infty\frac{d}{ds}\left(\chi^*(\boldsymbol{r}+s\boldsymbol{\Omega},E,\boldsymbol{\Omega})e^{-\Sigma_t s}\right)ds=\chi^*(\boldsymbol{r},E,\boldsymbol{\Omega})\\ &=\int_0^\infty\Sigma_t e^{-\Sigma_t s}\psi^*(\boldsymbol{r}+s\boldsymbol{\Omega},E,\boldsymbol{\Omega})ds \end{aligned} \tag{7.6}$$

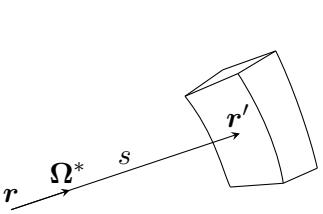

$$
\begin{aligned}
d\boldsymbol{A} &= s^2 d\boldsymbol{\Omega}^* \\
dV' &= s^2 d\boldsymbol{\Omega}^* ds \\
s &= |\boldsymbol{r}' - \boldsymbol{r}| \\
\boldsymbol{r}' &= \boldsymbol{r} + s\boldsymbol{\Omega}^* \\
\boldsymbol{\Omega}^* &= (\boldsymbol{r}' - \boldsymbol{r})/s
\end{aligned}
$$

Figure 7.1: Volume element with local coordinates used for the volume integration.

in which we've replaced $\boldsymbol{r}_0 = \boldsymbol{r}$.

It is convenient to write the right hand side of Eq. (7.6) as a volume integral. To that end, local spherical coordinates $(s, \boldsymbol{\Omega}^*)$ are introduced as in Fig. 7.1. Using these definitions we may proceed to write Eq. (7.6) as

$$\chi^*(\boldsymbol{r}, E, \boldsymbol{\Omega}) = \int_{4\pi} \int_0^\infty \Sigma_t e^{-\Sigma_t s} \psi^*(\boldsymbol{r} + s\boldsymbol{\Omega}, E, \boldsymbol{\Omega}) \delta(\boldsymbol{\Omega} - \boldsymbol{\Omega}^*) \frac{s^2 d\boldsymbol{\Omega}^* ds}{s^2} \tag{7.7}$$

Writing out the definitions from Fig. 7.1 results in

$$\chi^*(\boldsymbol{r}, E, \boldsymbol{\Omega}) = \int \Sigma_t e^{-\Sigma_t s} \psi^*(\boldsymbol{r}', E, \boldsymbol{\Omega}) \delta\left(\boldsymbol{\Omega} - \frac{\boldsymbol{r}' - \boldsymbol{r}}{|\boldsymbol{r}' - \boldsymbol{r}|}\right) \frac{dV'}{|\boldsymbol{r}' - \boldsymbol{r}|^2} \tag{7.8}$$

We could have taken into account the spatial dependence of the macroscopic cross section by introducing an integrating factor $\exp\left(-\int_0^s \Sigma_t(\boldsymbol{r}_0 + s'\boldsymbol{\Omega}, E) ds'\right)$, in stead of $\exp(-\Sigma_t s)$, before proceeding with Eq. (7.5). Taking the spatial dependence into account we can see that the right hand side of Eq. (7.8) contains the transition kernel adjoint to Eq. (2.16).

$$
\begin{aligned}
\chi^*(\boldsymbol{r}, E, \boldsymbol{\Omega}) &= \int \Sigma_t(\boldsymbol{r}', E) \exp\left\{-\int_0^{|\boldsymbol{r}'-\boldsymbol{r}|} \Sigma_t(\boldsymbol{r} + s\boldsymbol{\Omega}, E) ds\right\} \\
&\times \frac{\delta\left(\boldsymbol{\Omega} - \frac{\boldsymbol{r}'-\boldsymbol{r}}{|\boldsymbol{r}'-\boldsymbol{r}|}\right)}{|\boldsymbol{r}' - \boldsymbol{r}|^2} \psi^*(\boldsymbol{r}', E, \boldsymbol{\Omega}) dV' \\
&= \int T(\boldsymbol{r} \to \boldsymbol{r}', E, \boldsymbol{\Omega}) \psi^*(\boldsymbol{r}', E, \boldsymbol{\Omega}) dV'
\end{aligned} \tag{7.9}
$$

and that we have arrived at Eq. (2.41).

It is now time to follow the route backwards from integral to integro-differential form.

7.2 From integral to integro-differential form

Consider an equation of the form

$$f(\boldsymbol{r}, E, \boldsymbol{\Omega}) = \int T(\boldsymbol{r} \to \boldsymbol{r}', E, \boldsymbol{\Omega}) g(\boldsymbol{r}', E, \boldsymbol{\Omega}) dV' \tag{7.10}$$

and let us again assume, for sake of simplicity, that the total cross section is independent of position. From Fig. 7.1, and like in Eq. (7.7) and Eq. (7.6) we can write Eq. (7.10) as

$$\begin{aligned} &- \int_0^\infty \frac{d}{ds} \left\{ f(\boldsymbol{r} + s\boldsymbol{\Omega}, E, \boldsymbol{\Omega}) e^{-\Sigma_t s} \right\} ds \\ &= \int_0^\infty \Sigma_t e^{-\Sigma_t s} g(\boldsymbol{r} + s\boldsymbol{\Omega}, E, \boldsymbol{\Omega}) ds \end{aligned} \tag{7.11}$$

As this should hold for any value of $\Sigma_t \in [0, \infty)$ it is reasonable to assume that the arguments under the integral are equal for any s in the domain of integration and we can therefore write

$$\begin{aligned} &- \frac{d}{ds} \left(f(\boldsymbol{r} + s\boldsymbol{\Omega}, E, \boldsymbol{\Omega}) e^{-\Sigma_t s} \right) \\ &= \Sigma_t e^{-\Sigma_t s} g(\boldsymbol{r} + s\boldsymbol{\Omega}, E, \boldsymbol{\Omega}) \end{aligned} \tag{7.12}$$

from which we can see that.

$$-\boldsymbol{\Omega} \cdot \nabla f(P) + \Sigma_t(\boldsymbol{r}, E) f(P) = \Sigma_t(\boldsymbol{r}, E) g(P) \tag{7.13}$$

It is now possible to write an equation of the form Eq. (7.10) as Eq. (7.13). The interrelation between $f(P)$ and $g(P)$ then determines what the final equation will look like.

The necessary boundary condition can be obtained from Eq. (7.10)

$$f(\boldsymbol{r}_b, E, \boldsymbol{\Omega}_{out}) = 0 \tag{7.14}$$

in which $\boldsymbol{r}_b$ represents a boundary position and $\boldsymbol{\Omega}_{out}$ represents the outward direction at $\boldsymbol{r}_b$.

7.3 The second moment equation for collision estimators

The second moment of the score for a particle entering a collision at P, Eq. (4.33), contains an integral over the second moment at a post-event weight and two other 'source' terms which, for notational convenience, are written here as $\Lambda(P, W)$.

$$\begin{aligned} \Lambda(P, W) = W^2 I_0(P) + z_N(P, \kappa(P)W) W^2 \frac{N_{split} - 1}{N_{split}} \\ \times \kappa(P) \int K(P \to P') M_1^2(P') dP' \end{aligned} \tag{7.15}$$

Easing notation further by taking the event probabilities and the normalization of the kernel together to form

$$z(P, W) = \kappa(P)^{-1} \left\{ z_1(P, \kappa(P)W) + N z_N(P, \kappa(P)W) \right\} \tag{7.16}$$

Eq. (4.33) can be written as

$$M_2(P,W) = \Lambda(P,W) + z(P,W)\int\int C(\boldsymbol{r}, E \to E', \boldsymbol{\Omega} \to \boldsymbol{\Omega}') \times Q(\boldsymbol{r}, E', \boldsymbol{\Omega}', W^*(P, \kappa(P)W))dE'd\boldsymbol{\Omega}' \tag{7.17}$$

In this form the transition kernel is contained in the quantity Q. Notice that

$$Q(\boldsymbol{r}, E, \boldsymbol{\Omega}, W) = \int T(\boldsymbol{r} \to \boldsymbol{r}', E, \boldsymbol{\Omega}) M_2(\boldsymbol{r}', E, \boldsymbol{\Omega}, W)dV' \tag{7.18}$$

and note that this is exactly, asides from the weight dependence, the same form as Eq. (7.10). We can therefore proceed by stating the integro-differential form directly as

$$-\boldsymbol{\Omega} \cdot \nabla Q(P,W) + \Sigma_t(\boldsymbol{r}, E)Q(P,W) = \Sigma_t(\boldsymbol{r}, E)M_2(P,W) \tag{7.19}$$

Using the second moment definition from Eq. (7.17) we arrive at

$$\begin{aligned} &-\boldsymbol{\Omega} \cdot \nabla Q(P,W) + \Sigma_t(\boldsymbol{r}, E)Q(P,W) = \Sigma_t(\boldsymbol{r}, E)\Lambda(P,W) \\ &+ \Sigma_t(\boldsymbol{r}, E)z(P,W)\int\int C(\boldsymbol{r}, E \to E', \boldsymbol{\Omega} \to \boldsymbol{\Omega}') \\ &\times Q(\boldsymbol{r}, E', \boldsymbol{\Omega}', W^*(P, \kappa(P)W))dE'd\boldsymbol{\Omega}' \end{aligned} \tag{7.20}$$

with boundary condition

$$Q(\boldsymbol{r}_b, E, \boldsymbol{\Omega}_{out}, W) = 0 \tag{7.21}$$

Assuming that we are able to solve for $Q(P,W)$, more on that issue in section 7.6, the only thing that remains is using Eq. (7.17) or Eq. (7.19) to obtain the second moment of the score.

7.4 The number of collisions equation

For the number of collisions, Eq. (4.40), we write

$$n(P,W) = \varsigma(P) + z(P,W)\int\int C(\boldsymbol{r}, E \to E', \boldsymbol{\Omega} \to \boldsymbol{\Omega}') \times F(\boldsymbol{r}, E', \boldsymbol{\Omega}', W^*(P, \kappa(P)W))dE'd\boldsymbol{\Omega}' \tag{7.22}$$

in which $z(P,W)$ is as in Eq. (7.16) and

$$F(P,W) = \int T(\boldsymbol{r} \to \boldsymbol{r}', E, \boldsymbol{\Omega}) n(\boldsymbol{r}', E, \boldsymbol{\Omega}, W)dV' \tag{7.23}$$

is the form we are looking for. The full equation can therefore be written as

$$
\begin{aligned}
&-\boldsymbol{\Omega}\cdot\nabla F(P,W)+\Sigma_t(\boldsymbol{r},E)F(P,W)=\Sigma_t(\boldsymbol{r},E)n(P,W)\\
&=\Sigma_t(\boldsymbol{r},E)\varsigma(P)+\Sigma_t(\boldsymbol{r},E)z(P,W)\int\int C(\boldsymbol{r},E\rightarrow E',\boldsymbol{\Omega}\rightarrow\boldsymbol{\Omega}')\\
&\times F(\boldsymbol{r},E',\boldsymbol{\Omega}',W^*(P,\kappa(P)W))dE'd\boldsymbol{\Omega}'
\end{aligned}
\tag{7.24}
$$

with boundary condition

$$
F(\boldsymbol{r}_b,E,\boldsymbol{\Omega}_{out},W)=0 \tag{7.25}
$$

Once $F(P,W)$ is obtained, $n(P,W)$ is calculated from Eq. (7.24).

7.5 Track-length estimators

The most commonly used estimator in practice will be a track-length estimator. It is therefore necessary to treat the integro-differential form of the second moment equation for the track-length estimator here. Recall that for the derivation we looked at a neutron starting a flight rather than a neutron entering a collision. This meant that, from Fig. 4.3, there was first a transition from $\boldsymbol{r}$ to $\boldsymbol{r}'$. Recall $P_e=(\boldsymbol{r}',E,\boldsymbol{\Omega})$ and write Eq. (4.53) as follows

$$
\begin{aligned}
&M_{2tl}(P,W)=\int T(P\rightarrow P_e)S_{tl}(P_e)dV'+\int T(P\rightarrow P_e)z(P_e,W)\\
&\times\int\int C(P_e\rightarrow P')M_{2tl}(P',W^*(P_e,\kappa(P_e)W))dE'd\boldsymbol{\Omega}'dV'
\end{aligned}
\tag{7.26}
$$

from which the integro-differential form can immediately be obtained.

$$
\begin{aligned}
&-\boldsymbol{\Omega}\cdot\nabla M_{2tl}(P,W)+\Sigma_t(\boldsymbol{r},E)M_{2tl}(P,W)=\Sigma_t(\boldsymbol{r},E)S_{tl}(P,W)\\
&+\Sigma_t(\boldsymbol{r},E)z(P,W)\int\int C(\boldsymbol{r},E\rightarrow E',\boldsymbol{\Omega}\rightarrow\boldsymbol{\Omega}')\\
&\times M_{2tl}(\boldsymbol{r},E',\boldsymbol{\Omega}',W^*(P,\kappa(P)W))dE'd\boldsymbol{\Omega}'
\end{aligned}
\tag{7.27}
$$

The boundary condition is

$$
M_{2tl}(\boldsymbol{r}_b,E,\boldsymbol{\Omega}_{out},W)=0 \tag{7.28}
$$

We see that the different interpretation of the adjoint kernels $K(P\rightarrow P')$ and $L(P\rightarrow P')$ leads to a different interpretation of the equivalent integro-differential equations for the respective second moments. The result of (7.27) is actually more appealing than Eq. (7.20) as it is in closed form already; solving the equation immediately returns the second moment. The integral form, Eq. (4.53) was most definitely less appealing than Eq. (4.33).

For the number of collisions equation, Eq. (4.56), derived for a particle starting a flight we can write the following

$$
\begin{aligned}
&-\boldsymbol{\Omega}\cdot\nabla n_{tl}(P,W)+\Sigma_t(\boldsymbol{r},E)n_{tl}(P,W)=\Sigma_t(\boldsymbol{r},E)\varsigma(P)\\
&+\Sigma_t(\boldsymbol{r},E)z(P,W)\int\int C(\boldsymbol{r},E\rightarrow E',\boldsymbol{\Omega}\rightarrow\boldsymbol{\Omega}')\\
&\times n_{tl}(\boldsymbol{r},E',\boldsymbol{\Omega}',W^*(P,\kappa(P)W))dE'd\boldsymbol{\Omega}'
\end{aligned}
\tag{7.29}
$$

with boundary condition

$$
n_{tl}(\boldsymbol{r}_b,E,\boldsymbol{\Omega}_{out},W)=0 \tag{7.30}
$$

7.6 Practical implementation

There are several complications one faces when trying to obtain $\mathrm{Var}(W)$ and $N_c(W)$ by means of an algorithm, based on the possibility of solving the moment and number of collision equations at a certain weight with an existing deterministic neutron transport code.

First there is the choice which equations are the best starting point. While the integral forms of the second moment equation and the number of collisions equations for a particle entering a collision were more appealing than the integral forms of the equations for a particle starting a flight, it is the other way around for the integro-differential form. Asides from this fact there is the possibility to treat both collision estimators and track-length estimators with Eq. (7.27), given a proper choice of the scoring function $\eta_\psi(P,P_e)$. This is not the case for Eq. (7.20) because it can only handle collision estimators.

Now suppose the second moment and number of collisions are available at a certain weight. It is still a matter of evaluating the weighted integrals, for example $N_c(W)=\int S_1(P)n(P,W)dP$, to obtain the variance and number of collisions at a certain weight. Evaluating integrals containing the source of first collisions is less appealing from a practical point of view as the physical source will be available and the source of first collisions has to be calculated.

Calculating the source of first collisions can obviously be done by means of a deterministic code. The integro-differential form follows from the results obtained in previous sections quite readily

$$
\boldsymbol{\Omega}\cdot\nabla S_1(P)+\Sigma_t(\boldsymbol{r},E)S_1(P)=\Sigma_t(\boldsymbol{r},E)S(P) \tag{7.31}
$$

with boundary condition

$$
S_1(\boldsymbol{r}_b,E,\boldsymbol{\Omega}_{in})=0 \tag{7.32}
$$

Comparing Eq. (7.31) with Eq. (2.13) we see that, in order to obtain a solution, the correct source has to be given as input and scattering has to be put to zero.

The real difficulty lies in how to handle the weight dependence and how to handle the modified collision probabilities. Deterministic codes solve an equation of the form Eq. (7.1). The source is not an issue as it can simply be specified for any weight. The collision kernel, however, has to be modified according to

$$\tilde{C}(\boldsymbol{r}, E \to E', \boldsymbol{\Omega} \to \boldsymbol{\Omega}', W) = z(P, W) C(\boldsymbol{r}, E \to E', \boldsymbol{\Omega} \to \boldsymbol{\Omega}') \tag{7.33}$$

In existing deterministic neutron transport codes like PARTISN [Alcouffe and Baker, 2005], XSDRN [Green and Petrie, 1998], and DALTON [van Rooijen and Lathouwers, 2007], energy dependence is treated in energy groups g and discrete angles $\boldsymbol{\Omega}_m$ are used to treat angular dependence. Under the assumption that only a scattering event produces neutrons at the new energy and direction we can write the collision kernel as

$$C(\boldsymbol{r}, E \to E', \boldsymbol{\Omega} \to \boldsymbol{\Omega}') = \frac{\Sigma_s^{gg'}(\boldsymbol{r})}{\Sigma_s^g(\boldsymbol{r})} p(\boldsymbol{\Omega}_m \cdot \boldsymbol{\Omega}_{m'} | g \to g') \tag{7.34}$$

in which $p(\boldsymbol{\Omega}_m \cdot \boldsymbol{\Omega}_{m'} | g \to g')$ represents the probability to have a change in direction from $\boldsymbol{\Omega}_m$ to $\boldsymbol{\Omega}_{m'}$ given a change in energy from group g to g'. The scalar product stems from the fact that scattering usually only depends on the scattering angle cosine $\boldsymbol{\Omega}_m \cdot \boldsymbol{\Omega}_{m'}$

Somehow we have to incorporate $z(P, W)$ in the group-scatter cross sections. Strictly, $z(P, W)$ may still depend on direction, but we will drop this dependence as it will rarely be encountered in practice. We write a modified group scatter cross section as

$$\begin{aligned} \tilde{\Sigma}_s^{gg'}(\boldsymbol{r}, W) &= z(\boldsymbol{r}, g, W) \Sigma_s^{gg'}(\boldsymbol{r}) \\ &= \frac{\Sigma_t^g(\boldsymbol{r})}{\Sigma_s^g(\boldsymbol{r})} \left\{ z_1(\boldsymbol{r}, g, \kappa(\boldsymbol{r}, g) W) + N z_N(\boldsymbol{r}, g, \kappa(\boldsymbol{r}, g) W) \right\} \Sigma_s^{gg'}(\boldsymbol{r}) \end{aligned} \tag{7.35}$$

The event-probabilities $z_N(\boldsymbol{r}, g, \kappa(\boldsymbol{r}, g) W)$ and $z_0(\boldsymbol{r}, g, \kappa(\boldsymbol{r}, g) W)$ need to be calculated for a certain weight and possibly as a function of position. The cross section library has to be modified subsequently to arrive at a proper collision kernel.
Suppose this all works out, we can for example write Eq. (7.27) as

$$\begin{aligned} &- \boldsymbol{\Omega_m} \cdot \nabla n_{tl}(\boldsymbol{r}, g, \boldsymbol{\Omega}_m, W) + \Sigma_t(\boldsymbol{r}, g) n_{tl}(\boldsymbol{r}, g, \boldsymbol{\Omega}_m, W) = \tilde{\varsigma}(\boldsymbol{r}, g, \boldsymbol{\Omega}_m) \\ &+ \sum_{g'} \sum_{m'} \Sigma_t(\boldsymbol{r}, g) \tilde{C}(\boldsymbol{r}, g \to g', \boldsymbol{\Omega}_m \to \boldsymbol{\Omega}_{m'}, W) n_{tl}(\boldsymbol{r}, g', \boldsymbol{\Omega}_{m'}, W^*) \end{aligned} \tag{7.36}$$

in which $W^* = W^*(\boldsymbol{r}, g, \boldsymbol{\Omega}_m, \kappa(\boldsymbol{r}, g) W)$ and $\tilde{\varsigma}(\boldsymbol{r}, g, \boldsymbol{\Omega}_m) = \Sigma_t(\boldsymbol{r}, g) \varsigma(\boldsymbol{r}, g, \boldsymbol{\Omega}_m)$.

Despite Eq. (7.36) having the correct form to be solved by means of a deterministic code, the issue of the pre- and post-event weights not being equal remains.

At this point suppose that there is a constant weight window (in both energy and space), a constant κ and that always $\kappa(P)W_s \leq W_{th}$. Under these restrictions Eq. (7.36) at survival weight, or any of the above equations for that matter, can be written in the following form

$$\begin{aligned} &- \boldsymbol{\Omega}_m \cdot \nabla n_{tl}(\boldsymbol{r}, g, \boldsymbol{\Omega}_m, W_s) + \Sigma_t(\boldsymbol{r}, g) n_{tl}(\boldsymbol{r}, g, \boldsymbol{\Omega}_m, W_s) = \tilde{\varsigma}(\boldsymbol{r}, g, \boldsymbol{\Omega}_m) \\ &+ \sum_{g'} \sum_{m'} \Sigma_t(\boldsymbol{r}, g) \tilde{C}(\boldsymbol{r}, g \rightarrow g', \boldsymbol{\Omega}_m \rightarrow \boldsymbol{\Omega}_{m'}, W_s) \\ &\times n_{tl}(\boldsymbol{r}, g', \boldsymbol{\Omega}_{m'}, W_s) \end{aligned} \tag{7.37}$$

with boundary condition

$$n_{tl}(\boldsymbol{r}_b, g, \boldsymbol{\Omega}_{m,out}) = 0 \tag{7.38}$$

This equation is self consistent, in the correct form and can therefore be solved by means of a deterministic code. Once the solution of this equation is obtained, solutions at any weight can in principle be obtained by going from very low, approaching zero, weights to progressively higher weights. This is due to the fact that the post-event weight W^* will always be equal to the survival weight or lower than the pre-event weight, in which case the solution is available. Obviously also the equations for the only implicit capture and analog situations can be solved as there is no weight dependence present in that case.

Omitting the restrictions regarding the energy and spatial dependence of both weight window and non-absorption probability and also that $\kappa(P)W_s \nleq W_{th}$, will seriously complicate matters. We will not try to give an answer here as to how these complications can be overcome. In chapter 5 a great deal of effort went into solving issues like these. For general applications one would need to devise a smart, automated algorithm to handle the weight dependence.

Chapter 8

Discussion and Conclusions

8.1 Discussion

In chapter 4 the cost as a function of initial weight $f(W)$, a multiplication of expected variance and number of collisions resulting from a single neutron history, was introduced as a workable alternative to the Figure Of Merit. The necessary moment and number of collisions equations were derived from a probability score distribution, which proved to be a powerful and versatile concept. Despite the fact that the most commonly used non-analog simulation techniques were treated in this work, there are numerous other non-analog techniques possible, all of which would require their own derivation of moment and number of collisions equations. The formalism presented in chapter 4 should now make these derivations possible in most cases.

The derivations presented in chapter 4 were, however, concerned with fixed source problems. Dealing with a fission source, in which case the neutron transport equation becomes an eigenvalue equation for the effective multiplication factor k_{eff}, will require some extensions of the theory in order to arrive at an expression for the cost/efficiency of a simulation.

In practice, an initial fission source distribution is guessed, and after a number of cycles this distribution converges to the correct distribution, [Sjenitzer, 2009]. Collisions of neutrons may lead to fission events which generate the source for the next cycle. Despite this difference, once the correct eigenfunction is obtained we essentially still have a fixed source problem to which the formalism presented in chapter 4 is applicable. As an approximation the fission source may, for example, be calculated with an existing deterministic neutron transport code and used as input. The generation of offspring will not likely lead to complications[1] in the derivation of moment and number of collisions equations.

Exact analytic solutions to the variance and efficiency equations are dif-

[1] A splitting event may actually be considered as the production of offspring during a collision, which allows the concepts from section 4.3 to be used for the treatment of fission.

ficult, if not impossible, to obtain for any realistic simulation. Nevertheless, exact solutions to equations describing the efficiency of a Monte Carlo simulation in which the response is obtained with a collision estimator were found in chapter 5 for the simplified two-directional transport model. Most work went into solving issues arising from the fact that the equations contained different pre- and post-event weights. The expressions derived in 5 were put to the test in chapter 6. Numerous analytic computations were performed, all of which matched the results from Monte Carlo simulations perfectly, giving full confidence that the theory derived in chapter 4 is correct. The global minimum of the cost function was established at a particular choice of weight window thresholds.

From the investigation it followed that setting the weight window lower bound (the Russian roulette threshold weight W_{th}) has the largest effect on the overall cost/efficiency. The choice of survival weight and weight window upper bound (the splitting threshold W_{split}) have a marginal influence on the total cost. These parameters largely determine the discontinuities in the cost function but do not lead to a dramatic increase/decrease in cost.

It was shown that in some cases splitting is to be avoided from an efficiency perspective, leading to a lower bound for β (the ratio of the splitting and Russian roulette threshold). The default value in the general purpose Monte Carlo code MCNP for β is 5, which is quite close to the lower bound found for both the one-group finite system and the two-group infinite system. This poses the question if $\beta = 5$ will generally be best. $\alpha = 2$, the ratio of the survival weight threshold to the Russian roulette threshold, showed the best results consistently. From the simple systems studied in this work it is impossible to infer generalizations regarding the choice of parameters like α and β. It does show that an optimal choice can, and should, be given for each particular simulation and that the tools presented in this work allow to find an optimal choice in principle.

For a two-group infinite system, section 5.4 and 6.2, exact expressions were also obtained. The weight window was allowed to vary per group, which required extra effort to treat all the subtleties arising from the weight dependence of the equations. From a large number of computations it was shown that the analytic results agreed fully with results from Monte Carlo simulations and that in this case also an optimal choice of weight window thresholds can be obtained by minimizing the cost function.

Source biasing computations were also performed, which interestingly showed that biasing the source distribution with the adjoint flux is not necessarily the best option. Further investigation is required because in practice, biasing the source with the adjoint is an accepted strategy and it may turn out that this is not optimal.

If source biasing is implemented, the initial neutron weight becomes a function of phase space as well. The group wise effects have been studied and showed that it is best to choose the group weight window such that the neutron

should neither split nor play Russian roulette immediately at its first collision. This is a confirmation of what is accepted in practice. Further investigation is of course needed, especially of the spatial dependence.

Chapters 5 and 6 showed that in order to be able to use the theory in practice, numerical approximations to the variance and efficiency equations will be a necessity since analytic solutions are hard to come by.

The integro-differential forms derived in chapter 7 showed a number of interesting things. The moment and number of collisions equations for a track-length estimator (derived for neutrons starting a flight) have an appealing integro-differential form, whereas the integral form was rather unappealing. This observation is encouraging since track-length estimators are used most frequently in practice. As a side note, a proper choice of scoring function allows these expressions to be used for a collision estimator as well. It is not hard to incorporate the modified collision probabilities, now a function of weight, into a modified collision kernel. The efficiency of analog simulations and simulations containing only implicit capture can be obtained with only modest modifications.

The complications arising from the difference in pre- and post-event weights, however, remain. In chapters 5 and 6 some examples were given as to how to deal with these problems but the possibility of dealing with spatially varying weight windows, common in practice, was not treated. An algorithm needs to be devised to deal with this issue for the theory to be applied in a general context. Once such an algorithm exists, cost minimization can be employed to quickly initiate a particular simulation in an optimal way, general 'rules of thumb' like biasing the source with the adjoint flux and accepting default parameters like $\beta = 5$ can be studied. Essentially, the efficiency of practically all neutron transport Monte Carlo simulations would benefit from the development of such an algorithm.

8.2 Conclusions

- It is possible to obtain expressions for the a priori calculation of variance and efficiency of a neutron transport Monte Carlo simulation for a variety of non-analog simulation strategies.

- The formalism in which moment and number of collision equations are derived from a probability score distribution allows for easy extension to other simulation strategies and possibly to Monte Carlo applications in other fields as well.

- It is best to start the derivation of the cost function at a neutron entering a collision when using a collision estimator and at a neutron starting a flight when using a track-length estimator.

- Exact analytical expressions for the efficiency can be obtained for simple systems. Any realistic system will render this possibility obsolete.
- The cost function can be used for the a priori optimization of weight window thresholds and for finding optimal source biasing functions. Numerical results from actual Monte Carlo simulations show exact agreement with the analytical results obtained in this work.
- For the practical implementation of the theory presented in this work it will be necessary to devise an algorithm to cope with the weight dependence in the integro-differential form of the moment and number of collisions equations.
- Although it is impossible to infer generalizations from the two systems studied in this work, it has been shown that one needs to tread carefully when accepting general rules of thumb like biasing with a specific importance function or using default weight window thresholds, as it is questionable if these rules of thumb will be best in a particular situation.
- The theory of cost minimization to optimize neutron transport Monte Carlo simulation strategies a priori shows great potential and, if future developments lead to a quick and automated algorithm to perform (approximated) cost minimization, may significantly increase computational efficiency.

Bibliography

R. E. Alcouffe and R. S. Baker. Partisn: A time-dependent, parallel neutral particle transport code system. Technical Report LA-UR-05-3925, Los Alamos National Laboratory, 2005. [cited at p. 94]

G. I. Bell and S. Glasstone. *Nuclear Reactor Theory*. van Nostrand Reinhold, 1970. [cited at p. 10, 12, 87, 88]

J. G. Christiano. Differentiation of the repeated integral. *The American Mathematical Monthly*, 66(2):127–129, 1959. [cited at p. 52]

R. R. Coveyou and K. J. Yost V. R. Cain. Adjoint and importance in monte carlo application. *Nuclear Science and Engineering*, 27:219–234, 1967. [cited at p. 30]

J. J. Dunderstadt and L. J. Hamilton. *Nuclear Reactor Analysis*. John Wiley and sons, 1976. [cited at p. 3, 9, 10]

N. M. Green and L. M. Petrie. Xsdrnpm: A one-dimensional discrete ordinates code for transport analysis. NUREG/CR-0200 ORNL/NUREG/CSD-2/V2/R6, Oak Ridge National Laboratory, 1998. [cited at p. 78, 94]

A. Haghighat and J. C. Wagner. Monte carlo variance reduction with deterministic importance functions. *Progress in nuclear energy*, 42(1):25–53, 2003. [cited at p. 27]

J. E. Hoogenboom. *Adjoint Monte Carlo Methods in Neutron Transport Calculations*. Delft University Press, 1977. [cited at p. 13, 19, 107]

J. E. Hoogenboom. Theoretical and practical study of the variance and efficiency of a monte carlo calculation due to russian roulette. *Physor*, 160:1–22, 2004. [cited at p. 29]

J. E. Hoogenboom. The two-direction neutral particle transport model: a useful tool for research and education. *Transport theory and statistical physics*, 37:65–108, 2008. [cited at p. 48]

Los Alamos National Laboratories. Mcnp5 a general monte carlo n-particle transport code, version 5. Technical report, University of California, 2008. [cited at p. 27]

I. Lux and L. Koblinger. *Monte Carlo Particle Transport Methods: Neutron and Photon Calculations*. CRC Press, 1991. [cited at p. 12, 19, 23, 24, 29, 30, 103]

P. K. MacKeown. *Stochastic Simulation in Physics.* Springer Verlag, 1997. [cited at p. 5]

C. A. Laury Micoulaut. The nth centred moment of a multiple convolution and its applications in an intercloud gas model. *Astronomy and Astrophysics*, 51:343–346, 1976. [cited at p. 37, 38]

A. C. Pipkin. *A course on integral equations.* Springer Verslag, 1991. [cited at p. 14, 20, 64]

D. Porter and D. S. G. Stirling. *Integral Equations.* Cambridge university press, 1990. [cited at p. 64]

Y. Ronen. *CRC Handbook of Nuclear Reactors Calculations*, volume 3. CRC Press Inc., 1986. [cited at p. 15]

Stochastic signal analysis. *Nuclear Reactor Analysis.* John Wiley and sons, 1976. [cited at p. 103]

B. Sjenitzer. Variance reduction using the correcton method on criticality calculations. Master's thesis, Delft, University of technology, 2009. [cited at p. 97]

J. Spanier and E. M. Gelbard. *Monte Carlo Principles and Neutron Transport Problems.* Addison-Wesley, 1969. [cited at p. 19]

J. M. Thijssen. *Computational Physics.* Cambridge University Press, 2007. [cited at p. 6]

W.F.G. van Rooijen and D. Lathouwers. Sensitivity analysis of the kinetic behaviour of a gas cooled fast reactor to variations of the delayed neutron parameters. In *MC conference Monterey USA*, 2007. [cited at p. 94]

F. Vermolen, J. van Kan, and A. Segal. *Numerical Methods in Scientific Computing.* VSSD, 2008. [cited at p. 3]

Appendix A

Statistics and estimation

Some basic concepts from statistics and some notation used throughout this work require introduction here. The notation is based on [Lux and Koblinger, 1991] and for a more extensive treatment the reader is advised to consult [signal analysis, 1976].

A random variable represents the set of possible outcomes of some random event, like throwing dice (discrete), or the size of a solar flare (continuous). The probabilities associated with these outcomes are characterized by the *probability mass function* pmf (discrete) or *probability density function* pdf (continuous). Furthermore, any function of a random variable will itself be a random variable.

Suppose that we consider a random variable S with associated pdf $\pi(s)$. The expected value of the process $E[S] = \langle S \rangle_\pi$, or in light of applications in chapter 4, the first moment M_1, of this random variable is given by

$$E[S] = \int s\pi(s)ds = M_1 \tag{A.1}$$

for the continuous case. The integral runs over the ensemble of possible outcomes $\{s\}$ and $\pi(s)ds$ represents the probability to get an outcome of s in ds. For the discrete case obviously

$$M_1 = \sum_i s_i \pi(s_i) \tag{A.2}$$

The expected value or first moment represents the average outcome of the random event, described by the random variable S.

A measure for how much the outcomes of the random event will deviate from the average is given by the variance $\mathrm{Var}(S)$.

$$\mathrm{Var}(S) = E[\{S - E[S]\}^2] = E[S^2] - E[S]^2 = M_2 - M_1^2 \tag{A.3}$$

with the second moment $M_2 = E[S^2]$. Most outcomes of the random event are expected to be within one standard deviation $\sigma(S) = \sqrt{\mathrm{Var}(S)}$ from the expected value.

The expectation value and variance or standard deviation are usually enough to characterize the random event. It is possible to extend the theory to higher moments, but this is irrelevant for the purposes of this work.

Suppose now that we only have N independent random observations s_i of the random event and we want to know the expected value and the variance. We can estimate $E[S]$ with the sample mean estimator $\bar{S}$

$$\overline{S} = \frac{1}{N}\sum_{i=1}^{N} s_i \approx E[S] \tag{A.4}$$

in which the approximate sign may be dropped as $(N \to \infty)$, a result better known as the law of large numbers. This estimate is called unbiased;

$$\mathrm{Bias}(\overline{S}) = E[\bar{S}] - E[S] = 0 \tag{A.5}$$

since it delivers the expectation value on average.

The variance may be estimated from the limited number of samples as well. An unbiased estimate of the variance is given by

$$\begin{aligned}\widehat{\mathrm{Var}}(S) &= \frac{1}{N-1}\sum_{i=1}^{N}\left(s_i - \overline{S}\right)^2 \\ &= \frac{1}{N-1}\left\{\sum_{i=1}^{N} s_i^2 - \frac{1}{N}\left(\sum_{i=1}^{N} s_i\right)^2\right\}\end{aligned} \tag{A.6}$$

The devision by $(N-1)$ may be understood as loosing one degree of freedom to the calculation of $\overline{S}$.

The variance in the sample mean estimator is given by

$$\widehat{\mathrm{Var}}(\overline{S}) = \frac{1}{N(N-1)}\left\{\sum_{i=1}^{N} s_i^2 - \frac{1}{N}\left(\sum_{i=1}^{N} s_i\right)^2\right\} = \frac{\widehat{\mathrm{Var}}(S)}{N} \tag{A.7}$$

which shows that the variance in the mean scales with the number of samples. This is another way of expressing the law of large numbers since, given enough samples $(N \to \infty)$ the variance in the sample mean will tend to zero and therefore the sample mean, if unbiased, will tend to the true mean.

Appendix B

Adjoint Monte Carlo

In particular situations, adjoint Monte Carlo may be much better suited to estimate a response. The source and payoff functions are interchanged. Therefore, problems in which the payoff function is nonzero in a small region of phase space and the source is distributed over a large region in phase space, can in principle much better be treated by adjoint Monte Carlo.

The adjoint equations Eq. (2.34) and Eq. (2.36) can in principle be solved by means of Monte Carlo, but there are some complications arising from the adjoint interpretation of the transport kernels. The adjoint transport kernel in the form of a transposition of the forward kernel, $L(P \to P')$, is not well suited for MC implementation. Rather, we need an adjoint kernel of the form $L^*(P' \to P)$, or more explicitly; we are looking for a transformation such that we can play the adjoint game like a forward Monte Carlo game. The derivation that follows can also be done starting from the kernel $K(P \to P')$, but since the adjoint equations are so closely related this is more or less irrelevant for the final result.

As stated we are looking for a relation such that the adjoint Monte Carlo game can be played in a similar fashion as is the case in forward calculations. For the adjoint kernel L we demand the following relation

$$\begin{aligned} L(P \to P') &\equiv T(\boldsymbol{r} \to \boldsymbol{r}', E, \boldsymbol{\Omega}) C(\boldsymbol{r}', E \to E', \boldsymbol{\Omega} \to \boldsymbol{\Omega}') \\ L^*(P' \to P) &= T^*(\boldsymbol{r}' \to \boldsymbol{r}, E, \boldsymbol{\Omega}) C^*(\boldsymbol{r}', E' \to E, \boldsymbol{\Omega}' \to \boldsymbol{\Omega}) \end{aligned} \tag{B.1}$$

Next we will see that it is possible to show an equivalence between the transposed transition kernel and the desired transition kernel. Recall Eq. (2.16) and divide by the total cross section. After some manipulation and using the

substitution $s' = |\boldsymbol{r} - \boldsymbol{r}'| - s$ we see

$$\begin{aligned}\frac{T(\boldsymbol{r} \to \boldsymbol{r}', E, \boldsymbol{\Omega})}{\Sigma_t(\boldsymbol{r}', E)} &= \exp\Big\{ - \int_0^{|\boldsymbol{r}'-\boldsymbol{r}|} \Sigma_t(\boldsymbol{r}' - s\boldsymbol{\Omega}, E) ds \Big\} \frac{\delta(\boldsymbol{\Omega} - \frac{\boldsymbol{r}'-\boldsymbol{r}}{|\boldsymbol{r}-\boldsymbol{r}'|})}{|\boldsymbol{r} - \boldsymbol{r}'|^2} \\ &= \exp\Big\{ - \int_0^{|\boldsymbol{r}-\boldsymbol{r}'|} \Sigma_t(\boldsymbol{r} + s'\boldsymbol{\Omega}, E) ds' \Big\} \frac{\delta(\boldsymbol{\Omega}' + \frac{\boldsymbol{r}-\boldsymbol{r}'}{|\boldsymbol{r}-\boldsymbol{r}'|})}{|\boldsymbol{r} - \boldsymbol{r}'|^2} \\ &= \frac{T(\boldsymbol{r}' \to \boldsymbol{r}, E, -\boldsymbol{\Omega})}{\Sigma_t(\boldsymbol{r}, E)} \end{aligned} \tag{B.2}$$

From which we can obtain a reasonable choice for the adjoint transition kernel, suited for Monte Carlo sampling

$$T^*(\boldsymbol{r}' \to \boldsymbol{r}, E, \boldsymbol{\Omega}) = T(\boldsymbol{r}' \to \boldsymbol{r}, E, -\boldsymbol{\Omega}) \tag{B.3}$$

This is a 'normal' kernel, subject to the same normalization conditions as the regular transition kernel. Given this particular choice for the adjoint transition kernel we can see that apparently the adjoint 'particles' move in the direction opposite to their direction vector. Also from Eq. (B.2) the definition of the adjoint collision kernel can be obtained

$$C^*(\boldsymbol{r}', E' \to E, \boldsymbol{\Omega}' \to \boldsymbol{\Omega}) = \frac{\Sigma_t(\boldsymbol{r}', E)}{\Sigma_t(\boldsymbol{r}, E)} C(\boldsymbol{r}', E \to E', \boldsymbol{\Omega} \to \boldsymbol{\Omega}') \tag{B.4}$$

Note that this kernel is generally not normalized. Together with the definition of the collision kernel from Eq. (2.17) we now arrive at a transport kernel which, subjected to the right normalization conditions, can be sampled for MC purposes by first sampling the adjoint collision kernel for $(E, \boldsymbol{\Omega})$ and afterwards selecting a new collision site $\boldsymbol{r}$ from the adjoint transition kernel.

$$\begin{aligned} L^*(P' \to P) &= \frac{T(\boldsymbol{r}' \to \boldsymbol{r}, E, -\boldsymbol{\Omega}) \Sigma_t(\boldsymbol{r}', E)}{\Sigma_t(\boldsymbol{r}, E)} C^*(\boldsymbol{r}', E' \to E, \boldsymbol{\Omega}' \to \boldsymbol{\Omega}) \\ &= \frac{T(\boldsymbol{r}' \to \boldsymbol{r}, E, -\boldsymbol{\Omega})}{\Sigma_t(\boldsymbol{r}, E)} \\ &\quad \times \sum_A \sum_j \Sigma_{j|A}(\boldsymbol{r}', E) c_{j|A}(E) p_{j|A}(E \to E', \boldsymbol{\Omega} \to \boldsymbol{\Omega}) \end{aligned} \tag{B.5}$$

Although Eq. (B.5) might not seem as a direct improvement, it can be put to good use when the following transformation is made

$$\widetilde{\chi}(P) = \Sigma_t(\boldsymbol{r}, E) \chi^*(P) \tag{B.6}$$

$$\widetilde{\psi}(P) = \Sigma_t(\boldsymbol{r}, E) \psi^*(P) \tag{B.7}$$

This transformation makes sense from a physical point of view as well since the new function $\widetilde{\psi}(P)$, for example, will behave more like an event density,

in stead of a flux like quantity which is less suited for Monte Carlo implementation. We also see the factor $\Sigma_t(\boldsymbol{r}, E)$ in the denominator of Eq. (B.5).

The transformed equation for the transformed adjoint quantity, with respect to Eq. (2.36), can be written as

$$\widetilde{\chi}(P) = f_\chi(P) + \int \widetilde{L^*}(P' \to P)\widetilde{\chi}(P')dP' \tag{B.8}$$

in which

$$f_\chi(P) = \Sigma_t(\boldsymbol{r}, E)\eta_\chi(P) \tag{B.9}$$

The transformed kernel is written as

$$\begin{aligned}\widetilde{L^*}(P' \to P) &= \frac{\Sigma_t(\boldsymbol{r}, E)}{\Sigma_t(\boldsymbol{r}', E')} L^*(P' \to P) = T(\boldsymbol{r}' \to \boldsymbol{r}, E, -\boldsymbol{\Omega}) \\ &\times \sum_A \sum_j \frac{\Sigma_{j|A}(\boldsymbol{r}', E)}{\Sigma_t(\boldsymbol{r}', E')} c_{j|A}(E) p_{j|A}(E \to E', \boldsymbol{\Omega} \to \boldsymbol{\Omega}')\end{aligned} \tag{B.10}$$

The only thing missing now is proper normalization of collision part of the kernel. The normalization factor is given by

$$\begin{aligned}N^*(P') &= \frac{\int\int \sum_A \sum_j \Sigma_{j|A}(\boldsymbol{r}', E) c_{j|A}(E) f_{j|A}(E \to E', \boldsymbol{\Omega} \to \boldsymbol{\Omega}') dE d\boldsymbol{\Omega}}{\Sigma_t(\boldsymbol{r}', E')} \\ &= \frac{\Sigma^*(\boldsymbol{r}', E)}{\Sigma_t(\boldsymbol{r}', E)}\end{aligned} \tag{B.11}$$

The new quantity Σ^* appearing in Eq. (B.11) is called the adjoint cross section. It has some rather special characteristics which go beyond the scope of this thesis. A full treatment of the adjoint cross section can be found in Hoogenboom [1977]. Adjoint simulation can now be done by selecting $(E, \boldsymbol{\Omega})$ from the normalized 'adjoint' collision kernel

$$\begin{aligned}&C_N^*(\boldsymbol{r}', E' \to E, \boldsymbol{\Omega}' \to \boldsymbol{\Omega}) = \\ &\sum_A \sum_j \frac{\Sigma_{j|A}(\boldsymbol{r}', E)}{\Sigma^*(\boldsymbol{r}', E)} c_{j,A}(E) p_{j,A}(E \to E', \boldsymbol{\Omega} \to \boldsymbol{\Omega}')\end{aligned} \tag{B.12}$$

and selecting new collision sites from the transition kernel
$T(\boldsymbol{r}' \to \boldsymbol{r}, E, -\boldsymbol{\Omega})$. From Eq. (2.39) we see that $f_\chi(P)$ acts as a source of first collisions

$$f_\chi(P) = \int f_\psi(\boldsymbol{r}', E, \boldsymbol{\Omega}) T^*(\boldsymbol{r}' \to \boldsymbol{r}, E, \boldsymbol{\Omega}) dV' \tag{B.13}$$

in which $f_\psi(P) = \Sigma_t(P)\eta_\psi(P)$. From Eq. (2.41) and Eq. (2.42) we can deduce the following pair of equations for the transformed adjoint densities

$$\widetilde{\psi}(P) = f_\psi(P) + \int N^*(\boldsymbol{r}, E')C_N^*(\boldsymbol{r}, E' \to E, \boldsymbol{\Omega}' \to \boldsymbol{\Omega})\widetilde{\chi}(\boldsymbol{r}, E', \boldsymbol{\Omega}')dE'd\boldsymbol{\Omega}' \tag{B.14}$$

$$\widetilde{\chi}(P) = \int T(\boldsymbol{r}' \to \boldsymbol{r}, E, -\boldsymbol{\Omega})\widetilde{\psi}(\boldsymbol{r}', E, \Omega)dV' \tag{B.15}$$

For completeness and to see the striking resemblance with the forward situation, Eq. (2.21) and Eq. (2.24), let us express the transformed quantities in terms of themselves at other points in phase space by manipulating the equation pair, Eq. (B.14).

$$\widetilde{\psi}(P) = f_\psi(P) + \int T(\boldsymbol{r}' \to \boldsymbol{r}, E', -\boldsymbol{\Omega}') \times N^*(\boldsymbol{r}, E')C_N^*(\boldsymbol{r}, E' \to E, \boldsymbol{\Omega}' \to \boldsymbol{\Omega})\widetilde{\psi}(\boldsymbol{r}', E', \boldsymbol{\Omega}')dP' \tag{B.16}$$

$$\widetilde{\chi}(P) = f_\chi(P) + \int N^*(\boldsymbol{r}', E')C_N^*(\boldsymbol{r}', E' \to E, \boldsymbol{\Omega}' \to \boldsymbol{\Omega}) \times T(\boldsymbol{r}' \to \boldsymbol{r}, E, -\boldsymbol{\Omega})\widetilde{\chi}(\boldsymbol{r}', E, \Omega)dV' \tag{B.17}$$

from which we can see that $\widetilde{\psi}$ takes on the role of the forward emission density χ and $\widetilde{\chi}$ takes on the role of the forward collision density ψ.

The response can be expressed in terms of the transformed densities as follows

$$R = \int S(P)\frac{\widetilde{\chi}(P)}{\Sigma_t(P)}dP = \int S_1(P)\frac{\widetilde{\psi}(P)}{\Sigma_t(P)}dP \tag{B.18}$$

Now that we've seen how to treat transport the only thing that remains is the source density. Other than the fact that f_ψ need not be normalized this should given no complications. One can sample the normalized pdf $f_\psi(P)/\int f_\psi(P)dP$ and simply multiply the final result by $\int f_\psi(P)dP$.

The series expansion solution of the type two Fredholm integral equation pair, Equations (B.14) is the following

$$\widetilde{\psi}_0(P) = f_\psi(P) \tag{B.19}$$

$$\widetilde{\chi}_0(P) = \int T(\boldsymbol{r}' \to \boldsymbol{r}, E, -\boldsymbol{\Omega})\widetilde{\psi}_0(\boldsymbol{r}', E, \Omega)dV' \tag{B.20}$$

$i + 1 = 1, 2, ..., \infty$

$$\widetilde{\psi}_{i+1}(P) = \int N^*(\boldsymbol{r}, E')C_N^*(\boldsymbol{r}, E' \to E, \boldsymbol{\Omega}' \to \boldsymbol{\Omega})\widetilde{\chi}_i(\boldsymbol{r}, E', \boldsymbol{\Omega}')dE'd\boldsymbol{\Omega}' \tag{B.21}$$

$$\widetilde{\chi}(P)_{i+1} = \int T(\boldsymbol{r}' \to \boldsymbol{r}, E, -\boldsymbol{\Omega})\widetilde{\psi}_{i+1}(\boldsymbol{r}', E, \Omega)dV' \tag{B.22}$$

which directly leads to the Monte Carlo procedure for adjoint transport, depicted in Table B.1.

	Do for N 'particles' from $j = 1...N$
	set $i = 0$ and proceed until leakage or absorption
1:	Sample $f_\psi(P)/\int f_\psi(P)dP$ for initial coordinates $(\boldsymbol{r}_0, E_0, \boldsymbol{\Omega}_0)$
2:	Possibly score at an emission
3:	Sample $T(\boldsymbol{r}_i \rightarrow \boldsymbol{r}_{i+1}, E_i, -\boldsymbol{\Omega})_i$ for next collision site $\boldsymbol{r}_{i+1}$
4:	Possibly score at a collision
5:	Multiply weight by $N^*(\boldsymbol{r}_{i+1}, E_i)$
6:	Sample $C_N^*(\boldsymbol{r}_{i+1}, E_i \rightarrow E_{i+1}, \boldsymbol{\Omega}_i \rightarrow \boldsymbol{\Omega}_{i+1})$ for $(E_{i+1}, \boldsymbol{\Omega}_{i+1})$
	Set $P_i = (\boldsymbol{r}_{i+1}, E_{i+1}, \boldsymbol{\Omega}_{i+1})$ and return to 2:
	Determine $\widehat{R}_j$ from the score collected during history j and proceed with the next history

Table B.1: Monte Carlo procedure for adjoint, non-analog transport.

Appendix C

Coefficients

Let $I_0(x) = A_0 + A_1 \cosh(kx)$ with

$$A_0 = \eta_\phi^2 \left\{ \frac{2}{k^2} - \frac{1}{\Sigma_t^2} \right\}$$
$$A_1 = -\eta_\phi^2 \frac{2}{k^2} \frac{\Sigma_s}{k \sinh(kb) + \Sigma_t \cosh(kb)}$$

and let

$$l = \sqrt{\Sigma_t^2 - \Sigma_s^2}$$

From which the coefficients can be expressed more easily as

$$C_{a0} = \frac{\Sigma_t^2}{k^2} A_0$$
$$C_{a2} = -\Sigma_t \frac{\Sigma_s}{2k} A_1$$
$$C_{a1} = \frac{\Sigma_t \left(A_0 - C_{a0}\right) + \sinh(kb) \left(kA_1 - \Sigma_t b C_{a2} - C_{a2}\right) + \cosh(kb) \left(\Sigma_t A_1 - bkC_{a2}\right)}{k \sinh(kb) + \Sigma_t \cosh(kb)}$$
$$C_{i0} = \frac{\Sigma_t^2}{l^2} A_0$$
$$C_{i2} = -\frac{\Sigma_s}{k^2 - l^2} A_1$$
$$C_{i1} = \frac{\Sigma_t \left(A_0 - C_{i0}\right) + \sinh(kb) kA_1 - \sinh(lb) l C_{i2} + \cosh(kb) \Sigma_t A_1 - \cosh(lb) \Sigma_t C_{i2}}{k \sinh(kb) + \Sigma_t \cosh(kb)}$$
$$C_{M0} = C_{a0}$$
$$C_{M2} = C_{a2}$$
$$C_{M1} = C_{a1}$$

A PRIORI EFFICIENCY CALCULATIONS
FOR MONTE CARLO APPLICATIONS
IN NEUTRON TRANSPORT

PNR-131-2008-009

Andreas van Wijk

Delft, January 6, 2010